

AL/OE-TR-1995-00113



AN INVESTIGATION OF ACTIVE NOISE REDUCTION OF JET ENGINE RUNUP NOISE

Robert G. Gibson
Eric Stusnick

Wyle Laboratories
2001 Jefferson Davis Highway
Arlington, VA 22202

Jerome P. Smith
Ricardo A. Burdisso
Christopher R. Fuller

Virginia Polytechnic Institute and State University
Blacksburg, VA

OCCUPATIONAL AND ENVIRONMENTAL HEALTH DIRECTORATE
Bioenvironmental Engineering Division
Noise Effects Branch
2610 7th Street
Wright-Patterson AFB OH 45433-7901

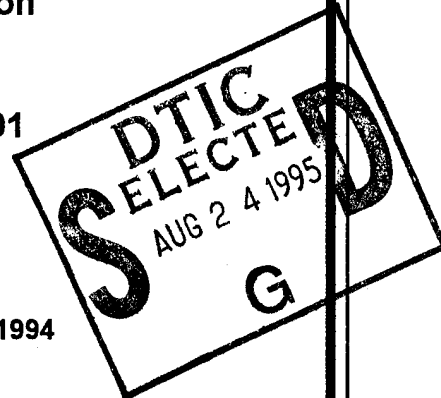
August 1995

Final Technical Report for Period July 1993 - October 1994

Approved for public release; distribution is unlimited.

AIR FORCE MATERIEL COMMAND
BROOKS AIR FORCE BASE, TEXAS

19950821 031



ARMSTRONG
LABORATORY

NOTICES

When US Government drawings, specifications, or other data are used for any purpose other than a definitely related Government procurement operation, the Government thereby incurs no responsibility nor any obligation whatsoever, and the fact that the Government may have formulated, furnished, or in any way supplied the said drawings, specifications, or other data, is not to be regarded by implication or otherwise, as in any manner licensing the holder or any other person or corporation, or conveying any rights or permission to manufacture, use, or sell any patented invention that may in any way be related thereto.

Please do not request copies of this report from the Armstrong Laboratory. Additional copies may be purchased from:

National Technical Information Service
5285 Port Royal Road
Springfield, Virginia 22161

Federal Government agencies registered with the Defense Technical Information Center should direct requests for copies of this report to:

Defense Technical Information Center
Cameron Station
Alexandria, Virginia 22314

DISCLAIMER

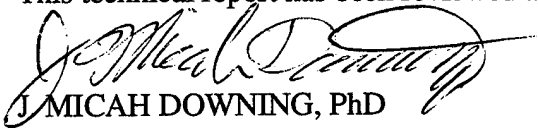
This Technical Report is published as received and has not been edited by the Technical Editing Staff of the Armstrong Laboratory.

TECHNICAL REVIEW AND APPROVAL


AL/OE-TR-1995-0113

This report has been reviewed by the Office of Public Affairs (PA) and is releasable to the National Technical Information Service (NTIS). At NTIS, it will be available to the general public, including foreign nations.

This technical report has been reviewed and is approved for publication.


J MICAH DOWNING, PhD
Acting Chief, Noise Effects Branch

FOR THE DIRECTOR


JAMES D. MONTGOMERY, LT COL, USAF, BSC
Chief, Bioenvironmental Engineering Division
Armstrong Laboratory

REPORT DOCUMENTATION PAGE

Form Approved
OMB No. 0704-0188

Public reporting burden for this collection of information is estimated to average 1 hour per response, including the time for reviewing instructions, searching existing data source, gathering and maintaining the data needed, and completing and reviewing the collection of information. Send comments regarding this burden estimate or any other aspect of this collection of information, including suggestions for reducing this burden, to Washington Headquarters Services, Directorate for Information Operations and Reports, 1215 Jefferson Davis Highway, Suite 1204, Arlington, VA 22202-4302, and to the Office of Management and Budget, Paperwork Reduction Project (0704-0188), Washington, D.C. 20503.

1. AGENCY USE ONLY (Leave Blank)		2. REPORT DATE August 1995	3. REPORT TYPE AND DATES COVERED Final Report for the period of July 1993 through October 1994	
4. TITLE AND SUBTITLE An Investigation of Active Noise Reduction of Jet Engine Runup Noise			5. FUNDING NUMBERS C: F41624-93-C-9001 PE: 63723F PR- 3037 TA: 303709 WU: 30370905	
6. AUTHOR(S) Robert G. Gibson and Eric Stusnick - Wyle Laboratories Jerome P. Smith, Ricardo A. Burdisso, and Chris R. Fuller - Virginia Polytechnic Institute and State University				
7. PERFORMING ORGANIZATION NAME(S) AND ADDRESS(ES) Wyle Laboratories 2001 Jefferson Davis Highway Arlington, VA 22202 Department of Mechanical Engineering Virginia Polytechnic Institute and State University Blacksburg, VA 24061			8. PERFORMING ORGANIZATION REPORT NUMBER WR 94-26	
9. SPONSORING / MONITORING AGENCY NAME(S) AND ADDRESS(ES) Armstrong Laboratory Occupational and Environmental Health Directorate Bioenvironmental Engineering Division, Noise Effects Branch 2610 7th Street Wright-Patterson Air Force Base, Ohio 45433-7901			10. SPONSORING / MONITORING AGENCY REPORT NUMBER AL/OE-TR-1995-0113	
11. SUPPLEMENTARY NOTES				
12a. DISTRIBUTION / AVAILABILITY STATEMENT Approved for public release; distributed is unlimited.			12b. DISTRIBUTION CODE	
13. ABSTRACT (Maximum 200 words) Active Noise Reduction techniques are used in this study to attenuate low-frequency broadband noise from jet engine exhaust. The low-frequency sound radiation from aircraft engine runup operations can result in a noise or vibration problem in nearby communities, even when aircraft are in test facilities such as hush houses or engine test cells. Experimental results are presented for the active reduction of broadband exhaust noise from both a stationary, unsuppressed jet engine and a jet engine installed in a small-scale simulated hush house. The control method is the feedforward filtered-x LMS algorithm and is implemented for both single-input, single-output and multi-input, multi-output systems. One-third octave band attenuations of up to 15 dB are achieved at error microphone locations, and large areas of significant noise reduction surround the error microphone locations. The areas of attenuation generally agree with analytical predictions.				
14. SUBJECT TERMS Active Noise Control Hush House Runup Noise Jet Engine Testing			15. NUMBER OF PAGES 144	
			16. PRICE CODE	
17. SECURITY CLASSIFICATION OF REPORT Unclassified	18. SECURITY CLASSIFICATION OF THIS PAGE Unclassified	19. SECURITY CLASSIFICATION OF ABSTRACT Unclassified	20. LIMITATION OF ABSTRACT Unlimited	

ACKNOWLEDGMENTS

The authors would like to thank Mr. Scott Hall of the U.S. Air Force Armstrong Laboratory for his encouragement and guidance throughout this project.

We also thank Dr. Robert Olsen and Dr. John Noble of the U.S. Army Research Laboratory, Battlefield Environment Directorate, for agreeing to provide us with the use of the Mobile Acoustic Source.

Accession For	
NTIS CRA&I	<input checked="checked" type="checkbox"/>
DTIC TAB	<input type="checkbox"/>
Unannounced	<input type="checkbox"/>
Justification	
By	
Distribution /	
Availability Codes	
Dist	Avail and/or Special
A-1	

TABLE OF CONTENTS

	<u>Page</u>
EXECUTIVE SUMMARY	1
INTRODUCTION	5
Background	5
Concept of Active Noise Reduction (ANR).	7
TECHNICAL CONSIDERATIONS IN THE APPLICATION OF ANR	9
Concepts of "Local" and "Global" Noise Reduction	9
Selection of Control Sources	10
The Importance of Reference and Error Signals	12
The Reference Signal	12
The Error Signal	13
Summary of Local and Global ANR Implementation	14
Use of an Electropneumatic Noise Source	16
ANALYTICAL MODEL.	19
Analytical Results	19
Discussion of Results	29
EXPERIMENTAL APPARATUS AND PROCEDURES	33
Test Site	33
Simulated Hush House	35
Unsuppressed Jet.	37
Electrodynamic Loudspeakers for Control	37
Electropneumatic Source (WAS 3000) for Control	39
Sound Power Output and Horn Characteristics	39
Mobile Acoustic Source	40
Performance Characteristics	41
Adaptive Controller	41
Reference Signal	42
Error Signal	43
Assessment of Noise Reduction	44
EXPERIMENTAL RESULTS	45
Local Active Noise Reduction	45
Preliminary Experiments on the Unsuppressed JT15D Engine	45
Simulated Hush House	47
Single-Input, Single-Output Configuration	51
Three-Input, Three-Output Configuration	67
Comparison of Results With Analytical Model	73
Unsuppressed Jet With WAS 3000 as Control Source	79

TABLE OF CONTENTS (Continued)

	<u>Page</u>
Global Active Noise Reduction	89
Simulated Hush House With Conventional Loudspeakers	89
Simulated Hush House With WAS 3000 Control Source.	91
Potential of WAS 3000 as a Control Source	103
Coherence	105
Feedback Removal	105
Control of a Broadband Disturbance at High Sound Level	108
CONCLUSIONS	117
REFERENCES.	119
APPENDIX A: Control Algorithm	121
Principles of Operation	121
System Identification of the Control Path Transfer Function(s)	124
Feedback Removal	126
REFERENCES FOR APPENDIX A	127
APPENDIX B: Description of the Analytical Model	129

LIST OF FIGURES

<u>Fig. No.</u>		
1	Noise Levels 100m From F-15 in USAF T-10 Hush House	6
2	Schematic Depiction of Active Noise Reduction (ANR)	8
3	Schematic Depiction of Local ANR	15
4	Photograph of the Cylinders of a WAS 3000	17
5	Overhead View of Experimental Facility Simulated in Analysis	20
6	SPL Reduction Contours for SI-SO Control Simulation at 40 Hz With Control Source at (30,0,1)m and Error Sensor at (40,0,1)m	22
7	SPL Reduction Contours for SI-SO Control Simulation at 80 Hz With Control Source at (30,0,1)m and Error Sensor at (40,0,1)m	23
8	SPL Reduction Contours for 3I-3O Control Simulation at 40 Hz With Control Sources at (30,0,1), (30,5,1), and (30,-5,1)m and Error Sensors at (40,0,1), (39,5,1), and (39,-5,1)m	24
9	SPL Reduction Contours for 3I-3O Control Simulation at 40 Hz With Control Sources at (30,0,1), (30,5,1), and (30,-5,1)m and Error Sensors at (40,0,1), (45,5,1), and (45,-5,1)m	26

LIST OF FIGURES (Continued)

<u>Fig. No.</u>		<u>Page</u>
10	SPL Reduction Contours for 3I-3O Control Simulation at 40 Hz With Control Sources at (30,0,1), (30,5,1), and (30,-5,1)m and Error Sensors at (40,0,1), (50,7.5,1), and (50,-7.5,1)m	27
11	SPL Reduction Contours for 3I-3O Control Simulation at 40 Hz With Control Sources at (30,0,1), (30,15,1), and (30,-15,1)m and Error Sensors at (40,0,1), (50,7.5,1), and (50,-7.5,1)m	28
12	SPL Reduction Contours for 7I-7O Control Simulation at 50 Hz	30
13	Photograph of the Turbo Lab and Test Cell	34
14	Photograph of the Simulated Hush House Exterior	36
15	Photograph of the Jet Aircraft Used for Local ANR Tests	38
16	Configuration for SI-SO Local ANR of the Unsuppressed JT15D Engine	46
17	Error Signal One-Third Octave Band Analysis, SI-SO Local ANR of Unsuppressed JT15D Engine	48
18	Total SPL Reduction Contours, SI-SO Local ANR of Unsuppressed JT15D Engine; Control Source at (30,0)m and Error Microphone at (40,0)m	49
19	SPL Reduction Contours in 50 Hz One-Third Octave Band, SI-SO Local ANR of Unsuppressed JT15D Engine; Control Source at (30,0)m and Error Microphone at (40,0)m	50
20	First Configuration for SI-SO Local ANR of the Simulated Hush House	52
21	Coherence Between Reference Microphone and Error Microphone, SI-SO Local ANR of Simulated Hush House	53
22	Coherence Between Input to Control Loudspeaker and Error Microphone, SI-SO Local ANR of Simulated Hush House	54
23	Error Microphone Spectra, SI-SO Local ANR of Simulated Hush House	56
24	Error Microphone One-Third Octave Band Analysis, SI-SO Local ANR of Simulated Hush House	57
25	Total SPL Reduction Contours, SI-SO Local ANR of Simulated Hush House; Control Source at (30,0)m and Error Microphone at (40,0)m	58
26	SPL Reduction Contours in 40 Hz One-Third Octave Band, SI-SO Local ANR of Simulated Hush House; Control Source at (30,0)m and Error Microphone at (40,0)m	59

LIST OF FIGURES (Continued)

<u>Fig. No.</u>		<u>Page</u>
27	SPL Reduction Contours in 80 Hz One-Third Octave Band, SI-SO Local ANR of Simulated Hush House; Control Source at (30,0)m and Error Microphone at (40,0)m.	60
28	Second Configuration for SI-SO Local ANR of Simulated Hush House . . .	61
29	Coherence Between Reference Microphone and Error Microphone, SI-SO Local ANR of Simulated Hush House	63
30	Error Microphone One-Third Octave Band Analysis, SI-SO Local ANR of Simulated Hush House	64
31	Total SPL Reduction Contours, SI-SO Local ANR of Simulated Hush House; Control Source at (17,0)m and Error Microphone at (40,0)m	65
32	SPL Reduction Contours in 63 Hz One-Third Octave Band, SI-SO Local ANR of Simulated Hush House; Control Source at (17,0)m and Error Microphone at (40,0)m.	66
33	First Configuration for 3I-3O Local ANR of the Simulated Hush House. . .	68
34	Error Microphone One-Third Octave Band Analysis, 3I-3O Local ANR of Simulated Hush House	69
35	Total SPL Reduction Contours, 3I-3O Local ANR of Simulated Hush House; Control Sources at (30,0), (30,5), and (30,-5)m and Error Microphones at (40,0), (45,5), and (45,-5)m	70
36	SPL Reduction Contours in 40 Hz One-Third Octave Band, 3I-3O Local ANR of Simulated Hush House; Control Sources at (30,0), (30,5), and (30,-5)m and Error Microphones at (40,0), (45,5), and (45,-5)m	71
37	SPL Reduction Contours in 100 Hz One-Third Octave Band, 3I-3O Local ANR of Simulated Hush House; Control Sources at (30,0), (30,5), and (30,-5)m and Error Microphones at (40,0), (45,5), and (45,-5)m	72
38	Second Configuration for 3I-3O Local ANR of Simulated Hush House . . .	74
39	Error Microphone One-Third Octave Band Analysis, 3I-3O Local ANR of Simulated Hush House	75
40	Total SPL Reduction Contours, 3I-3O Local ANR of Simulated Hush House; Control Sources at (30,0), (30,5), and (30,-5)m and Error Microphones at (40,0), (50,7.5), and (50,-7.5)m	76

LIST OF FIGURES (Continued)

<u>Fig. No.</u>		<u>Page</u>
41	SPL Reduction Contours in 40 Hz One-Third Octave Band, 3I-3O Local ANR of Simulated Hush House; Control Sources at (30,0), (30,5), and (30,-5)m and Error Microphones at (40,0), (50,7.5), and (50,-7.5)m	77
42	SPL Reduction Contours in 80 Hz One-Third Octave Band, 3I-3O Local ANR of Simulated Hush House; Control Sources at (30,0), (30,5), and (30,-5)m and Error Microphones at (40,0), (50,7.5), and (50,-7.5)m	78
43	Configuration for SI-SO Local ANR of Unsuppressed Jet Aircraft, Using WAS 3000	80
44	Photograph of Unsuppressed Jet Aircraft and WAS 3000 for Local ANR	82
45	Coherence Between Reference Microphone and Error Microphone, SI-SO Local ANR of Unsuppressed Jet Aircraft	83
46	Coherence Between Input to WAS 3000 and Error Microphone, SI-SO Local ANR of Unsuppressed Jet Aircraft, 10 to 100 Hz	84
47	Error Microphone Spectra, SI-SO Local ANR of Unsuppressed Jet Aircraft Using WAS 3000	85
48	Error Microphone One-Third Octave Band Analysis, SI-SO Local ANR of Unsuppressed Jet Aircraft, Using WAS 3000	87
49	SPL Reductions in 100 Hz One-Third Octave Band, SI-SO Local ANR of Unsuppressed Jet Aircraft, Using WAS 3000; Control Source at (0,-53)m and Error Microphone at (0,0)m	88
50	Configuration for SI-SO Global ANR of Simulated Hush House, Using Loudspeakers	90
51	Coherence Between Reference Microphone and Error Microphone, SI-SO Global ANR of Simulated Hush House, Using Loudspeakers	92
52	Coherence Between Input to Loudspeakers and Error Microphone, SI-SO Global ANR of Simulated Hush House	93
53	Error Microphone One-Third Octave Band Analysis, SI-SO Global ANR of Simulated Hush House, Using Loudspeakers	94
54	Total SPL Reduction Contours, SI-SO Global ANR of Simulated Hush House, Using Loudspeakers; Control Source at (8,0)m and Error Microphone at (40,0)m	95

LIST OF FIGURES (Continued)

<u>Fig. No.</u>		<u>Page</u>
55	SPL Reduction Contours in 31.5 Hz One-Third Octave Band, SI-SO Global ANR of Simulated Hush House, Using Loudspeakers; Control Source at (8,0)m and Error Microphone at (40,0)m	96
56	SPL Reduction Contours in 50 Hz One-Third Octave Band, SI-SO Global ANR of Simulated Hush House, Using Loudspeakers; Control Source at (8,0)m and Error Microphone at (40,0)m	97
57	Photograph of Simulated Hush House and WAS 3000 Horn for Global ANR	99
58	Configuration for SI-SO Global ANR of Simulated Hush House, Using WAS 3000	100
59	Coherence Between Reference Microphone and Error Microphone, SI-SO Global ANR of Simulated Hush House, Using WAS 3000.	101
60	Coherence Between Input to WAS 3000 and Error Microphone, SI-SO Global ANR of Simulated Hush House, 10 to 100 Hz.	102
61	Error Microphone One-Third Octave Band Analysis, SI-SO Global ANR of Simulated Hush House, Using WAS 3000.	104
62	Coherence Between Input to WAS 3000 and Error Microphone, WAS 3000 at 1.5 psi and 2 amps.	106
63	Coherence Between Input to WAS 3000 and Error Microphone, WAS 3000 at 2.5 psi and 4 amps.	107
64	Coherence Between Input to WAS 3000 and Reference Microphone, WAS 3000 at 3.5 psi and 2 amps, Bandwidth = 10 to 100 Hz	109
65	Reference Microphone One-Third Octave Band Analysis of Feedback Removal, WAS 3000 at 3.5 psi and 2 amps, Bandwidth = 10 to 100 Hz	110
66	Configuration for ANR of Loudspeaker Noise at High Level, Using WAS 3000; Reference Microphone Not in Use	111
67	Coherence Between Input to WAS 3000 and Error Microphone, ANR of Loudspeaker Noise at High Level, WAS 3000 at 3.5 psi and 6 amps, Bandwidth = 10 to 100 Hz	113
68	Coherence Between Input to Disturbance Loudspeakers (Reference Signal) and Error Microphone, ANR of Loudspeaker Noise at High Level	114
69	Error Microphone One-Third Octave Band Analysis, ANR of Loudspeaker Noise at High Level, Using WAS 3000, Bandwidth = 25 to 100 Hz	115

EXECUTIVE SUMMARY

The purpose of this program was to investigate the effectiveness of Active Noise Reduction (ANR) technology in reducing the noise generated by jet engine runup operations conducted in hush houses and on airport property. The noise associated with such operations is typically dominated by low-frequency energy which can propagate easily over a great distance and can be a source of annoyance to local communities around air bases. Reduction of such noise using traditional, or "passive," noise control techniques is often difficult or impractical.

An example of such a low-frequency noise source is the Air Force T-10 hush house, which is very effective at reducing the mid- and high-frequency noise of jet engine runup operations, but which results in high noise levels at low frequencies, particularly between 10 and 100 Hz.

Active noise reduction is a relatively new acoustic technology which has been successfully applied over recent years to low-frequency noise from a variety of sources. Preliminary assessment of the characteristics of noise from hush houses and jet aircraft runup operations suggested that successful attenuation of such noise over large areas might result from the application of ANR.

Active noise reduction is a technique based on the principle that the superposition of one acoustic wave with another wave which is "out of phase" (sometimes referred to as "anti-sound") will result in destructive interference, or "cancellation" of the noise field. ANR utilizes noise sources such as loudspeakers to produce the "anti-sound," or control noise, to cancel the offending, or disturbance noise. Although complete cancellation is not achieved in practice, significant noise reductions can be obtained.

This report presents the results of a series of experiments in which ANR was applied to noise from a jet aircraft and from a small-scale simulated hush house. The control sources used were conventional loudspeakers and a high-intensity electro-pneumatic noise source, the WAS 3000, designed and fabricated by Wyle Laboratories. Two ANR configurations, local and global control, were investigated.

Local control, or attenuation over a specific localized area, of noise from both the simulated hush house and the unsuppressed jet aircraft was studied. Local ANR is applicable where noise is only of concern in one specific region, for example, near a residence. In this configuration, one or more control sources can be placed near the receiver, and these sources need to produce much less acoustic power than the offending source since cancellation over only a limited area is required.

Global noise control, or attenuation over a very large area, was only investigated for the simulated hush house. Global ANR is required where noise needs to be reduced in all directions from the offending source. In this configuration, a control source or sources must be placed very near the offending source and must have the capability of high sound output power, comparable to that of the offending source. The global control of noise from an unsuppressed jet engine is currently infeasible due to the high sound levels produced and the extended nature of the noise source itself.

In this program, the application of local ANR to the simulated hush house resulted in noise reduction of up to 15 dB when measured over one-third octave bands in the range of 31.5 to 100 Hz. Large areas of significant noise reduction in the local region of interest were measured; noise reduction of greater than 5 dB in certain one-third octave bands has been demonstrated over an area in excess of 20m x 25m. For these experiments, conventional loudspeakers were used as the control sources. Similar results were obtained for the application of local ANR to the low-frequency noise from an unsuppressed jet engine.

The application of global ANR to the simulated hush house resulted in smaller attenuations, noise reduction up to 4 dB when measured over one-third octave bands. These results were achieved using conventional loudspeakers as control sources.

Application of the WAS 3000 noise source in a local ANR system resulted in noise reduction of up to 6 dB in one-third octave bands. Global ANR of the simulated hush house using the WAS 3000 was not successful due to causality problems and because the WAS 3000 was operated at the lower end of its design range, where its output was highly nonlinear. A series of experiments studying the WAS 3000 indicate that it should perform well as a control source if applied to ANR of a noise source that is significantly louder than the disturbance sources used in this

program. When operated at high noise levels, the sound output of the WAS 3000 is significantly more linear, or coherent with the input, than at low noise levels. The WAS 3000 was used to reduce the noise from loudspeakers by up to 14 dB in one-third octave bands.

This study presents important results which suggest that active noise reduction may be a powerful technique for the effective attenuation of low-frequency jet engine runup noise. Control sources suitable for local ANR are readily available. Provided an adequate reference signal can be obtained, the WAS 3000 should be suitable for global ANR of hush house noise. Similar experiments on a larger scale are required to demonstrate that the technique can be practically applied to full-scale military aircraft and hush houses.

The *INTRODUCTION* of this report provides a detailed introduction to the study, *TECHNICAL CONSIDERATIONS IN THE APPLICATION OF ANR* reviews the requirements for successful application of ANR, and *ANALYTICAL MODEL* describes an analytical model which was developed to assist in the design of ANR configurations. *EXPERIMENTAL APPARATUS AND PROCEDURES* and *EXPERIMENTAL RESULTS* describe the experimental apparatus, procedures, and results, and the last section summarizes conclusions. Appendices A and B describe the control algorithm and the analytical model in detail.

INTRODUCTION

Background

The noise from aircraft operations at military air bases can be a continuing source of annoyance to local communities. As would be expected, the major offenders are aircraft flight operations both on the runways and in the airspace surrounding the base. However, a not insignificant contribution to the local noise environment is the testing of aircraft engines, which occurs not only on open test pads but also in hush houses and engine test cells.

Hush houses were specifically designed to eliminate the community noise resulting from the testing of jet aircraft and aircraft engines on open test pads. By and large, they have been fairly successful in reducing the annoyance, by greatly attenuating high- and mid-frequency engine noise. However, the radiated noise from hush houses is characterized by a very low-frequency noise component, in the range of 100 Hz and below, that propagates with little attenuation (other than that due to geometrical spreading) over large distances, and is difficult to eliminate. Engine test cells are similar in function to hush houses; their very low-frequency noise component is not so prevalent as it is in hush houses, but community disturbance still occurs because testing cycles can be lengthy. Noise levels measured during operation of a U.S. Air Force T-10 hush house are shown in Figure 1.¹

Both hush houses and engine test cells have been designed using so-called "passive" noise reduction techniques – namely, techniques that rely on the acoustic absorption and transmission loss properties of materials to reduce the high sound levels generated at the source. In recent years, however, there has been increased interest in the application of so-called "active" methods of noise reduction, where out-of-phase acoustic noise is used to "cancel" unwanted noise. These methods, known as Active Noise Reduction or Active Noise Control, have been shown to be most effective at fairly low frequencies, and therefore may be ideal for application to low-frequency noise from hush houses and test cells. Active methods may also be useful for application to other types of noise sources on air bases, particularly the engine runup of aircraft which are stationary but are not in a hush house, since at large distances from such aircraft the noise may be dominated by low-frequency components.

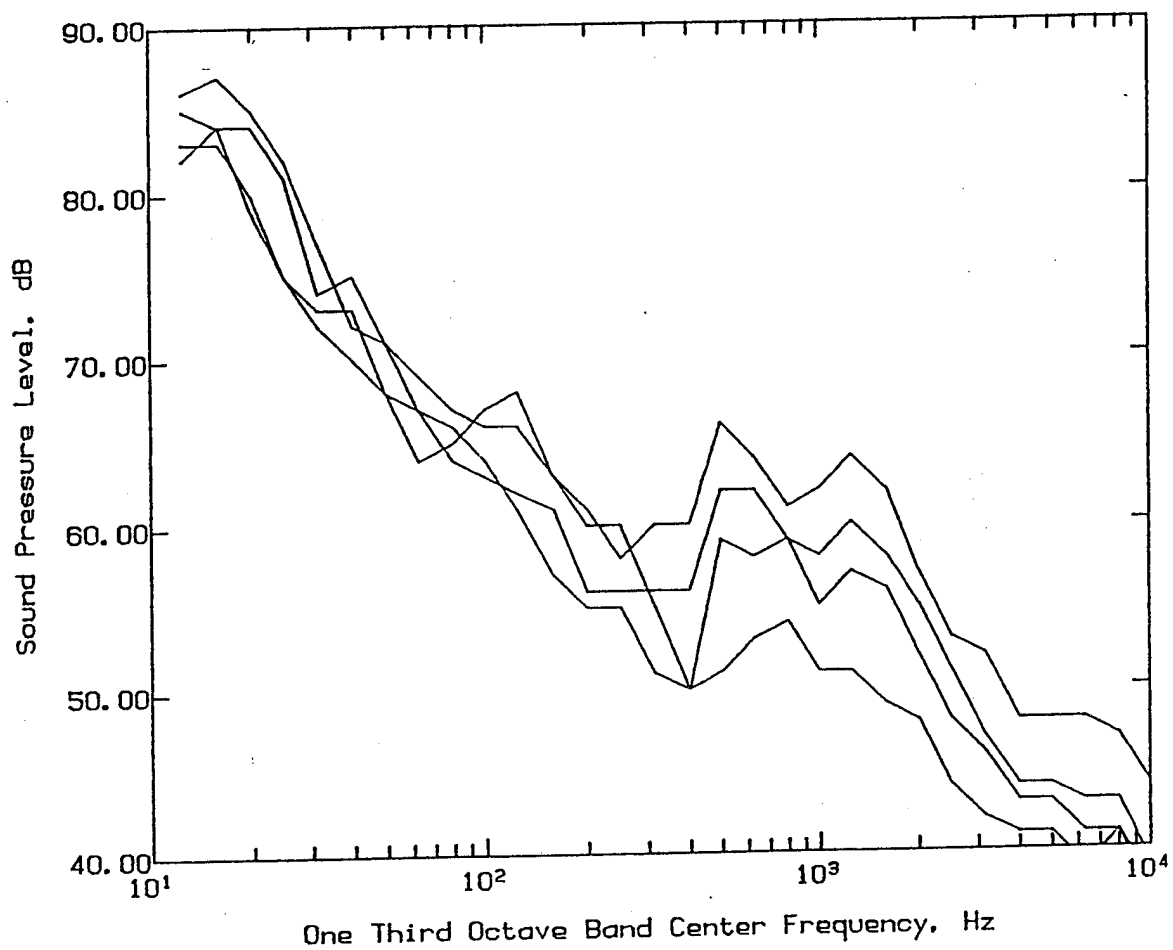


Figure 1. Noise Levels 100m From F-15 in USAF T-10 Hush House.

Concept of Active Noise Reduction (ANR)

Active Noise Reduction (ANR) or Active Noise Control (ANC) is a noise mitigation technique based on the principle that the superposition of coherent acoustic waves will produce an interference pattern. ANR involves the use of secondary acoustic sources, such as loudspeakers, to generate an "anti-sound" field that destructively interferes with the primary, unwanted noise field. Thus the control sources serve to "cancel" the effect of the disturbance source in the radiation field.

The concept of ANR was demonstrated as far back as 1936 when it was shown that the pressure due to a simple sound wave propagating in a duct could be reduced with a loudspeaker.² In more recent years, the advancements in high-speed digital signal processing have made ANR techniques practical and realizable. The technique of ANR has been shown to be most effective at low frequencies, where passive noise control techniques are ineffective.

The basic concept of an ANR system employing the technique known as "feed-forward" control is illustrated in Figure 2. The heart of the controller shown in the figure is a microprocessor that reads the signal detected by the reference sensor and computes the optimal control signal to be sent, or "fed forward", to the control source (typically a loudspeaker), which transmits the control signal so that the unwanted noise is reduced. The resultant reduced noise is detected by the error sensor and minimized by the controller, which adapts the output signal to the loudspeaker. The controller is adaptive in that it has the ability to adjust to gradual changes in system parameters. This means that, even as the frequency or amplitude of the unwanted sound changes, the control system is able to account for these changes and maintain its control performance.

In theory, this method can result in complete cancellation of the noise; in practice, complete cancellation is not achieved, although dramatic results have been demonstrated in cases where noise of only a single frequency is to be cancelled.

ANR has proven to be an effective method of noise mitigation in several industrial applications, typically in situations where the noise is predominantly distributed over a narrow band of low frequencies and initially contained within a confined duct. For instance, air flow and exhaust fan noise in large ducts have been significantly

reduced using ANR.³ Similarly, there have been considerable advances in the application of active noise control in reducing automobile exhaust noise. Another application of ANR has been in the so-called "active" headphones, which cut down the background noise while allowing the user to listen to speech frequencies relatively unhampered.

Initially, digital signal processor (DSP) speeds allowed ANR to be applied only to tonal and very narrowband signals. As the operation speed of these processors has increased, ANR has been successfully applied to broadband noise sources. For broadband noise, more computational effort is required to apply ANR, and therefore noise reductions are typically of a lesser magnitude than for single frequencies. Recent reviews of the theory and practice of Active Noise Control are presented in a textbook by Nelson and Elliott⁴ and in References 5 and 6.

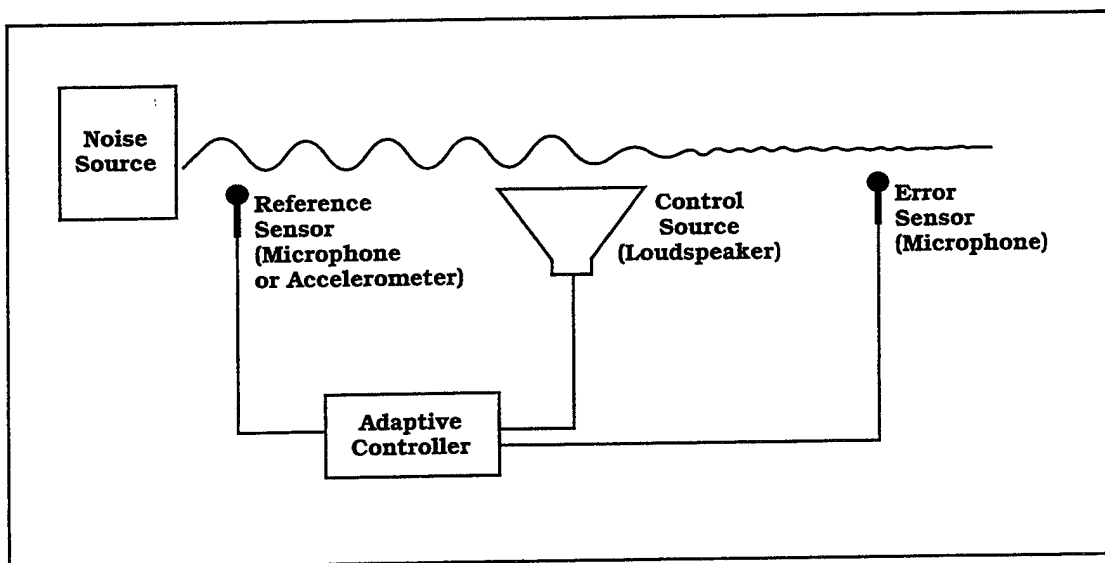


Figure 2. Schematic Depiction of Active Noise Reduction (ANR).

TECHNICAL CONSIDERATIONS IN THE APPLICATION OF ANR

Concepts of "Local" and "Global" Noise Reduction

Two configurations of ANR systems to control low-frequency broadband noise have been investigated in this study. In the first, noise cancellation is attempted over a specific limited area or sector at some large distance from the disturbance noise source. In this configuration, referred to in this report as "local" ANR, the objective is to minimize the noise level in one specific region – for example, at the location of a house or group of residences. In the second configuration, noise cancellation is attempted over a very large area, potentially in all directions from the noise source; this is referred to as "global" ANR. The potential of local ANR has been investigated in this study for two types of noise source, a hush house and an unsuppressed jet engine. The potential of global ANR has been investigated only for a hush house.

Previous studies by other researchers have shown some encouraging results for both local and global control; however, the majority of these studies which have addressed broadband noise have been in laboratory environments. One example of local ANR applied to broadband noise in the laboratory was performed by Hasebe *et al.*⁷ They were able to demonstrate good global reduction of a three-dimensional sound field over a 1500 Hz bandwidth. In addition, Hasebe demonstrated that an attenuation "shadow" was created in the region beyond the error microphone. Similar results, using multiple speakers and error microphones in a laboratory, were obtained more recently by Peterson *et al.*⁸

Outside of laboratory settings, tonal noise from devices such as transformers has been controlled over large areas; an example of this is in work by Angevine.⁹ An attempt at global control of broadband exhaust noise from a combustion turbine was made by Hill and Wheeler,¹⁰ but the results were not successful. The same researchers then attempted local control of the same source (described in the same report), and achieved some noise reduction, on the order of 3 dB at one measurement point; results were not measured over a large area.

Selection of Control Sources

In general, the process of minimizing the sound pressure at the error sensor with active methods will result in a "zone of cancellation" about the error sensor. The separation distance between the disturbance source and the control source dictates to some extent the area in which noise attenuation will be observed. The closer the control source is to the disturbance source, the larger and more global the expected area of attenuation about the error sensor. As a general rule of thumb, for a control source to be effective in a global ANR application, it must be located near the offending source and must be capable of generating sound levels similar to those produced by the offending source, with a similar directivity.

Alternatively, if localized noise reduction is required, then the control source can be located closer to the local area of interest, and only needs to be capable of generating sound pressure levels similar to those produced by the offending source in the specified area.

If a control source has a sound power output capability similar to the offending source and is placed close to that source, within a small fraction of an acoustic wavelength, then global noise reduction may be possible. With the control source close to the offending source, a combined dipole source may be formed (if both sources are assumed to be acoustic monopoles). It has been demonstrated that a dipole has a very poor global radiation efficiency when the source separation is much less than one wavelength.¹¹ Since the peak frequency of interest for hush house noise is about 20 Hz, corresponding to a wavelength of 17m, it is feasible to achieve spacing of much less than a wavelength between the hush house exhaust and a control source, allowing for the possibility of noise reduction in all angular directions, if the monopole model is valid.

If a control source is used to provide localized noise reduction, a directional "wedge" or "shadow" of noise reduction can be created; this "shadow" could cover significant areas far away from the noise source. However, the difference in curvature of the acoustic wavefronts from the distant source and the controlling source poses an inherent limit to the size of this controlled area. In either the local or global configuration, it should be possible to increase the area of reduction by increasing the number of control sources.

For the application of ANR to local control of engine runup noise, the control sources should be a considerable distance away from the aircraft or hush house, in the vicinity of potentially affected receivers in the community, and therefore standard loudspeakers may be acceptable for this application. The noise from an unsuppressed jet aircraft is spread over a fairly wide frequency range, but at a distance in excess of 1000m from the source, the combined effects of ground and air absorption will modify the spectrum so that the sound energy may be concentrated in the low-frequency range and should be well within the power range of standard loudspeakers.

For global control of hush house noise, on the other hand, the control source has to be capable of generating extremely high levels of low-frequency sound energy, since jet engines operating at full capacity in a hush house can produce sound power levels (re 10^{-12} watts) on the order of 140 dB at infrasonic frequencies. Conventional loudspeakers can, in theory, be used to create the high levels produced by hush houses, but in practice, this means using cumbersome banks of large and powerful loudspeakers. In order to achieve the very high levels of low-frequency noise characteristic of hush house emissions, a high-intensity source known as the WAS 3000, described in *Use of an Electropneumatic Noise Source*, has been utilized in this program.

In addition to sound power level, another important aspect of a control source is the source's linearity, or the coherence between electrical signal input and acoustic output. Coherence is a measure of the linear relationship between two signals, expressed as a function of frequency, and is measured on a scale from 0 to 1, the former indicating no relation between the two signals, and the latter indicating an exact linear relationship. If the linearity or coherence of a source is poor, then the cancellation noise will not be an adequate representation of the intended control output, and the amount of noise attenuation will be reduced.

The Importance of Reference and Error Signals

The Reference Signal

Obtaining an appropriate reference signal is an important aspect of the design of a feedforward active noise reduction system. This reference signal can come from any of a number of types of transducer, provided that the signal has good coherence across the frequency range of interest with the acoustic field that is to be cancelled. This means that a relationship must exist such that the noise to be cancelled can be predicted from the reference signal to some extent. If the reference signal and a representative acoustic signal in the sound field to be controlled are not coherent, the ability of the control system to cancel the unwanted noise will suffer.

For applications where noise is propagating – for example, down a duct – an upstream microphone is typically used to provide a reference signal for controlling downstream noise. For applications to single-frequency noise from rotating machinery, a tachometer signal is often used as a reference. For other machinery noise applications, an accelerometer on a machine surface may provide a vibration signal which is coherent with radiated noise. In some applications, multiple reference sensors may be used.

Difficulties may exist in the identification of a good reference signal in certain cases. It may not be possible to obtain an adequate reference signal in the near field of the noise source since the pressure fluctuations may not be well correlated with the propagating acoustical disturbance that reaches the far field. In the case of aerodynamic noise from a high-velocity jet exhaust, for example, a reference microphone or pressure transducer in or near the exhaust flow may have poor coherence with an error signal obtained in the far field due to the non-linear acoustic path from a turbulent jet to the acoustic far field, and due to the large spatial extent of the aerodynamic source. Hill and Wheeler¹⁰ encountered this problem while applying ANR technology to a power generation gas turbine. When using a reference signal obtained from a microphone in the case of a complex acoustical source propagating into a free field, it is generally desirable from the point of view of maximizing coherence to obtain the reference signal from a point in the far field of the noise source.

Other difficulties in selection of a reference microphone location may arise due to two issues in active control: causality and control feedback. Causality describes the requirement that the reference signal must be obtained early enough both to allow the controller to calculate the required acoustic output and then to allow that output to reach the error microphone at the same time as the acoustic wave from the disturbance source. If the control output arrives too late, then no control can be achieved. The causality issue is of particular importance when dealing with broadband random disturbances.¹²

Control feedback describes the contamination of the reference signal by the acoustic output of the control source. The reference microphone ideally should sense only noise from the disturbance source; if this microphone instead senses a large component of noise from the control speakers, then a loss of coherence and feedback problems can develop. These issues are described in more detail in Appendix A.

As a result of these constraints, the selection of a location for a reference microphone will involve tradeoffs between coherence (which may require that the microphone be far from the disturbance source), causality (which may require that the microphone be near the disturbance source), and control feedback (which may require that the microphone be far from the control source).

The Error Signal

The error signal is obtained by a sensor that provides a signal characteristic of the quantity to be minimized. In this case, since sound attenuation is desired, a microphone is the obvious choice for the error transducer, since microphones provide a signal directly related to the acoustic pressure. Error microphone locations are generally chosen to be in the area where noise cancellation is most desired. Since the controller's function is to minimize sound pressure at the error microphone, or at a number of error microphones, the highest levels of noise attenuation are generally at the error microphone locations. For the free-field propagation applications investigated here, the appropriate error microphone locations are in the direction of desired attenuation.

The number of error microphones to employ in an ANR system is a matter of compromise. Using a single error microphone has the advantage of placing the least computational load on the adaptive controller. This allows the controller to operate at a greater sampling rate, thus increasing the applicable bandwidth. In addition, higher attenuations are possible with a single error microphone. A single error microphone, however, limits the ANR system's area of attenuation. Adding more error microphones can increase the area of attenuation at the cost of decreasing the magnitude of attenuation. This is because the adaptive controller strives to minimize the mean square value of all of the error signals combined. Multiple error microphones also increase the computational burden on the adaptive controller which will decrease the operational bandwidth.

Summary of Local and Global ANR Implementation

Choice of the locations for system components in the implementation of ANR for local control is fairly straightforward since it is relatively easy to satisfy the requirements outlined in *Selection of Control Sources* and *The Importance of Reference and Error Signals*, provided that the area where cancellation is desired is relatively far from the disturbance source. A schematic of local ANR for free-field propagation is shown in Figure 3. A coherent reference is obtained with a microphone between the disturbance (D) and the control source (C) as long as the distance between the disturbance and the reference (R) is sufficient for the acoustical propagation characteristics to have developed and for the disturbance to appear as a compact source. The control feedback into the reference signal is minimal if the distance between the reference and the control source is sufficient or if the control source is somewhat directional and pointed away from the reference. The power requirements of the control source for local ANR are typically satisfied by standard professional loudspeakers, particularly if the control source and the error microphone (E) are fairly close together. The input and output coherence requirement of the control source is also usually met by high-quality loudspeakers. The causality issue is also easily satisfied since the controller is typically fast enough to maintain a causal system if the components of the ANR system are sufficiently spread out and in the disturbance-reference-control-error geometry of Figure 3.

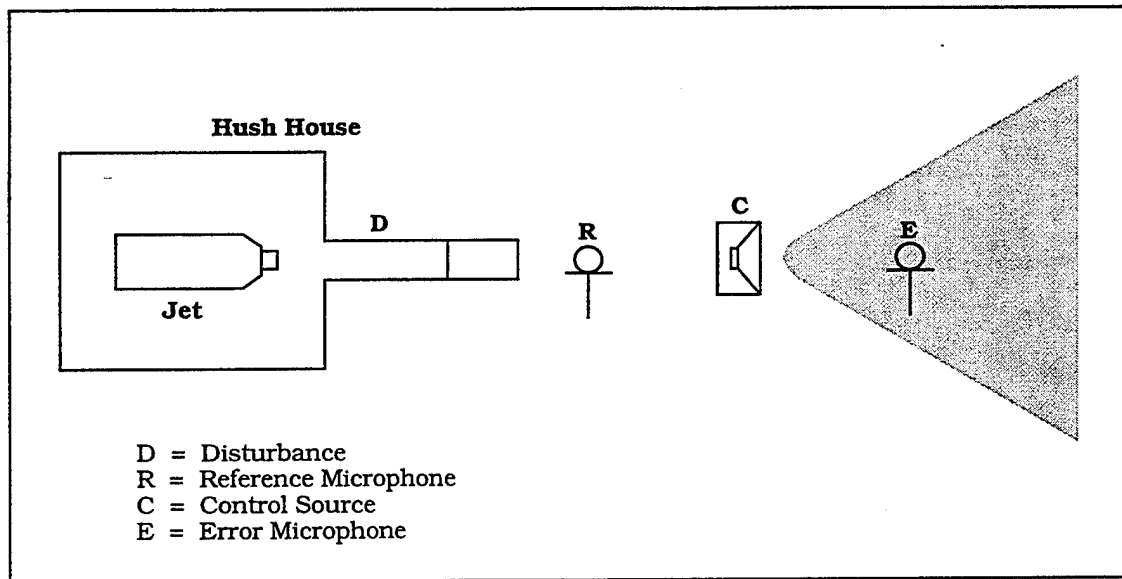


Figure 3. Schematic Depiction of Local ANR.

Global control can be more difficult to achieve since satisfying the requirements becomes somewhat more complex when the control source is moved close to the disturbance. First, the problem of finding a coherent reference signal without picking up feedback from the control source is a more difficult one. With a microphone as a reference sensor, the feedback from the control source into the reference signal is more significant if there is little separation distance between the control and the reference, particularly at low frequencies. Second, for disturbance sources which are somewhat distributed, a reference microphone near the disturbance may not allow enough distance between the disturbance and the reference for the acoustical propagation characteristics to have developed. For aeroacoustic noise sources, there may be limited measurable physical quantities that are coherent with the acoustic signal in the far field, and thus a limited number of sensors capable of providing a coherent reference. Third, the power requirements of a control source in close proximity to the disturbance can be greater than that provided by typical linear acoustic sources. Fourth, maintaining a causal system can be more difficult with a small distance between the reference sensor and the control source, since this allows little time for the control computations to be performed. The system will be acausal if the reference is moved away from both the control and the disturbance sources and into the far field.

Thus, for many reasons, global ANR may be more difficult to achieve than local ANR. For some situations, minimizing the noise in a localized area is sufficient, as in attenuating the noise at a group of houses near an air facility. In this research, both the global and local approaches to ANR are investigated for their potential of controlling low-frequency broadband exhaust noise.

Use of an Electropneumatic Noise Source

The use of an electropneumatic noise source as a control source in a global ANR system has been investigated in this program. An electropneumatic noise source, sometimes called a compressed air loudspeaker, is an extremely powerful acoustic source that generates sound by modulating a pressurized flow of air. Such sources have been used extensively for over three decades, primarily to generate high-intensity sound fields in reverberant chambers designed for the structural testing of aerospace vehicles and components. The basic principles of operation of this type of source have been described mathematically by Meyer¹³ and more recently by Chapman and Glendinning.¹⁴ Sources of this type differ from sirens in that the modulation mechanism is driven by a voice coil, enabling broadband noise rather than only tonal noise to be generated.

One example of a commercially available electropneumatic source is the Wyle Acoustic Source, or WAS 3000, manufactured by Wyle Laboratories. The heart of the WAS 3000 consists of two concentric cylinders, each having circumferential rows of modulation slots. The cylinders are connected together at one end to a firm base; a voice coil is wrapped around the other end of the outermost cylinder and is surrounded by a permanent magnet. The slots in the two cylinders are arranged such that, in the quiescent state, the slots of one cover exactly one-half the area of the slots in the other. The application of an electrical signal to the voice coil will produce axial motion of the outer cylinder and a resulting variation of the slot opening area at the frequency of the input signal. A photograph of the cylinders of a WAS 3000 is shown in Figure 4; the voice coil and slot openings can be seen at the top of the cylinders.

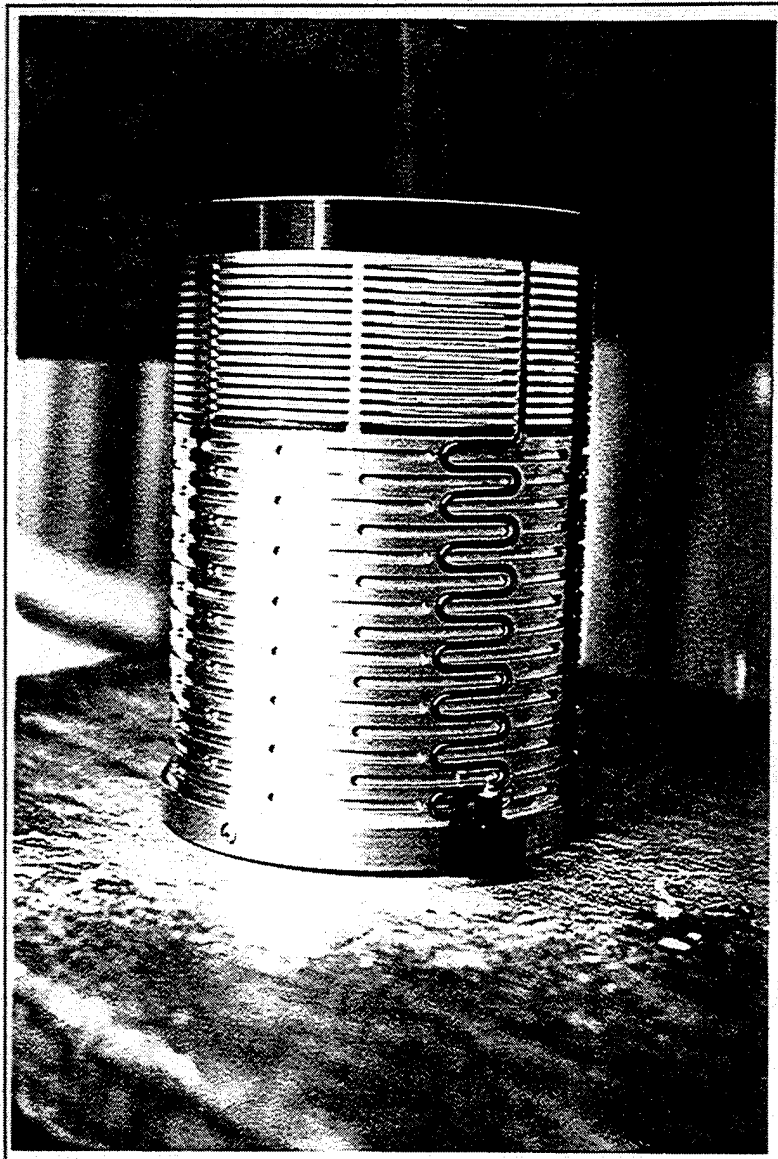


Figure 4. Photograph of the Cylinders of a WAS 3000.

Air pressure applied to the outside of the cylinders causes air to pass through the slots, the air flow being dependent on the open area of the slots. As this open area varies with the electrical input signal, so will the flow of air through the slots. The cylinders thus will modulate the stream of air passing through them, producing a pulsating flow of air which acts as a monopole source of sound.

The potential use of this type of source in active noise control for application to exhaust noise has been considered by a team at the University of Southampton.^{15,16} Their measurements indicated that commercially available electropneumatic sources suffered from high harmonic distortion and were not sufficiently linear for application to active control at low frequencies. As a result, a version with more linear response was designed. Although a small prototype source was fabricated and evaluated, no results are reported regarding its application to active control. Investigation of the linearity of the WAS 3000, and its potential for application to control of exhaust noise, were undertaken in the study described in this report.

ANALYTICAL MODEL

This section describes an analytical study performed to simulate the far-field localized cancellation of jet engine exhaust noise using active noise control methods. The disturbance and control sources are modelled as ideal acoustic monopoles, radiating spherically and harmonically. The control inputs required in order to minimize the acoustic pressure at one or more far-field locations are calculated, once the source locations are defined in the model. Both single-input, single-output (SI-SO) and multiple-input, multiple-output (MI-MO) cases are examined; an input is defined as an error sensor and an output is defined as a control source. The simulation is performed with MATLAB software. This analytical study is conducted in order to gain insight into some of the physical aspects of active noise control, such as the effects of the locations of the control sources and error sensors, and the relative magnitude of the control energy required for cancellation. The simulation program can also be used to design and predict the performance of practical ANR configurations and to provide guidelines for experimental system design.

A detailed description of the model is provided in Appendix B.

Analytical Results

A diagram of one basic physical arrangement to be simulated by the model is shown in Figure 5. The disturbance source represents the exhaust noise of an engine test cell located at the Virginia Tech Airport, described further in the following section, *EXPERIMENTAL APPARATUS AND PROCEDURES*. The array of points on the right in Figure 5 represents the area where noise cancellation is desired. Point C in the diagram, the control source, is 30 meters from the engine exhaust, and point E, the error sensor, is 40 meters from the engine exhaust. The disturbance, control source, and error microphone are all colinear in this configuration; the line formed by these locations is referred to here as the control axis.

The disturbance magnitude, A_d (described in Appendix B), used for all cases was 5 Pa, since this value resulted in similar sound pressure levels to those actually measured in the field for typical engine operation at the experimental facility. A 31 x 31 field point matrix with a spacing between points of 1 meter was used to determine the effects of control on and around the error locations in the model. The

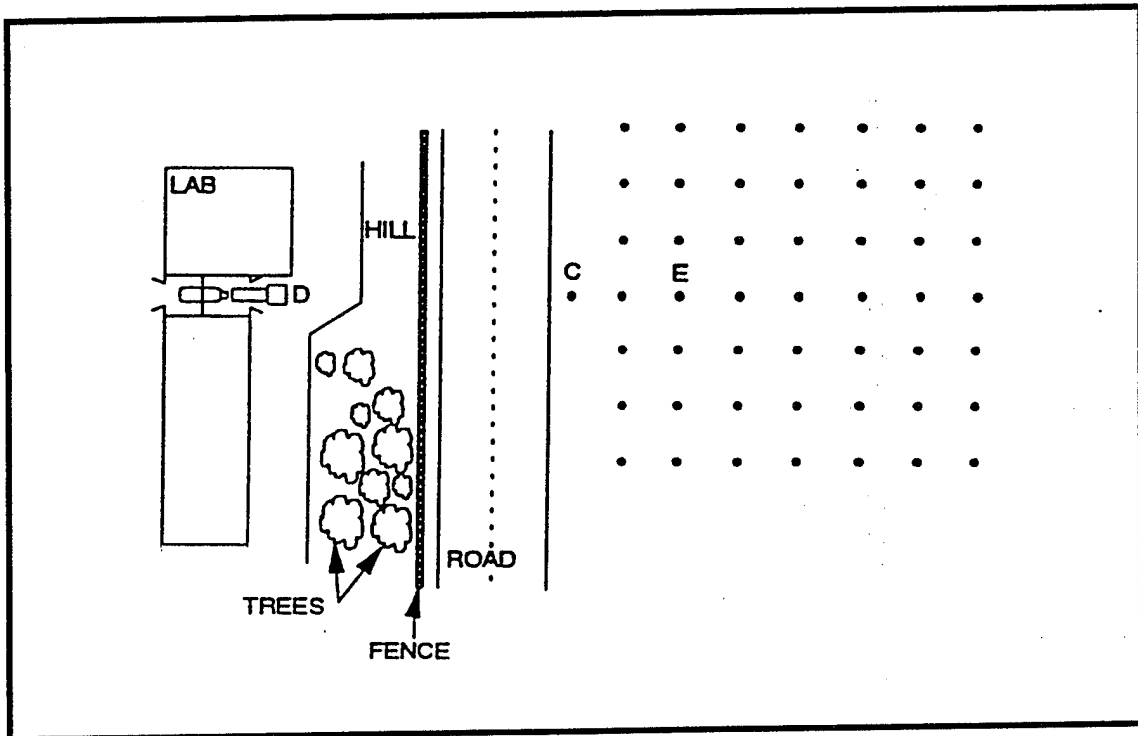


Figure 5. Overhead View of Experimental Facility Simulated in Analysis.

error locations are the observation points at which the pressure is minimized; experimentally, these correspond to points where microphone error sensors would be located. The control source locations represent the points where actual control loudspeakers would be located. The heights of sources and sensors are modeled as 1m above the ground. The field point matrix is a rectangular array which is aligned with the control axis.

Both SI-SO and MI-MO systems were examined in the analysis. The simulation computes results for a single frequency at a time, and the center frequencies of the standard one-third octave bands were usually chosen as the test frequencies.

Contour plots showing lines of equal noise reduction in the plane containing the disturbance, control sources, and error sensors were created to evaluate each configuration. For these contour plots, each contour line represents an integer noise reduction multiple of 5 dB. Negative reductions indicate an increase in sound pressure level after control. The horizontal axis of these plots shows the x-coordinate (parallel to the control axis) in meters, and the vertical axis indicates the y-coordinate (perpendicular to the control axis) in meters. For all configurations, the disturbance was located at (0,0,1) meters. The error microphone locations are marked with asterisks on the contour plots. The control locations are not shown; they are off the left edge of the frame for the cases presented here.

Figure 6 contains a contour plot of the reduction obtained utilizing a SI-SO system, with the error sensor located at (40,0,1) meters and the control source located at (30,0,1) meters. The disturbance frequency was 40 Hz. The contour lines exhibit a "cone" or "wedge" of reduction, with the "point" of the cone located at the control source position. Figure 7 contains a plot with the same configuration, except at a frequency of 80 Hz. Note that substantial areas of noise reduction are achieved, and that the width of the cone of reduction is narrower at the higher frequency. The magnitude of the required control inputs for both 40 Hz and 80 Hz were approximately the same value (1.3 Pa). Higher frequencies result in a more radically varying pressure field since the wavelength of the sound is much shorter at higher frequencies.

A multiple-input, multiple-output configuration, in this case, 3I-3O, with three control sources and three error sensors, is shown in Figure 8. This case had control sources at (30,0,1), (30,5,1), and (30,-5,1) meters with the error points positioned at

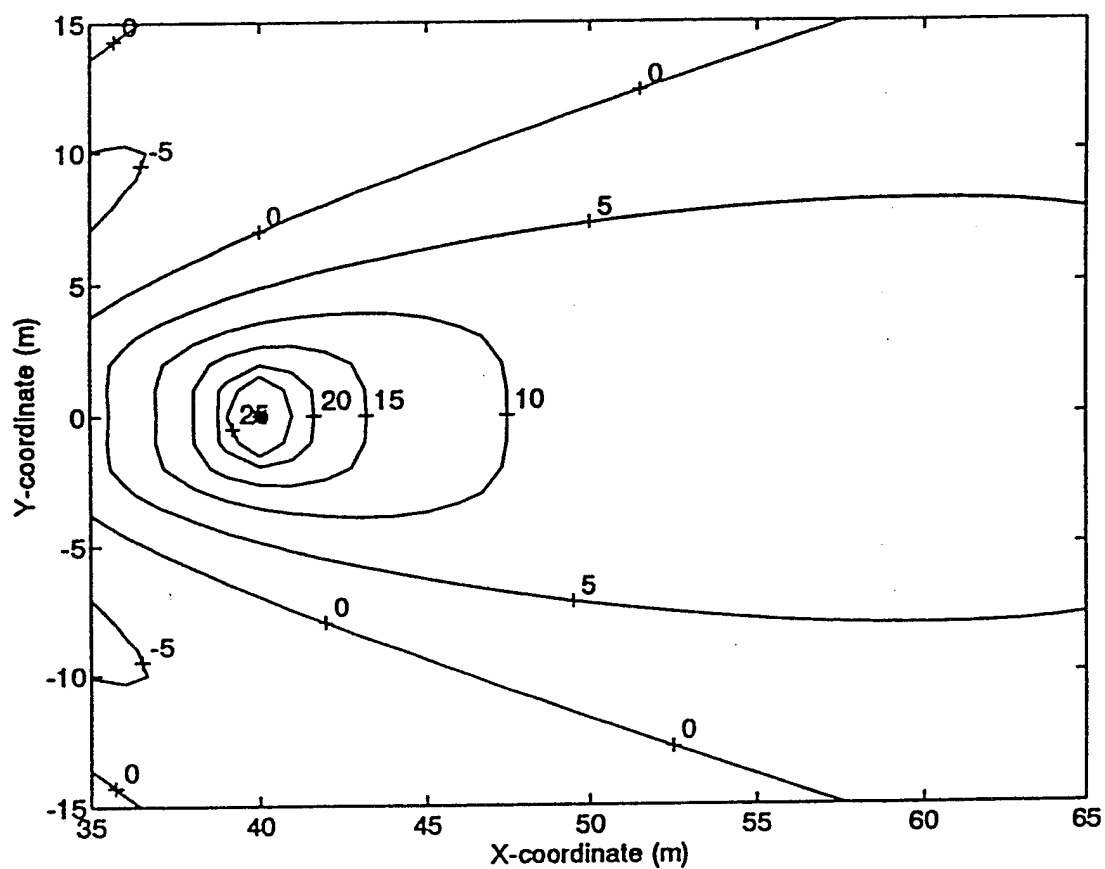


Figure 6. SPL Reduction Contours for SI-SO Control Simulation at 40 Hz With Control Source at (30,0,1)m and Error Sensor at (40,0,1)m.

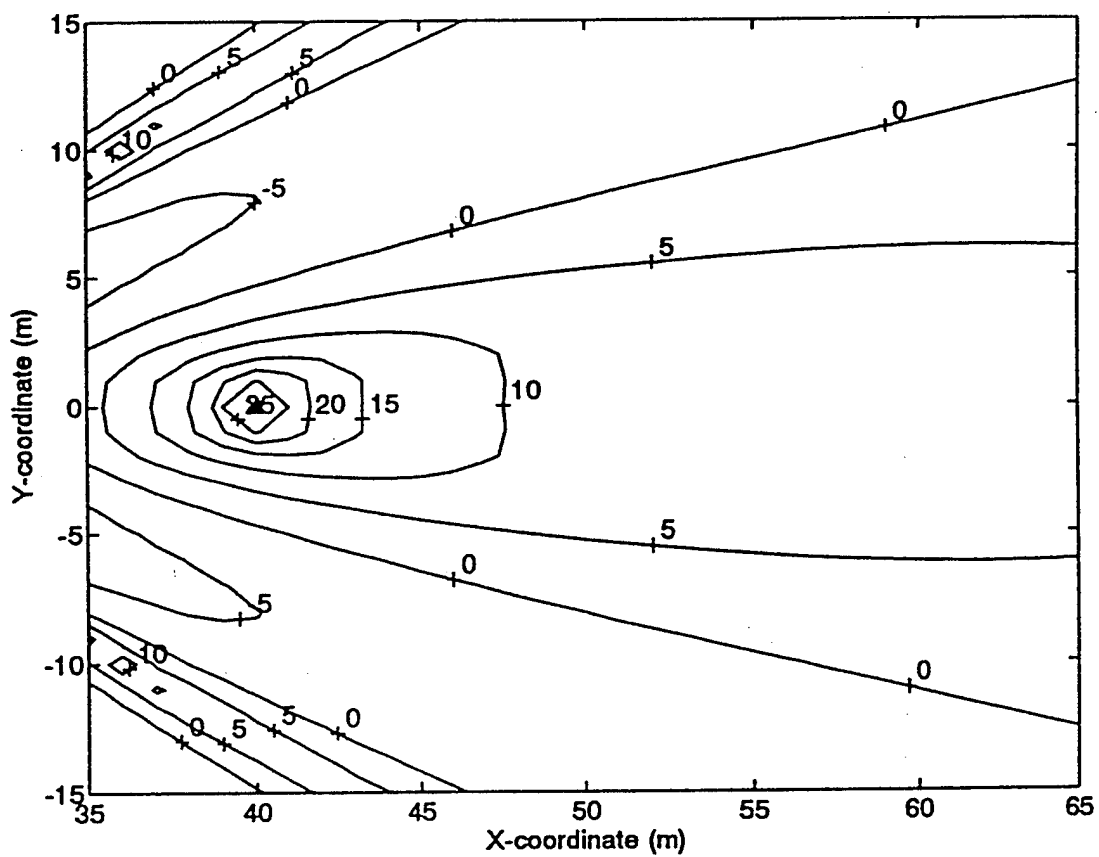


Figure 7. SPL Reduction Contours for SI-SO Control Simulation at 80 Hz With Control Source at (30,0,1)m and Error Sensor at (40,0,1)m.

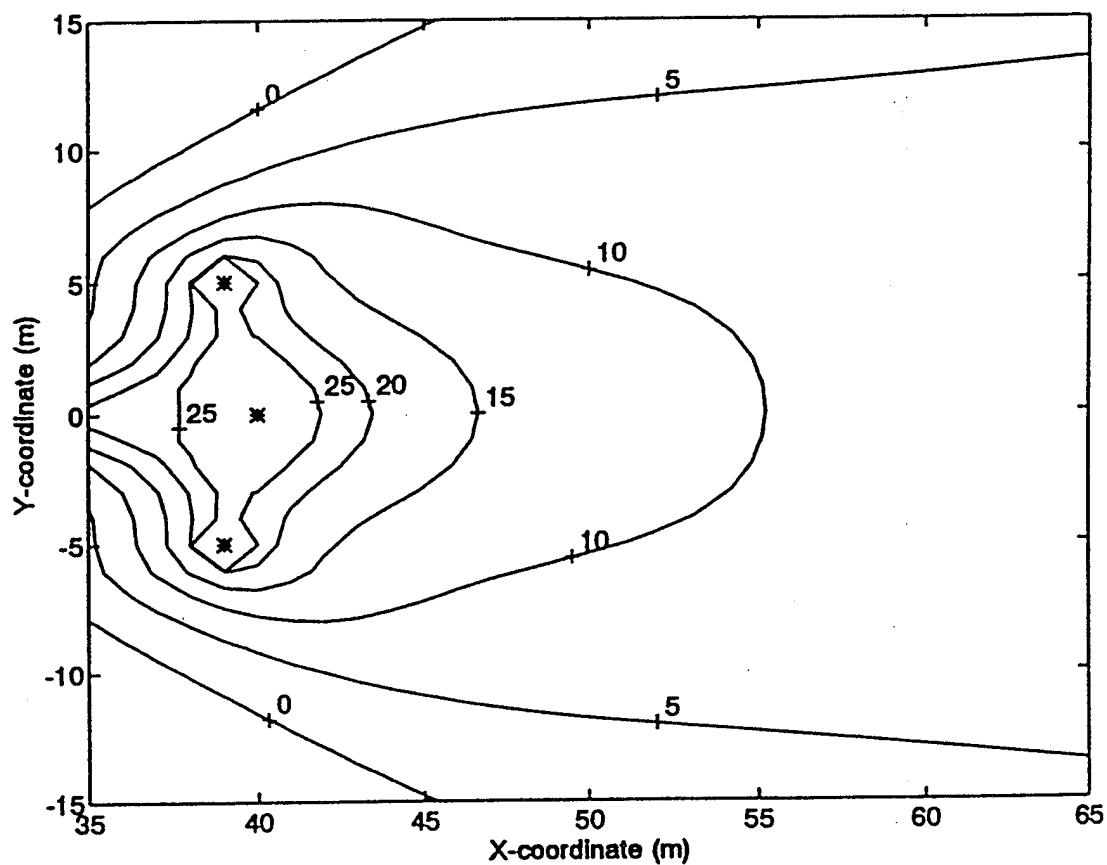


Figure 8. SPL Reduction Contours for 3I-3O Control Simulation at 40 Hz With Control Sources at (30,0,1), (30,5,1), and (30,-5,1)m and Error Sensors at (40,0,1), (39,5,1), and (39,-5,1)m.

(40,0,1), (39,5,1), and (39,-5,1) meters. Thus the control sources were positioned along a straight line perpendicular to the control axis, and the error sensors were located along a shallow arc. A contour plot showing the achieved reduction at 40 Hz is shown. As expected, the area of significant attenuation is larger with the 3I-3O system than with the similar SI-SO system (Figure 5), and attenuation of greater than 10 dB is predicted in a large area near the error sensors. The magnitudes of the control inputs were 2.2, 0.90, and 0.90 Pa, respectively. Thus the center control source contributed the most control energy.

A 3I-3O configuration with control sources again located at (30,0,1), (30,5,1), and (30,-5,1) meters with the error locations in a triangular configuration at (40,0,1), (45,5,1), and (45,-5,1) meters is shown in Figure 9. The contour plot showing the achieved reduction at 40 Hz for this case shows that the triangular error configuration resulted in a larger area of greater than 10 dB of attenuation compared with the shallow arc error configuration (Figure 8). The required magnitude of the control inputs were 1.8, 0.66, and 0.66 Pa, respectively.

A third 3I-3O case at a frequency of 40 Hz with the same control locations as the last two cases, but with the error locations at (40,0,1), (50,7.5,1), and (50,-7.5,1) meters, is shown in Figure 10. The error locations form a larger triangle than the case in Figure 9. The larger triangular error configuration resulted in more reduction and a larger area of attenuation than the system with the errors in the smaller triangular configuration, but more control energy was required. The required control magnitudes were 2.2, 0.90, and 0.90 Pa, respectively. Thus the center speaker requires most of the control energy in both of these configurations.

The effect of moving the control speakers farther apart is shown in Figure 11. The control sources were located at (30,0,1), (30,15,1), and (30,-15,1) meters. The error points were located in the large triangular formation used in Figure 10, i.e., at (40,0,1), (50,7.5,1), and (50,-7.5,1) meters. The result at 40 Hz shows that spreading out the control sources and error sensors too much can result in areas of little attenuation between the error sensors. In this case attenuation is achieved only in the proximity of each error sensor. The required control magnitudes were calculated to be 1.7, 0.43, and 0.43, respectively. Thus less control energy was required with a larger spacing of the control sources.

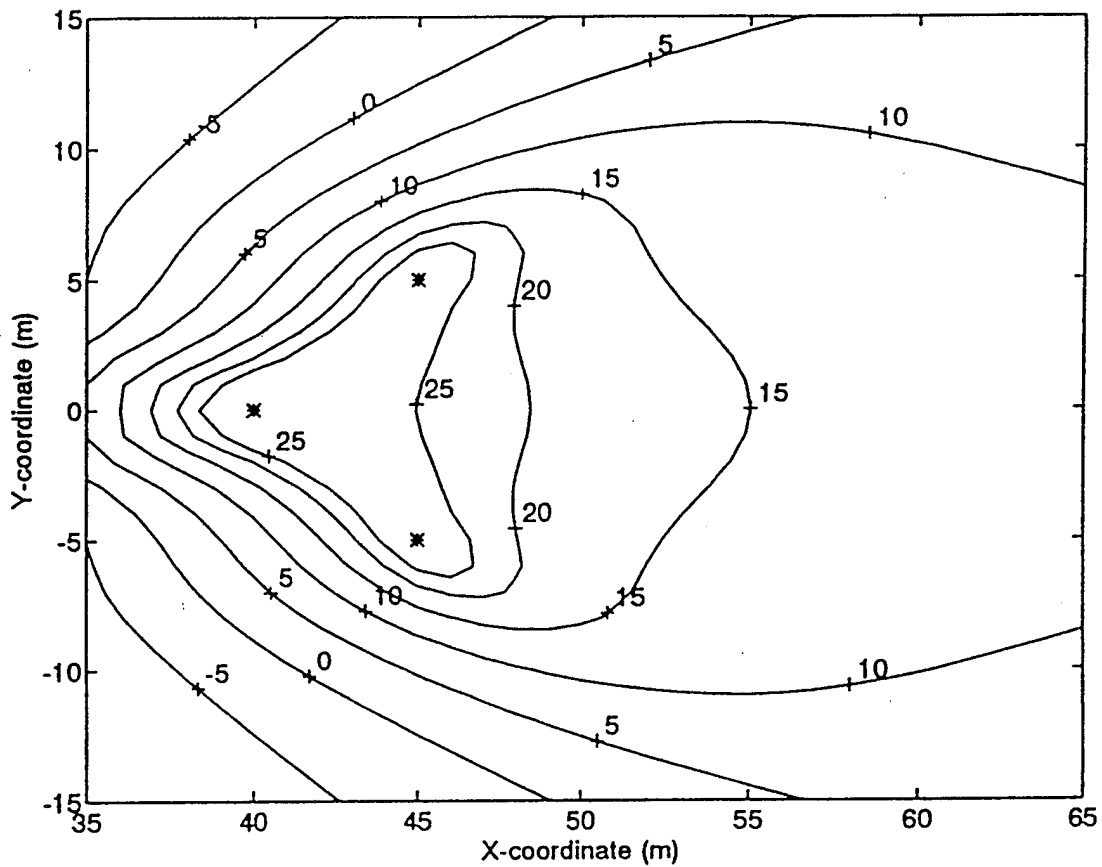


Figure 9. SPL Reduction Contours for 3I-3O Control Simulation at 40 Hz With Control Sources at (30,0,1), (30,5,1), and (30,-5,1)m and Error Sensors at (40,0,1), (45,5,1), and (45,-5,1)m.

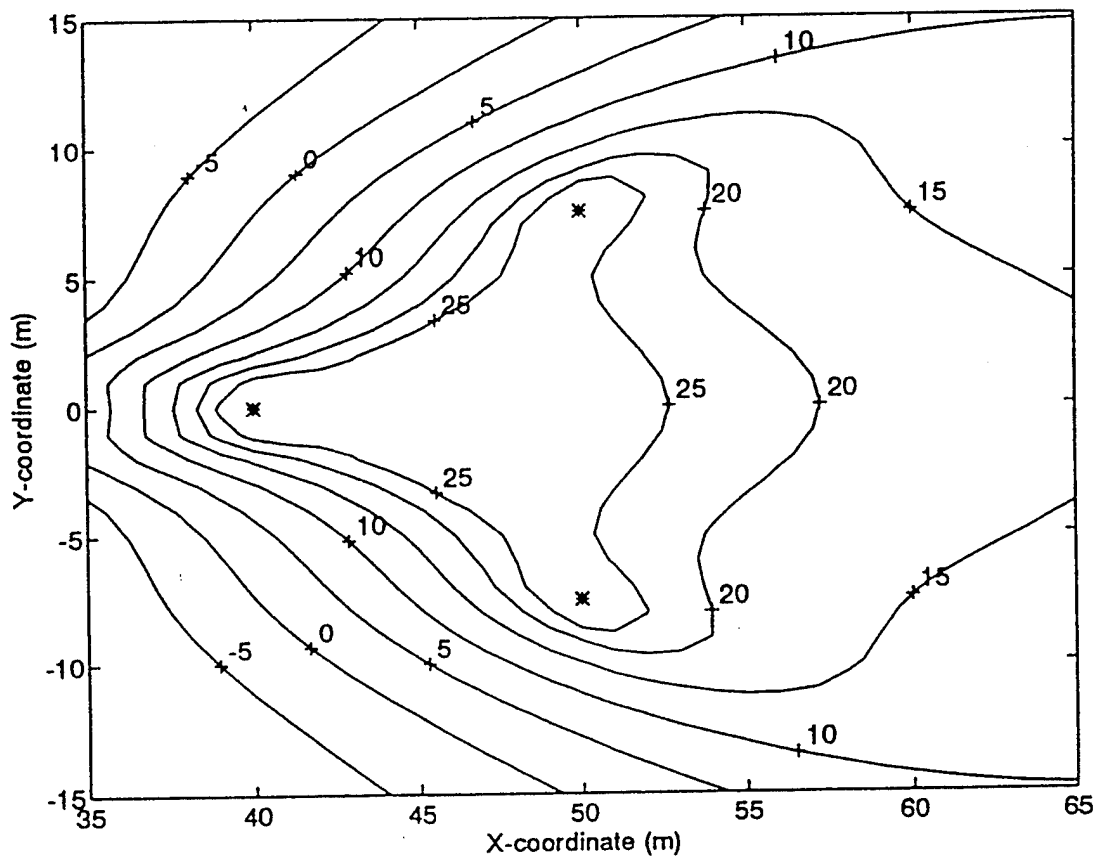


Figure 10. SPL Reduction Contours for 3I-3O Control Simulation at 40 Hz With Control Sources at (30,0,1), (30,5,1), and (30,-5,1)m and Error Sensors at (40,0,1), (50,7.5,1), and (50,-7.5,1)m.

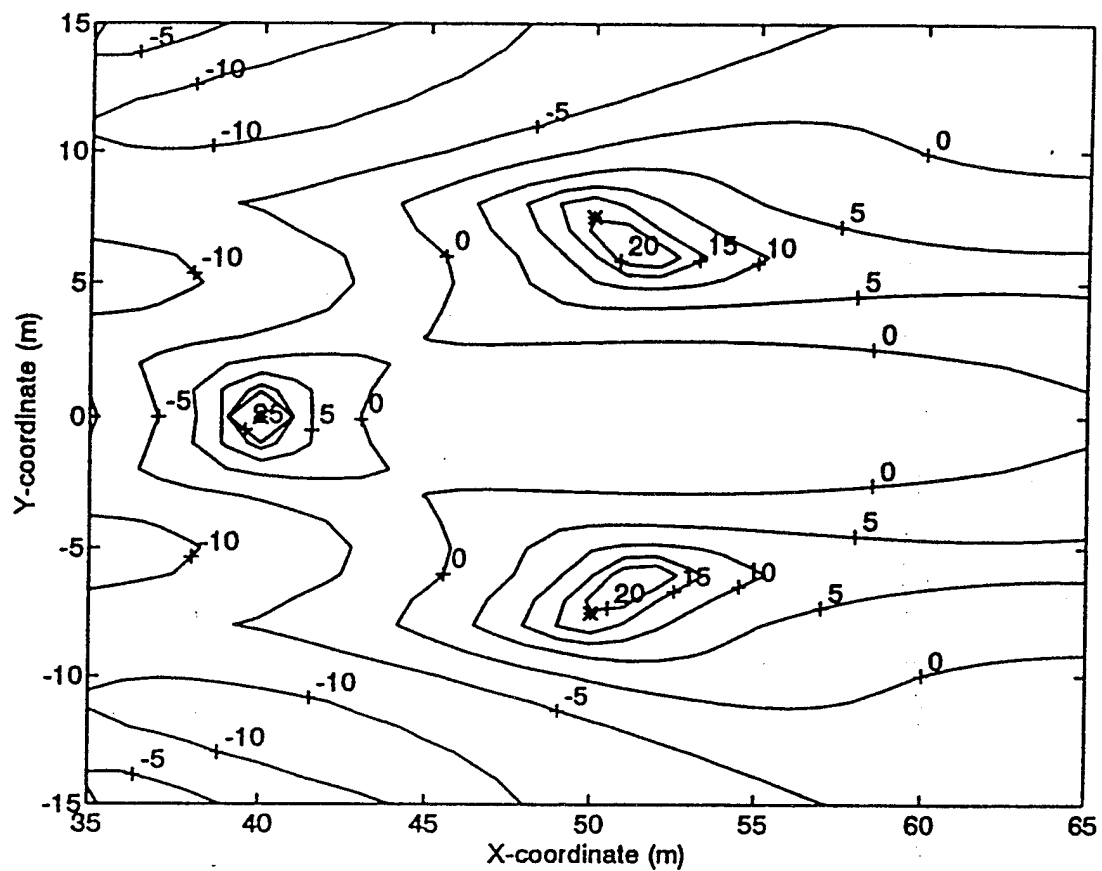


Figure 11. SPL Reduction Contours for 3I-3O Control Simulation at 40 Hz
 With Control Sources at (30,0,1), (30,15,1), and (30,-15,1)m
 and Error Sensors at (40,0,1), (50,7.5,1), and (50,-7.5,1)m.

Discussion of Results

The analytical study performed here can be used to gain insight into some of the physical aspects of an active noise control system designed for localized attenuation. The physical aspects include evaluation of the location and number of control sources and error sensors required to achieve a desired area of cancellation, the amount of attenuation potentially achievable, and the power required of the control sources.

As shown, a SI-SO configuration in general will result in a cone of sound attenuation, the point of which is approximately located at the control source position. As the frequency is increased, the cone of attenuation gets narrower and the pressure distribution can become more radically varying as a function of location due to the shortening of the wavelengths. Increasing the number of error sensors can increase the area of attenuation but generally results in less attenuation at each of the error locations. Increasing the number of control sources can increase the amount of reduction and the area of attenuation, depending on the configuration. The locations of the control sources and error sensors were found to dictate the amount of attenuation and the area of reduction. A limitation exists on obtaining a uniformly distributed area of attenuation between the error sensors when spreading out the sources and sensors in attempt to enlarge the area of attenuation.

Some control source configurations may result in the need for very powerful sources, or a very unequal distribution of control energy among the sources, which may not be practical to implement. Spreading or rearranging the sources may result in lower or more equally distributed control energy requirements, depending on the configuration of the error sensors.

Prediction of results for more than three control sources and three error sensors can yield areas of attenuation even greater than those shown previously. It is expected that in practical application, extremely large areas of attenuation may be achievable but will require a large number of control sources. An example of increasing the number of control sources is shown in Figure 12, which shows noise reduction contours at 50 Hz, using a 7I-7O system. However, in experimental implementation, limitations on maximum digital signal processing speed constrain the practical sample rate and calculation speed of the controller, and limit the control system

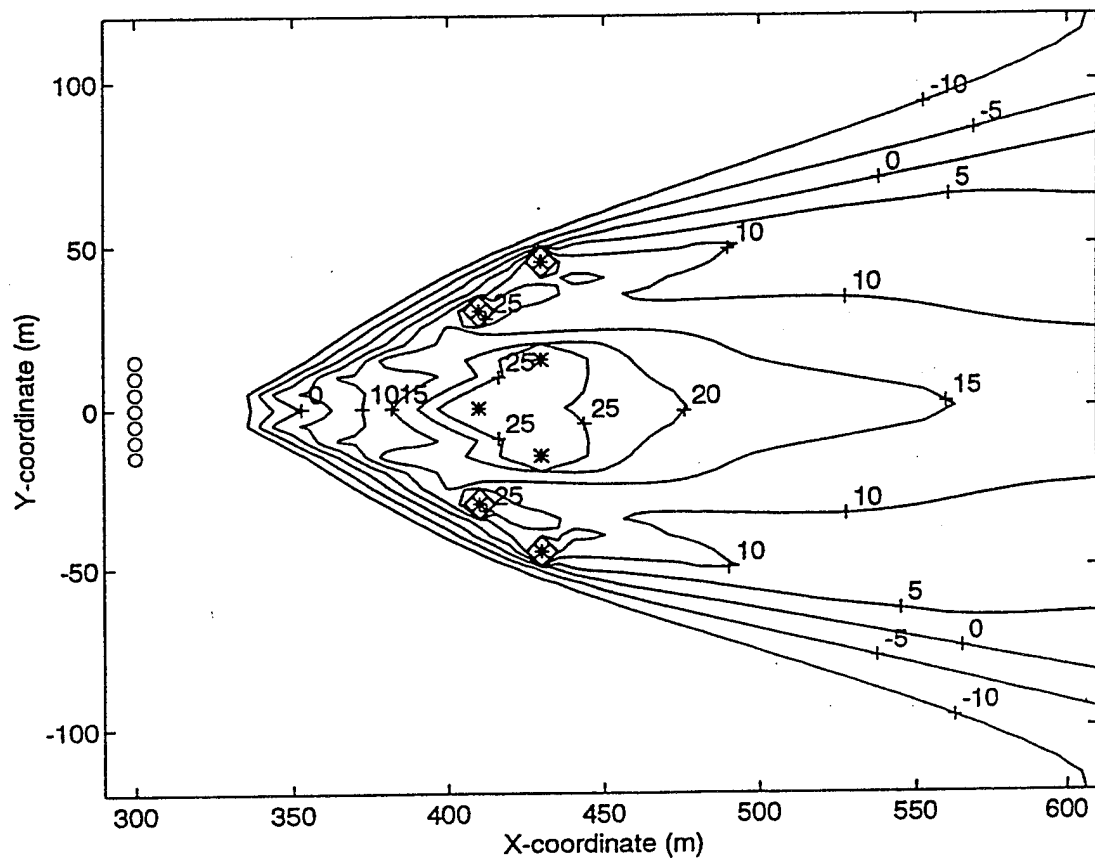


Figure 12. SPL Reduction Contours for 71-70 Control Simulation at 50 Hz.

used in this program, as described in *Adaptive Controller* and Appendix A, to 3I-3O. Nevertheless, it is possible to implement a large number of acoustic sources but simultaneously keep the number of control channels down to three by grouping the sources on each channel. Thus each channel of control could have a number of control sources, each at a different location. Furthermore, the magnitudes and phasing between the sources of a channel can be varied. For example, a single channel with three sources can have two of the sources in-phase and one source out-of-phase. In this way, the distribution of sources controlled by a 3I-3O system can be expanded, and the predicted attenuation results of configurations like this can be modeled.

EXPERIMENTAL APPARATUS AND PROCEDURES

Test Site

The experimental portion of the program was carried out at the Virginia Polytechnic Institute and State University (VPI&SU) Airport in Blacksburg, VA, which, in addition to being an active airport, is the site of the VPI&SU Mechanical Engineering Turbomachinery Laboratory (or Turbo Lab). Two areas of the airport were utilized for this study: a large, flat, grassy area adjacent to the main runway was the site of the unsuppressed jet experiments, and a smaller banked area adjacent to the Turbo Lab was the site of the simulated hush house experiments.

In the unsuppressed jet experiments, a jet aircraft was parked with its exhaust directed over the flat grassy area. A WAS 3000 noise source and a number of microphones mounted on tripods were set up on the grassy area in a direction of approximately 45 degrees off the axis of the aircraft exhaust. Because of the relatively flat terrain and the absence of large buildings, the acoustical propagation path from the aircraft across the area of study during the experiment was fairly simple.

In the suppressed jet, or engine test cell, experiments, the exhaust from a simulated hush house was directed over a small paved area immediately adjacent to the Turbo Lab building, an irregularly shaped structure approximately 16 feet high. Beyond the paved area, in the direction of the engine exhaust, is a steep bank approximately 10 feet high, covered with a few small trees, low brush, and grass. At the top of the bank is a chain link fence marking the edge of the airport property, beyond which is a two-lane paved road, not heavily used, and a slightly sloping grassy area where most of the microphones were located during the experiment. Beyond the grassy area, approximately 225 feet from the Turbo Lab, is another building, which limited the distance from the exhaust at which microphones could be placed. A photograph of the Turbo Lab building, taken from the grassy area where the microphones were placed, is shown in Figure 13. The location of the test cell can be seen toward the right of the photograph, between the tripod and the mouth of the horn. Because of the irregular terrain and reflections from the buildings, the acoustical propagation path was not an ideal free field, making the sound field somewhat more complex than that during the unsuppressed jet experiments.

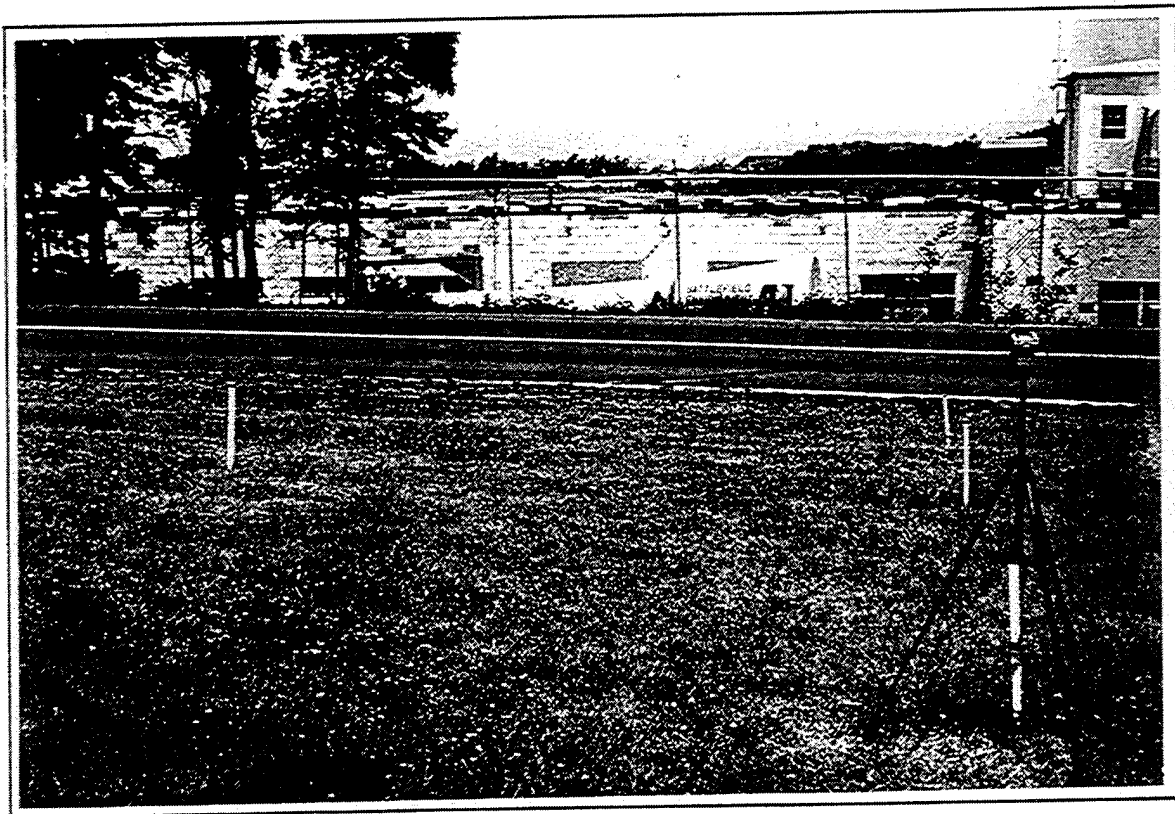


Figure 13. Photograph of the Turbo Lab and Test Cell.

Simulated Hush House

A Pratt & Whitney JT15D engine, with a bypass ratio of approximately 3.3:1, was mounted on a stand in a test cell in the VPI&SU Turbo Lab. The inlet side of the test cell is fitted with acoustically absorptive treatment. As part of this research program, the exhaust side of the test cell was modified by the addition of a lined duct as an exhaust tube, a ramp enclosed in a box as an exhaust deflector, and acoustically absorbent inlet air ducts. With these modifications, the test cell more closely approximated the exhaust and noise characteristics of an Air Force hush house, although on a much smaller scale.

The intent of the simulated hush house was to modify the jet exhaust plume in order to create a relatively compact acoustical noise source centered near the exhaust deflector. Low-frequency noise from the engine exhaust would not be attenuated significantly by the exhaust tube, although energy at higher frequencies, which was of little interest in this study, would be attenuated. It was also essential that the exhaust tube and inlet ducts should not increase the back pressure on the engine to an extent that could result in damage. Design of the simulated hush house was subcontracted to Hessler Associates, Inc., of Cabin John, MD, and construction and assembly were performed by a local contractor. A photograph of the exterior of the simulated hush house is shown in Figure 14.

The exhaust tube is 12 feet (3.66m) long with an inner diameter of 36 inches (0.914m) and contains approximately 2 inches of absorptive lining between the inner and outer walls. The exhaust enclosure fixed to the outlet of the tube is made of aluminum plates, 0.5 inch thick, and is approximately 4 feet square in plan and 6 feet high; inside this enclosure is an aluminum deflector ramp, 0.5 inch thick, set at an angle of approximately 55 to 60 degrees above the horizontal.

For safety purposes, the JT15D engine was usually operated at a running speed (in RPM) of no greater than 60 percent of its maximum. The total exhaust airflow resulting from operation at this speed is approximately 27 lbm/sec (12 kg/sec), and the core exhaust temperature is approximately 860°F.

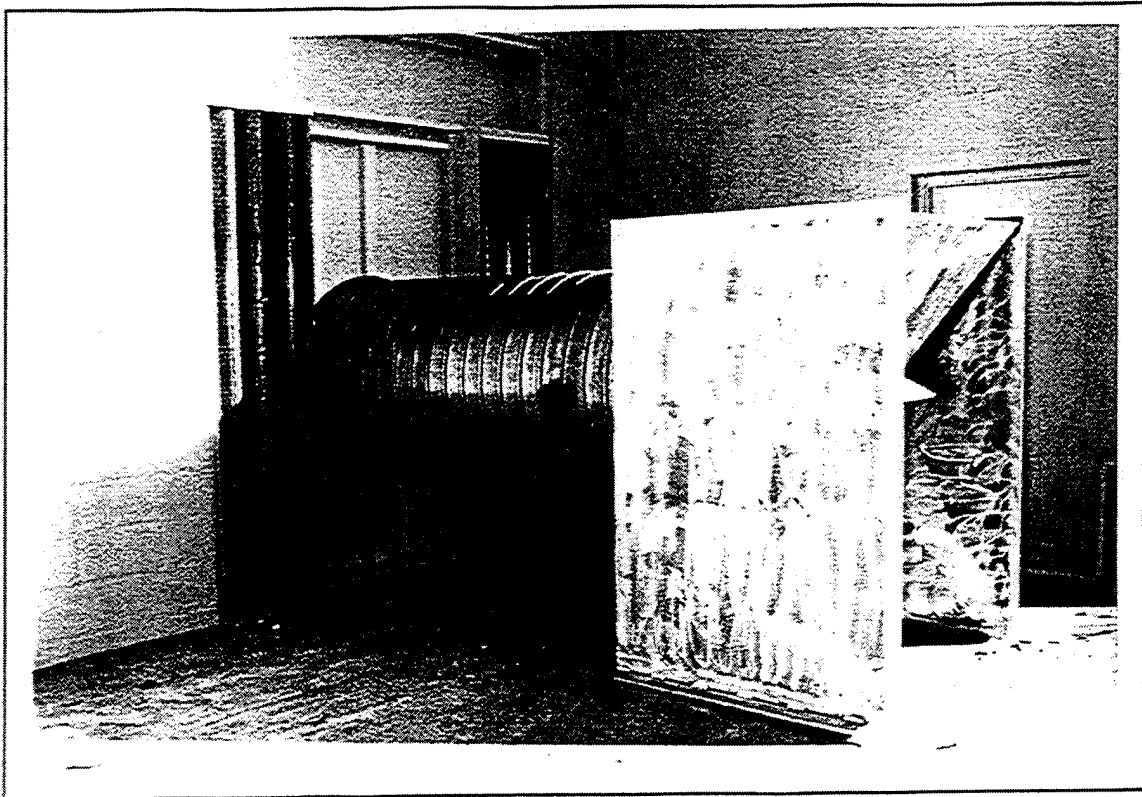


Figure 14. Photograph of the Simulated Hush House Exterior.

Unsuppressed Jet

The unsuppressed jet experiments were conducted using a Spanish-made Saeta HA-200 two-engine jet aircraft of 1950s vintage. This aircraft, which is privately owned by a pilot in the Blacksburg, VA area, was operated with both engines running at approximately 75 percent of their maximum speed during the experiments. A photograph of the aircraft is shown in Figure 15.

Electrodynamic Loudspeakers for Control

The first and simplest type of control source used in this experimental program was a conventional electrodynamic loudspeaker in a cabinet enclosure. Compact speakers of this type were used during the tests of local ANR of the simulated hush house. Advantages of this type of loudspeaker are relatively low cost, high linearity, compactness, and ease of installation. The primary disadvantage of this loudspeaker type is limited acoustic power output, particularly at low frequencies. Most standard loudspeakers, including bass drivers designed for professional applications, have frequency response curves which roll off quickly below 30 or 40 Hz, making it difficult or impossible to obtain very high output levels at very low frequencies.

Speakers from two manufacturers were used in this study. During preliminary tests, before the installation of the simulated hush house, an Electro-Voice MTL-4A speaker was used; this speaker has four low-frequency drivers in a single cabinet. In subsequent tests with the simulated hush house, Klipsch Chorus II speakers, with one low-frequency driver and one passive radiator per cabinet, were used. Both of these loudspeakers have nominally flat frequency responses down to approximately 40 Hz, with response 10 dB down at approximately 30 Hz, according to the manufacturer's specifications. The Electro-Voice speaker has flat response up to only 225 Hz, which was sufficiently high for the purposes of this study. The Klipsch speakers, which also have high-frequency and mid-range drivers, can respond up to approximately 20 kHz, although this high-frequency capability was not used in these experiments. For all of the local area control tests at the simulated hush house, the loudspeakers were placed on the ground, facing away from the hush house and reference microphone and toward the local area of interest for ANR.



Figure 15. Photograph of the Jet Aircraft Used for Local ANR Tests.

Electropneumatic Source (WAS 3000) for Control

Sound Power Output and Horn Characteristics

A WAS 3000 electropneumatic noise source, described briefly in *Use of an Electropneumatic Noise Source*, was used for local control experiments with the unsuppressed jet, and for global control experiments with the simulated hush house.

The moving cylinders of a WAS 3000 convert 3,000 cubic feet per minute (scfm) of air at 30 pounds per square inch (psig) to 30,000 acoustic watts. This maximum sound power output is equivalent to a sound power level (PWL) of 165 dB re 10^{-12} watts. To generate the maximum sound power it is necessary to match the output impedance of the WAS 3000 to the surrounding medium by means of an acoustic horn. The exponential horn is the most efficient for this purpose in terms of achieving the maximum transfer of sound power for the shortest horn length.

The dimension of the mouth of the horn determines the lowest frequency, f_1 , at which maximum power is radiated. Assuming an omnidirectional source, which is generally the case at low frequencies, this lower frequency limit is given approximately by the expression $kr = 2$, where k is the wave number, equal to $2\pi f_1/c$, c is the speed of sound in air, and r is the radius of the horn mouth. Thus, if maximum sound power radiation is required at frequencies greater than 100 Hz, the radius of the horn mouth must be 1.1 m. If the required lower frequency limit is 50 Hz, the mouth radius must be 2.2 m.

At frequencies below f_1 , the sound power radiated for a given horn mouth size decreases with the square of the frequency, so that for a horn with a mouth radius of 1.1 m, the effective PWL at 20 Hz is 14 dB less than it is at 100 Hz. Thus the maximum PWL for a WAS 3000 coupled to such a horn is 165 dB if all the energy is concentrated at 100 Hz, but only 151 dB at 20 Hz.

The sound levels produced by the WAS 3000 at any given location are dependent on the sound power output (PWL) and the distance from the source. Setting aside for the moment the effect of ground and air absorption (which will be the same for both the disturbance and control sources), the sound pressure level, SPL, as a function of distance, d , is normally given by the expression:

$$\text{SPL} = \text{PWL} - 20 \log(d) - 8, \text{ dB}$$

where d is measured in meters. Thus, with a 1.1 m radius horn, the WAS 3000 will produce a maximum sound level of about 117 dB at 100 meters for energy concentrated at frequencies above 100 Hz. For energy concentrated at 20 Hz, the same configuration will produce a maximum level of 103 dB.

Comparison of the potential WAS 3000 sound levels with hush house noise levels indicates that the WAS 3000 may be suitably powerful to serve as a global control source, provided a sufficiently large horn is installed. Noise levels measured at various U.S. Air Force hush houses indicates levels at around 20 Hz in the range of 90 to 105 dB at 100m, depending on the aircraft and engine operating mode.

Mobile Acoustic Source

An existing installation of a WAS 3000 system, mounted on a portable platform, property of the U.S. Army Research Laboratory's Battlefield Environment Directorate in White Sands, NM, was used in this program. This apparatus, known as the Mobile Acoustic Source (MOAS), was designed and assembled at the Jamie Whitten National Center for Physical Acoustics at the University of Mississippi.^{17,18}

The MOAS consists of a WAS 3000, along with all the hardware required for its operation, mounted on a flatbed truck. The MOAS system includes an exponential horn, designed to have a lower cutoff frequency of 10 Hz; the horn is 56 feet (17.1m) long, with a mouth radius of 46 inches (1.17m), and is connected to a WAS 3000. Airflow is provided by a rotary lobe blower, manufactured by the German firm Aerzen, powered by a 130 HP (97 kW) six-cylinder diesel engine. The air leaving the compressor passes through an electric heat exchanger to be cooled before entering the WAS 3000. A microcomputer is also installed on the truck to enable communication with a remote operator and to monitor operational parameters.

The MOAS was designed to produce up to 20 kW of acoustic power (163 dB) by providing airflow of up to 1800 cfm at 10 psi to the WAS 3000. While this is not the maximum output of the WAS 3000, it was judged to be sufficient for the purposes of the application, particularly when used with the horn capable of high output down to 10 Hz.

Arrangements were made to borrow the MOAS system for use at VPI&SU and to transport it from New Mexico to Virginia and back. The MOAS was operated during the experiments by technicians from the Physical Science Laboratory, New Mexico State University, Las Cruces, NM, and the U.S. Army Research Laboratory, White Sands, NM.

Performance Characteristics

The sound output of the MOAS is determined by the air pressure supplied to the WAS 3000 and the electric current supplied to the modulator coil. Air pressures in the range of approximately 1.5 to 10 psig and currents in the range of approximately 0 to 10 amps (rms) are available and can be selected independently, depending upon the sound output required.

Sound output level, directivity characteristics, and harmonic distortion of the MOAS have previously been assessed at a variety of operating points.^{18,19} Additional data from the MOAS were measured and analyzed during the early part of this program to assess the input-to-output coherence of the WAS 3000. Based on this preliminary coherence data, the MOAS was judged to be a good candidate as a control source for the reduction of hush house noise.

Adaptive Controller

The hardware which comprised the adaptive controller included a digital signal processing board installed in an Intel 80386-based microcomputer. The control algorithm was implemented on a Texas Instruments TMS320C30 digital signal processing (DSP) board equipped with expansion boards to allow 3-input, 3-output control. The codes used to operate the DSP were written in "C" language with embedded assembly code instructions. The user interface codes implement MATLAB software to allow the user to execute or halt the controller, set the sampling rate, and adjust the parameters that dictate convergence and control.

The control algorithm used an adaptive Finite Impulse Response (FIR) filter as the controller. System identification was performed before each test, using either a FIR or an Infinite Impulse Response (IIR) filter. A feedback removal algorithm could be implemented if necessary. For a description of the algorithm in more detail, refer to Appendix A.

Reference Signal

The reference signal for the ANR experiments was provided by a Bruel & Kjaer Type 4134 1/2-inch microphone, mounted on a tripod, and equipped with a foam windscreen to reduce the wind-induced signal content. The reference signal was band-pass filtered using an Ithaco filter with rolloff characteristics of 24 dB/octave, and amplified using a single channel of a Ithaco Model 455 amplifier before being input to the controller. The filtering was performed to restrict the signal content to the bandwidth of interest, and cutoff frequencies were chosen based on the requirements of each experiment.

For each test, the reference microphone location was chosen based on geometric considerations (as discussed in *The Importance of Reference and Error Signals* and *Summary of Local and Global ANR Implementation*) so as to minimize feedback from the control source and to provide an accurate representation of the propagating noise. For each candidate reference microphone location, the coherence function was measured between the reference microphone and an error microphone in the area of interest in the far field; some fine tuning of the reference location was performed in order to maximize the coherence. In general, the greater the coherence between the reference and error microphone signals, the greater the achievable attenuation.

Attempts were made to identify alternative signals which would provide an adequate reference, particularly for use in global control, where a microphone outside the exhaust airflow was susceptible to feedback from the control source. These attempts included accelerometers mounted at various locations on the jet engine, exhaust tube, deflector plate, exhaust box, and surrounding structure. However, coherence between acceleration and far-field noise was generally poor.

Microphones in the exhaust duct were also tried as reference sensors in a number of configurations. An array of microphones was mounted through holes drilled in the outer wall of the exhaust duct so that acoustic pressures were measured behind the absorptive liner of the duct; in this manner, flow over the microphones was minimized. Signals could be used singly or added together in an attempt to find a coherent reference, but the results were not successful. In a further test, a microphone was mounted at the end of a metal tube with a slit cut along its length; the tube was wrapped with cloth and the far end of the tube terminated in a streamlined nosecone. This method has been described in a number of references as a successful technique for measuring acoustic noise in flow.^{20,21,22} However, the results of these tests did not result in good coherence with the far field, most likely due to the high flow speed in the jet exhaust.

Microphones located near the exhaust deflector, on top of the lab building, inside the test cell, and at other locations were tested for coherence with the far-field microphones. Microphones located near the rear of the deflector resulted in relatively good coherence compared to other sensors in the near field of the source; however, these were not as good as the results obtained with the reference microphone located at the top of the bank, or hill, colinear with the exhaust deflector and the far-field error microphone. This is the location used for the reference microphone in the majority of the tests at the hush house site.

For the unsuppressed jet engine experiments, a reference microphone was located approximately 15m from the jet engine exhaust, roughly in the direction of the WAS 3000 control source and the error microphone.

Error Signal

Microphones were used to provide the error signals. A microphone is a logical choice since it provides directly the quantity to be minimized (i.e., sound pressure level) at a single point in space. The error signals were provided by Bruel & Kjaer Type 4134 and Type 4166 1/2-inch microphones mounted on tripods at some distance from the exhaust noise source. The signals from the error microphones were band-pass filtered with Ithaco 24 dB/octave filters, and each amplified with a single channel of an Ithaco Model 455 amplifier before being input to the controller.

Each test was conducted with either one or three error microphones. At the simulated hush house facility, one of the error microphones was located approximately 40m from the jet engine exhaust (point E in Figure 5). When three error microphones were in use, they were arranged in a line or a triangle near point E.

For the unsuppressed jet experiments, the error microphone was placed approximately 115m from the jet exhaust at an angle of 45 degrees off the exhaust axis.

Assessment of Noise Reduction

The results of ANR over the area of interest were evaluated by placing a 1/2-inch microphone mounted on a tripod at a number of predefined locations in an array, and performing a Fast Fourier Transform (FFT) frequency analysis of the noise over a period of approximately 5 seconds, using a B&K 2032 spectrum analyzer. When each analysis was completed, the 800-line spectrum was stored in a computer file, the microphone was moved to another location, and the process was repeated. Since the engine noise and controller output were stationary in time, it was not necessary to record the microphone signals at all the positions simultaneously. For most of the tests, measurements were made first at all the locations with the controller on, and then again at all locations with the controller off, or vice versa. However, for one or two tests during which it was somewhat windy, measurements were made at a single location with the controller first off and then on before moving to the next location, so that wind speeds would be similar in the two tests at each location.

Following acquisition and storage of the data, the spectra were further analyzed, including synthesis into one-third octave bands, via software operations.

EXPERIMENTAL RESULTS

In this section, experimental results are shown in a variety of graphical formats. Experimental configurations are shown in schematic drawings depicting overhead views of system components. Results of noise levels before and after active noise reduction are presented in graphs of narrowband spectra, showing sound level data in bandwidths of constant frequency, and in graphs of one-third octave spectra. All spectra are unweighted, with levels in decibels re 20 μ Pa. Noise reduction from the uncontrolled case to the controlled case is calculated in one-third octave bands, both for the error microphone and for microphones in an array in the far field. The noise reduction values in a particular one-third octave band are shown in contour plots over the microphone array; lines connect points of constant noise reduction. Values of total reduction, representing the overall difference in the unweighted noise levels integrated over the bandwidth, were also calculated and are shown on contour plots.

Also shown are coherence functions, measured to evaluate both the quality of the reference signal (reference to error coherence) and the quality of the control source output (source input and output coherence). A knowledge of the coherence values as a function of frequency helps in understanding and interpreting the results of the active noise reduction experiments.

Local Active Noise Reduction

Preliminary Experiments on the Unsuppressed JT15D Engine

A preliminary ANR experiment, before the hush house assembly was constructed, was performed using the unsuppressed JT15D engine. Microphones were used as the reference and error sensors, and the control speaker was a single Electrovoice MTL-4A low-frequency loudspeaker.

A single-input, single-output (SI-SO) control system (one error microphone and one control source) was implemented, with the locations of the reference microphone, the error microphone, and the control loudspeaker as shown in Figure 16. The error microphone was located 40m from the jet engine exhaust nozzle, along the axis of the engine. The control speaker was also located along the engine axis at a distance

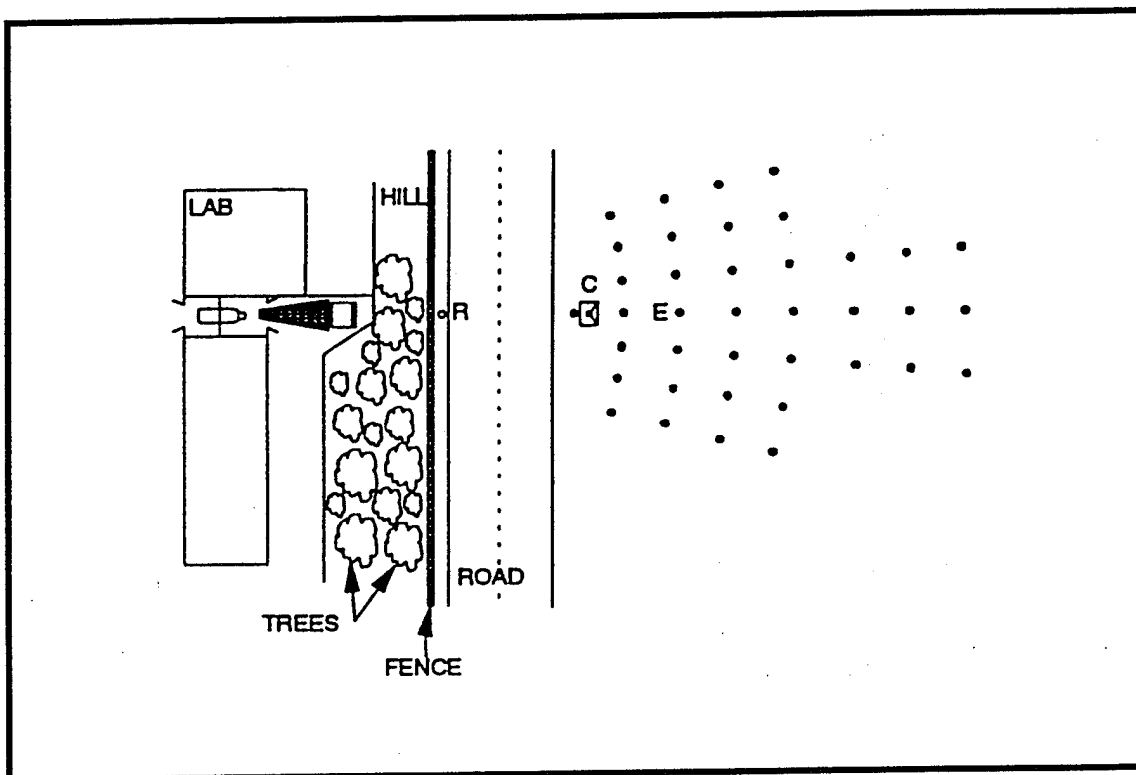


Figure 16. Configuration for SI-SO Local ANR of the Unsuppressed JT15D Engine.

of 30m from the engine exhaust. The reference microphone, R, was located at the top of the hill, on the axis of the engine in line with the control speaker and error microphone, about 15m from the engine exhaust. The locations to the right in the far field indicate microphone positions in an array.

The error, reference, and control output signals were bandpass filtered between 40 and 160 Hz. This range was dictated by limitations on the speaker output, and thus defined the frequency range of interest for ANR. The adaptive control FIR filter used 100 coefficients, and the system identification IIR filter, performed off-line, contained 50 numerator coefficients and 50 denominator coefficients, corresponding to 50 poles and 50 zeros. The sample rate of the controller was 800 Hz, and the controller was allowed to converge for approximately 60 seconds. Error microphone spectra and noise spectra at each of the field points in Figure 16 were obtained before and after control.

Figure 17 shows one-third octave band spectra at the error microphone before and after control. The total reduction of the error signal, integrated over the 40 to 160 Hz bandwidth, was 8.2 dB. Good reduction of the error signal is evident over the controllable frequency range, especially where the error signal was highest before control. Reduction in the 50 Hz one-third octave band was about 11 dB. Figure 18 contains a contour plot of the total SPL reduction over the field points, and Figure 19 contains a contour plot of the SPL reduction in the 50 Hz one-third octave band. Note that the scale in these plots is somewhat distorted, since the contour plot is in rectangular coordinates and the field point data were obtained in a polar coordinate system. This is the only experiment for which the polar field point matrix was used, and therefore these are the only distorted contour plots in this report. A considerable area of reduction around the error sensor is evident.

Simulated Hush House

A series of local ANR tests, using conventional loudspeakers as control sources, was performed on the JT15D jet engine in the simulated hush house described earlier. Both single-input, single-output (SI-SO), and three-input, three-output (3I-3O) tests were conducted.

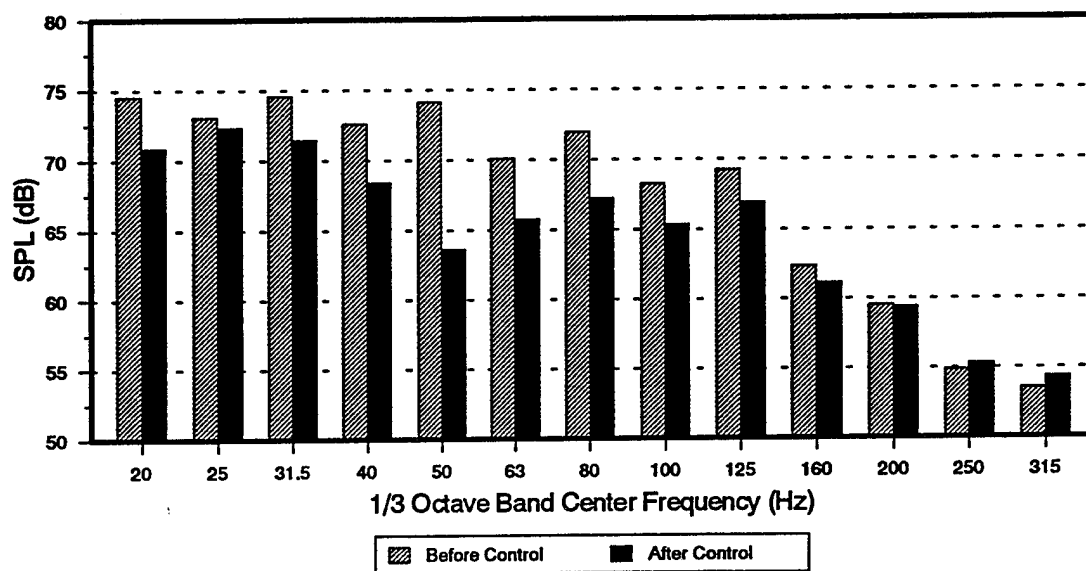


Figure 17. Error Signal One-Third Octave Band Analysis, SI-SO Local ANR of Unsuppressed JT15D Engine.

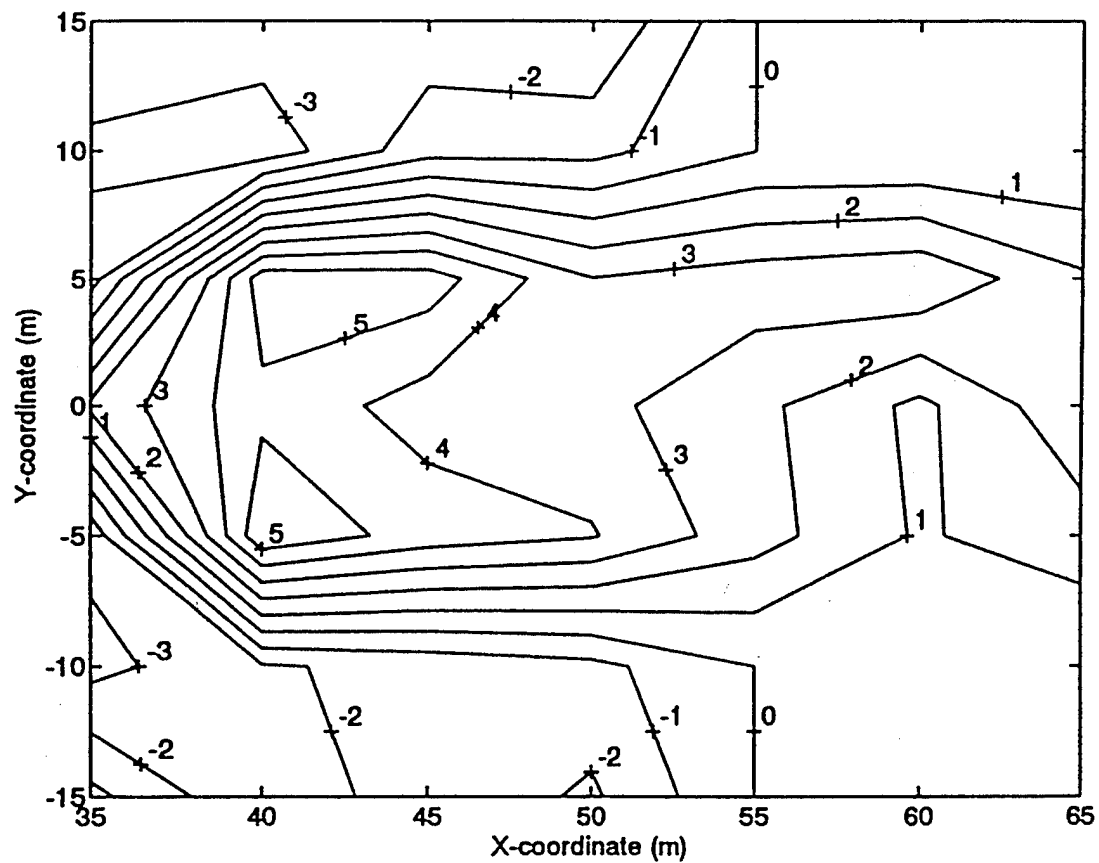


Figure 18. Total SPL Reduction Contours, SI-SO Local ANR of Unsuppressed JT15D Engine; Control Source at (30,0)m and Error Microphone at (40,0)m.

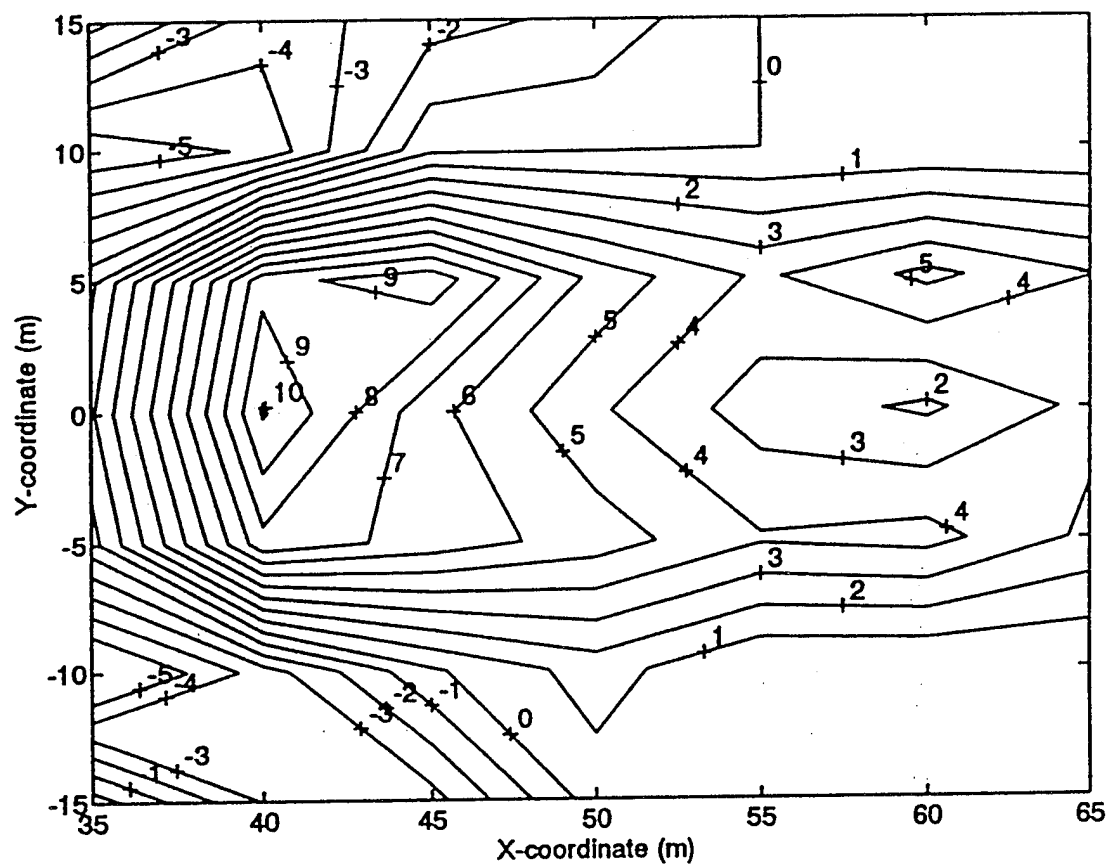


Figure 19. SPL Reduction Contours in 50 Hz One-Third Octave Band, SI-SO Local ANR of Unsuppressed JT15D Engine; Control Source at (30,0)m and Error Microphone at (40,0)m.

Single-Input, Single-Output Configuration

For the SI-SO experiment, microphones were used as the reference and error sensors, and the control source was a single Klipsch Chorus II loudspeaker. A SI-SO control system was implemented, with the locations of the reference microphone, the control loudspeaker, and the error sensor as shown in Figure 20. The loudspeaker was 30m from the jet engine exhaust nozzle, and the error sensor was 40m from the engine exhaust, both along the exhaust tube axis. The reference sensor was located approximately 14m from the engine. Note that the field points are in a rectangular pattern, 30m x 30m, with 5m spacing between points, which allowed for easier post-processing of the data.

The control, error, and reference signals were bandpass filtered between 25 and 250 Hz, defining the controllable bandwidth of interest. The adaptive control FIR filter used 100 coefficients, and the sample rate was 800 Hz. The system identification was performed on the DSP board with an FIR filter containing 200 coefficients. The controller was allowed to converge for approximately 60 seconds.

The coherence between the reference microphone and the error microphone with the engine running is shown in Figure 21. Although the coherence shown here is not ideal (less than 0.9 across most of the band), this represents one of the most coherent reference locations obtained with any sensor or reference microphone position at the hush house test location. The dips in the coherence may be due to the complex geometry around the source (laboratory building, hill, etc.) and resulting reflection, multipath, or propagation effects, which would probably not be present in a real hush house situation. As can be seen in the figure, the coherence between the reference and error microphones is best below about 100 Hz.

During the controller's system identification process, white noise was input to the control loudspeaker. The coherence between the white noise signal into the speaker and the error microphone signal is shown in Figure 22. This figure represents the input to output coherence of the loudspeakers, taking into account the acoustical propagation path from control source to error microphone in the far field. The coherence of this speaker is seen to be good across the controllable frequency range of interest, and very good, greater than 0.95, between 60 and 250 Hz.

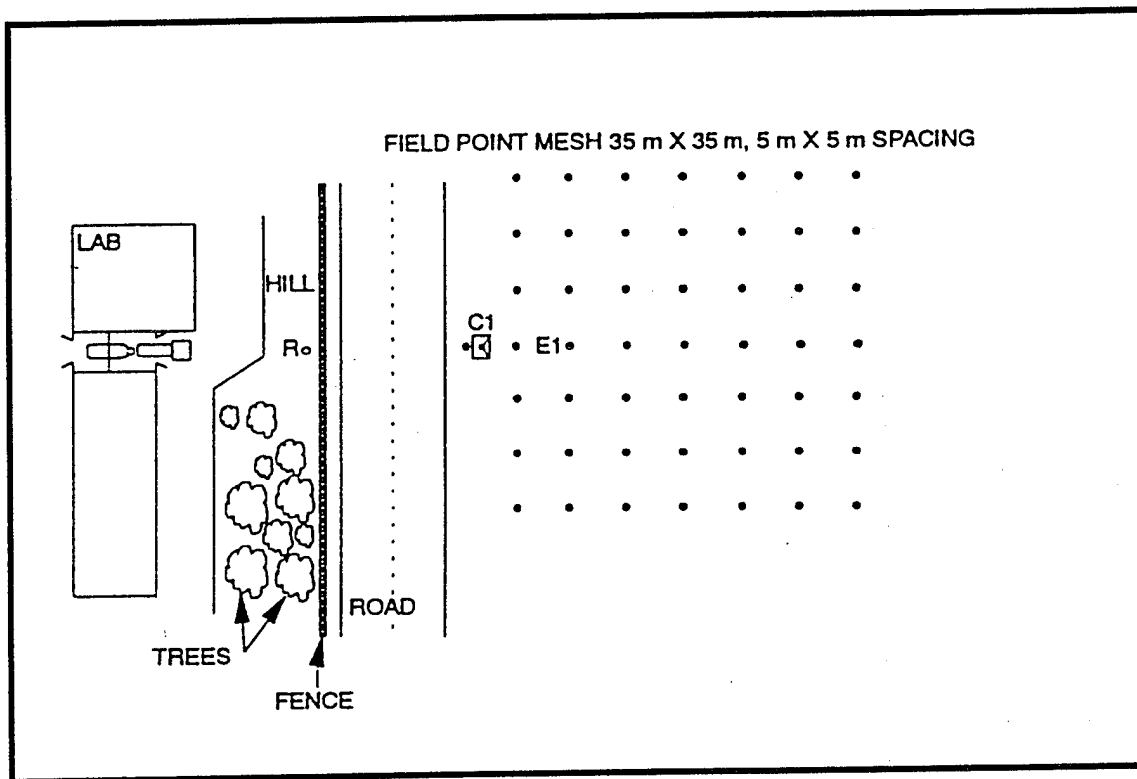


Figure 20. First Configuration for SI-SO Local ANR of the Simulated Hush House.

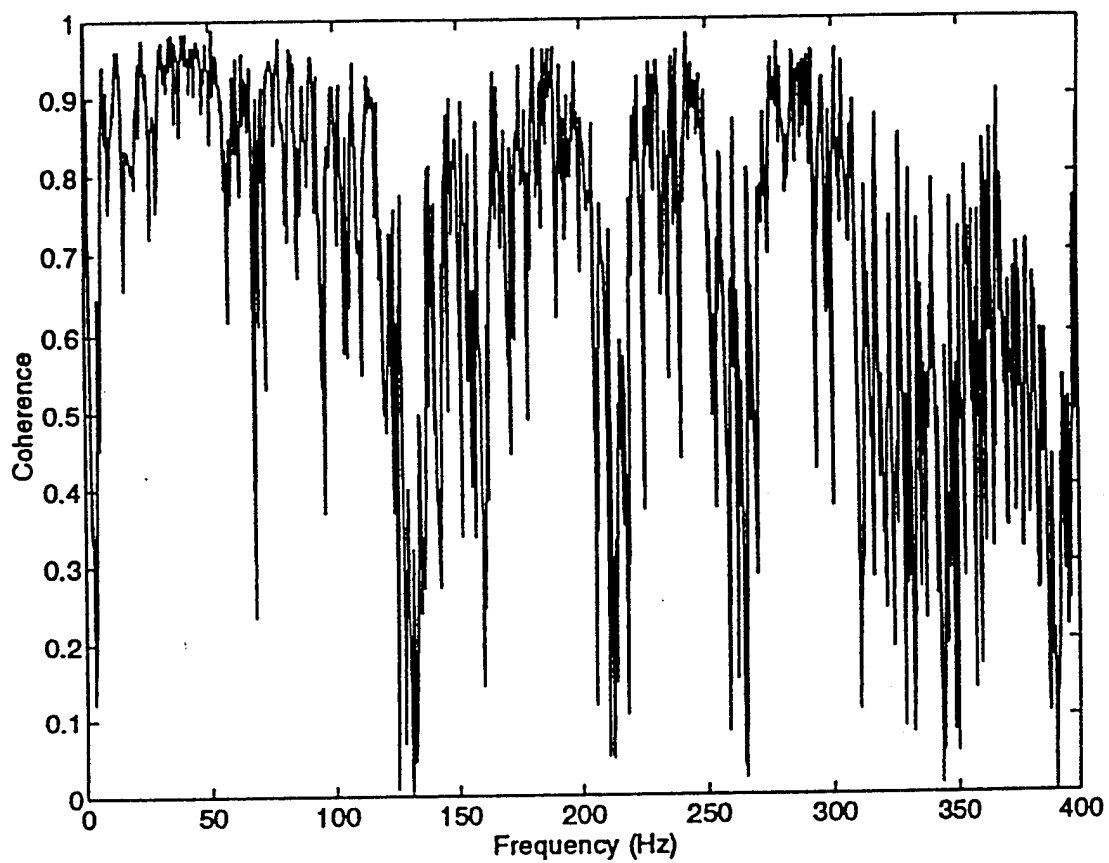


Figure 21. Coherence Between Reference Microphone and Error Microphone, SI-SO Local ANR of Simulated Hush House.

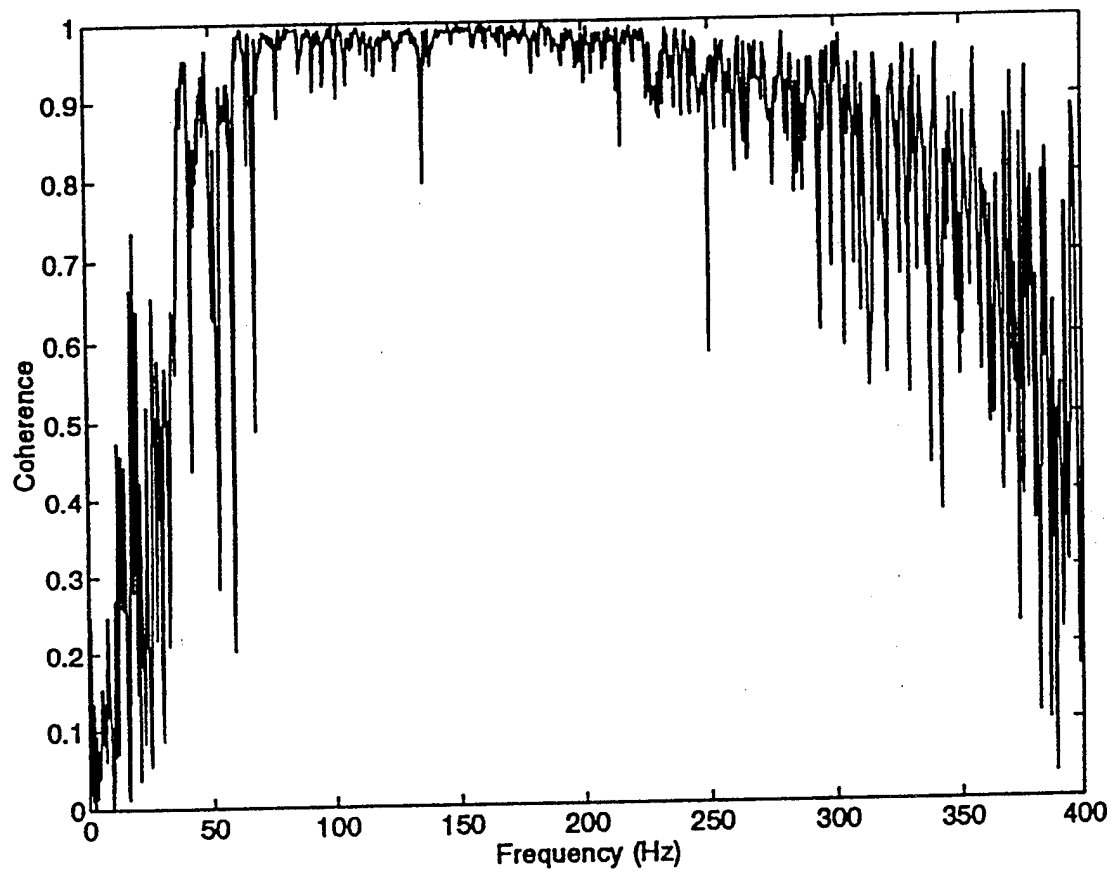


Figure 22. Coherence Between Input to Control Loudspeaker and Error Microphone, SI-SO Local ANR of Simulated Hush House.

Figure 23 contains a plot of the error microphone narrowband spectra, before and after control. The total reduction at the error microphone, integrated over the 25 to 250 Hz bandwidth, was 7.2 dB. Broadband control is clearly achieved across the frequency range of interest, and the amount of reduction is largest where the level before control is highest. The reduction starts diminishing below about 35 Hz, which is below the designed operating range of the speaker. One-third octave band levels at the error microphone are shown in Figure 24. Reductions on the order of 10 to 13 dB were obtained in the one-third octave bands which had the highest levels before control. There is even some reduction evident in the 25 Hz one-third octave band, which is below the designed operating range of the speaker.

Figures 25, 26, and 27 contain contour plots over the 30m x 30m field point matrix, of the total SPL reduction, and the SPL reduction in the 40 Hz and 80 Hz one-third octave bands, respectively. Again a considerable area of reduction is achieved around the error sensor, even with only a SI-SO control system. A "cone" of reduction emanating from the control source location is apparent with the SI-SO experiments, as predicted by the analytical model. Note that the origin of the contour plots for the simulated hush house tests is at the same location as for the tests on the unsuppressed jet and for the analytical model, at the exhaust of the jet engine.

Another SI-SO experiment was performed with microphones again used as the reference and error sensors, and two adjacent speakers driven in parallel with the same signal, making up a single control source. The locations of the reference microphone, the control loudspeakers and the error sensor are shown in Figure 28. This experiment is similar to the previous SI-SO experiment presented, with the exception of the locations of the control source and reference sensor, and the strength of the control source. The control speakers were located at the top of the hill at approximately 17m from the engine exhaust. Note that this is closer to the disturbance source than for the previous test (shown in Figure 20). The reference microphone was located at the bottom of the hill, approximately 7m from the engine. This configuration utilizes a larger spacing between the control source and error sensor, which is why two speakers were used in order to provide more acoustic power in the control source.

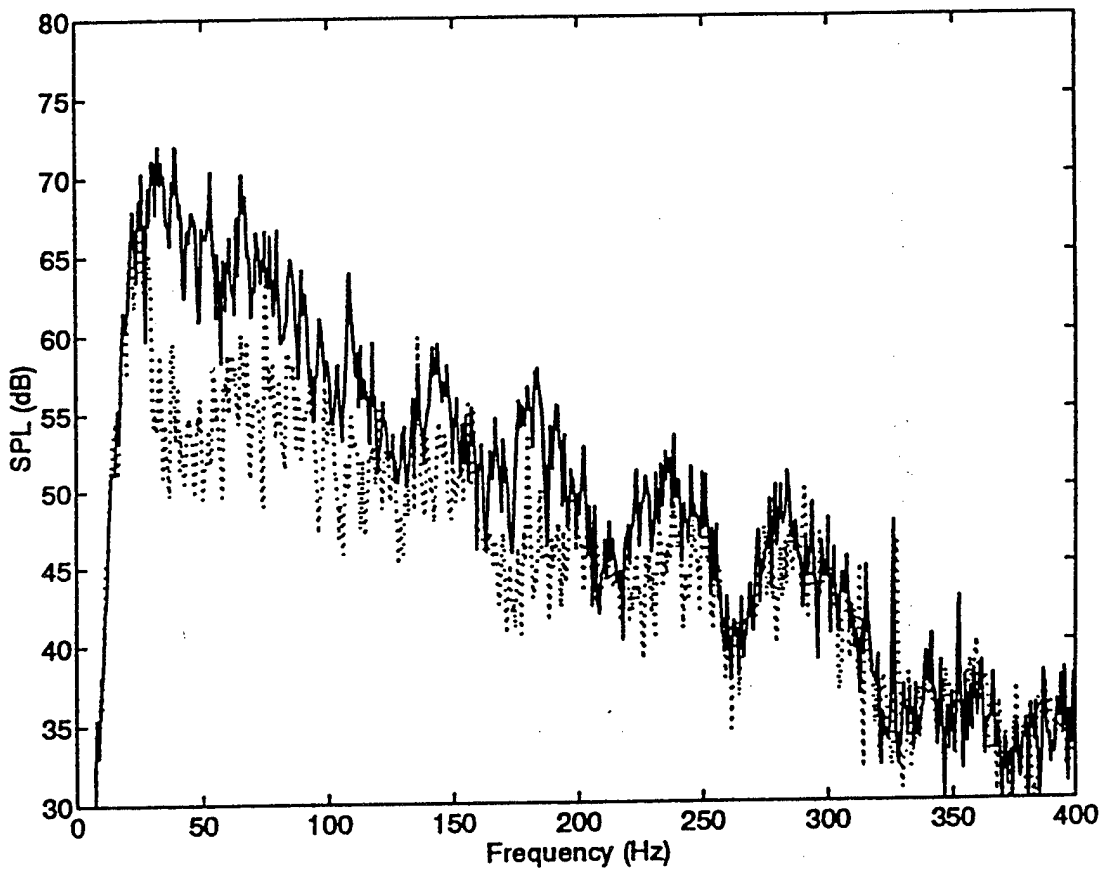


Figure 23. Error Microphone Spectra, SI-SO Local ANR of Simulated Hush House.
—— before control; after control.

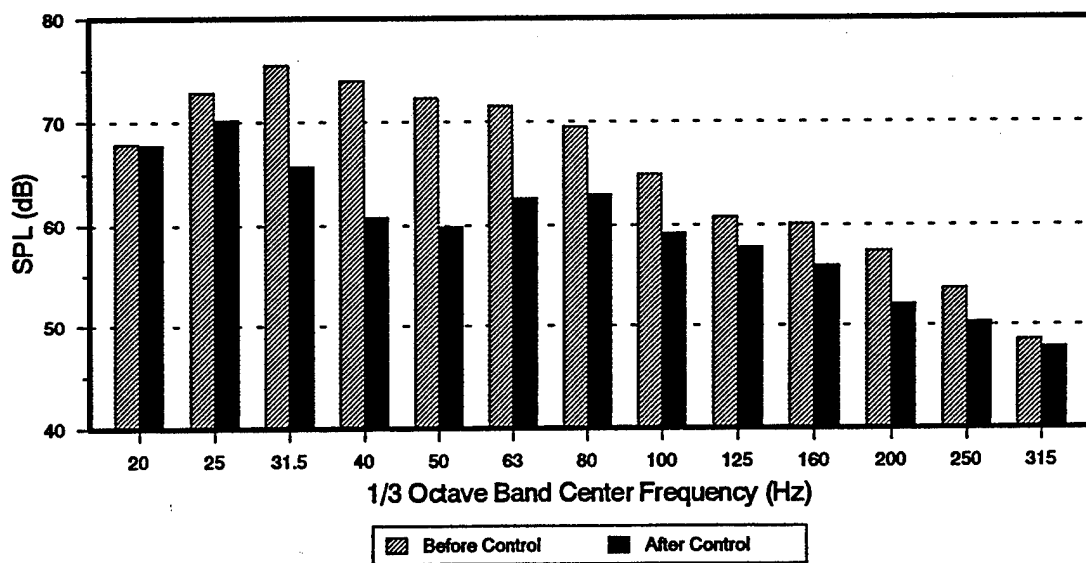


Figure 24. Error Microphone One-Third Octave Band Analysis, SI-SO Local ANR of Simulated Hush House.

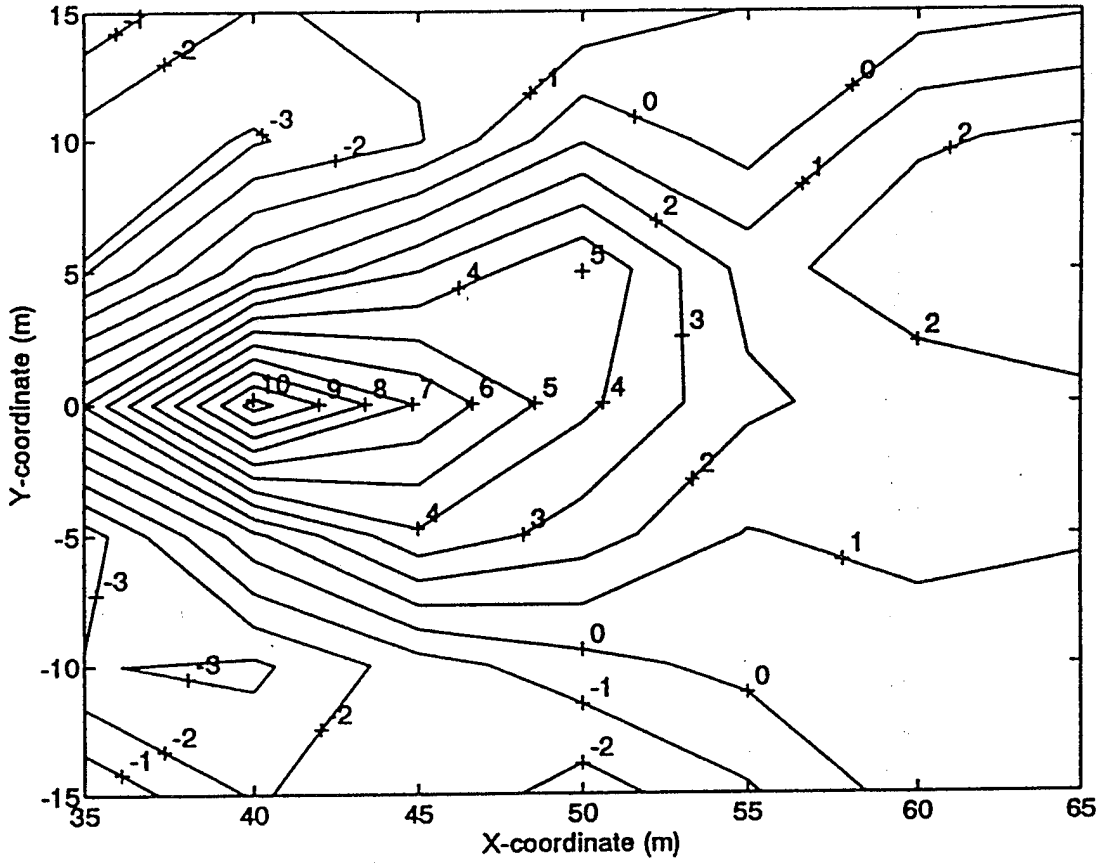


Figure 25. Total SPL Reduction Contours, SI-SO Local ANR of Simulated Hush House; Control Source at (30,0)m and Error Microphone at (40,0)m.

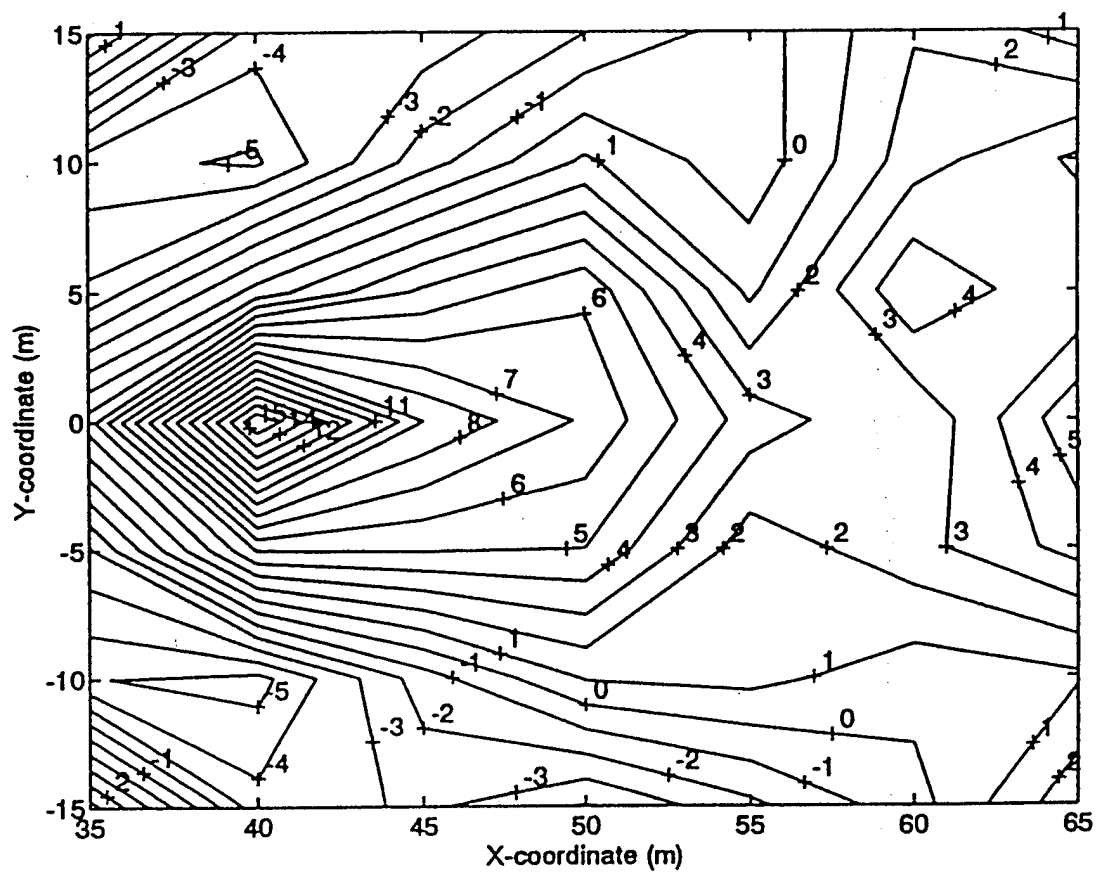


Figure 26. SPL Reduction Contours in 40 Hz One-Third Octave Band, SI-SO Local ANR of Simulated Hush House; Control Source at (30,0)m and Error Microphone at (40,0)m.

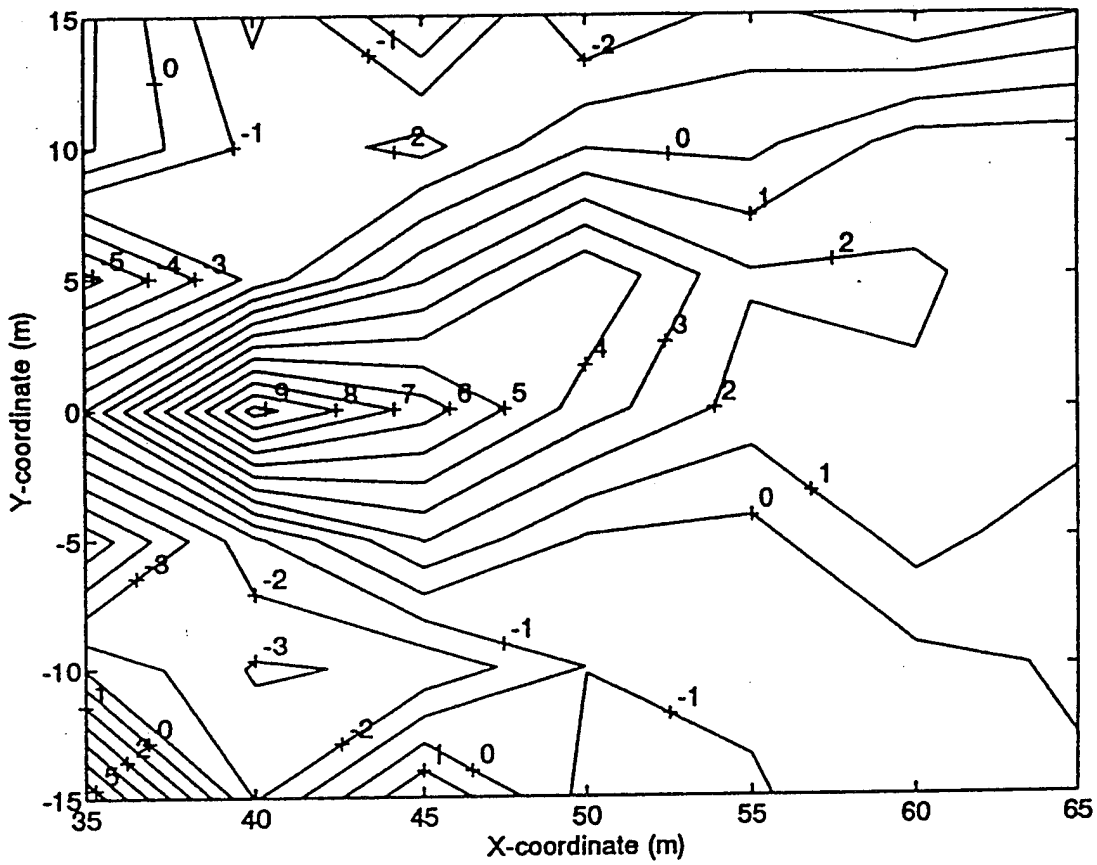


Figure 27. SPL Reduction Contours in 80 Hz One-Third Octave Band, SI-SO Local ANR of Simulated Hush House; Control Source at (30,0)m and Error Microphone at (40,0)m.

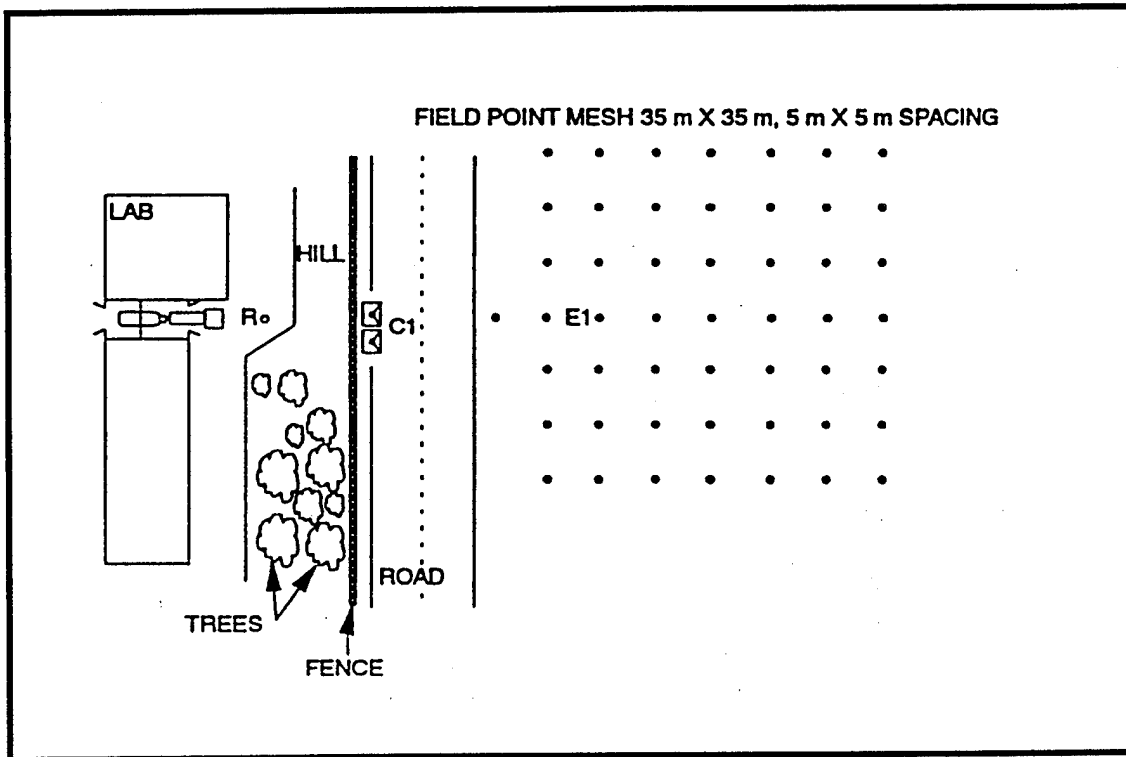


Figure 28. Second Configuration for SI-SO Local ANR of Simulated Hush House.

The control, error, and reference signals were again bandpass filtered between 25 and 250 Hz, defining the controllable bandwidth of interest. The adaptive control FIR filter contained 100 coefficients, and the sample rate was 800 Hz. The system identification was performed on the DSP board with an FIR filter containing 200 coefficients. The controller was allowed to converge for approximately 60 seconds.

The coherence between the reference microphone and the error microphone with the engine running is shown in Figure 29. Note that there was some degradation of the coherence primarily at the higher frequencies due to the reference microphone being located closer to the disturbance and down the hill from the level of the control sources and error sensors. The control source input to output coherence was similar to that observed in the previous experiment.

The one-third octave band spectra at the error microphone are shown in Figure 30. The total reduction of the error signal, integrated over the 25 to 250 Hz bandwidth, was 6.2 dB. Reductions ranging from 6 to 10 dB were obtained in the one-third octave bands with the highest levels before control. There is again some reduction evident in the 25 Hz one-third octave band, which is below the designed operating range of the speaker. Note that the amount of attenuation at the error microphone is less, in this experiment, with the larger spacing between the control source and the error sensor, than that shown previously (Figure 24).

Figures 31 and 32 contain contour plots over the 30m x 30m field point matrix of the total SPL reduction and the SPL reduction in the 63 Hz one-third octave band, respectively. Note that a larger area of attenuation was achieved around the error sensor with the control source closer to the disturbance source and with the larger spacing between the control source and the error sensor. Attenuation over almost the entire field point matrix was obtained in this and most of the other one-third octave bands with this SI-SO control configuration. Thus moving the control source closer to the disturbance resulted in a larger area of reduction, as expected. Comparing this test with the previous SI-SO test demonstrates the tradeoff between the amount of attenuation and the area over which attenuation occurs, as expected.

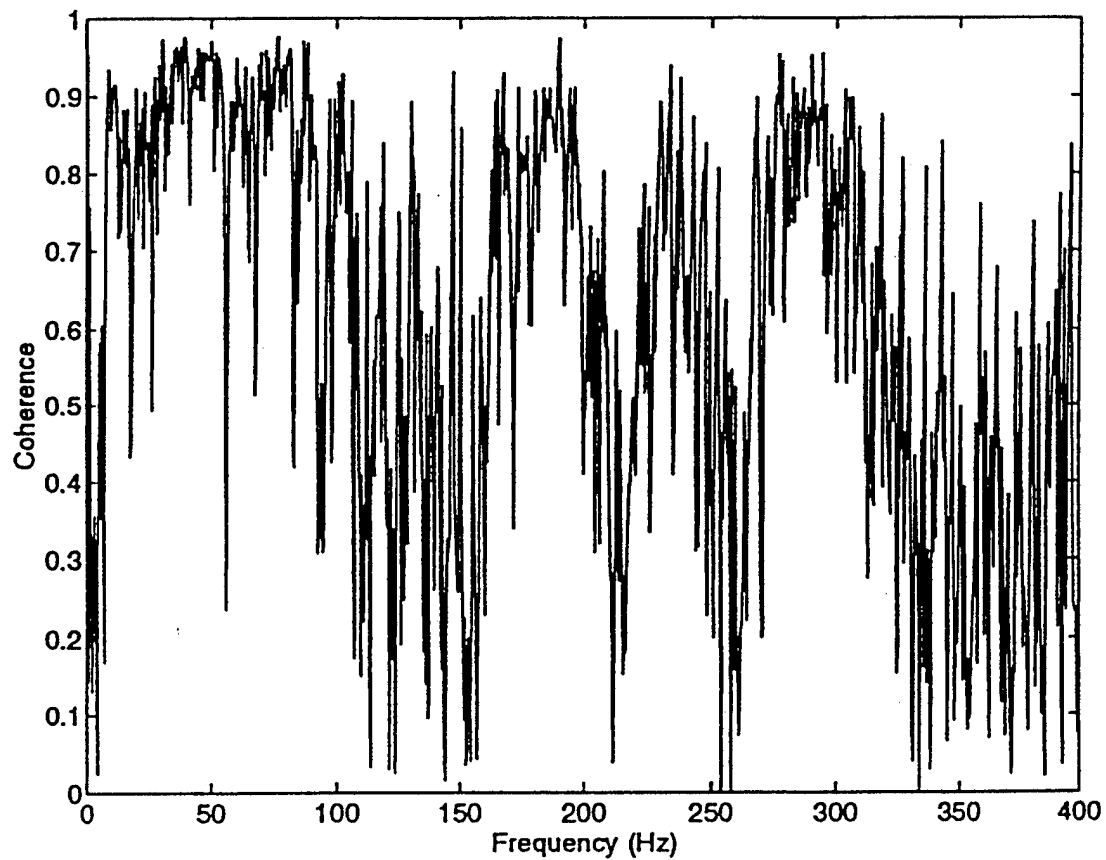


Figure 29. Coherence Between Reference Microphone and Error Microphone, SI-SO Local ANR of Simulated Hush House.

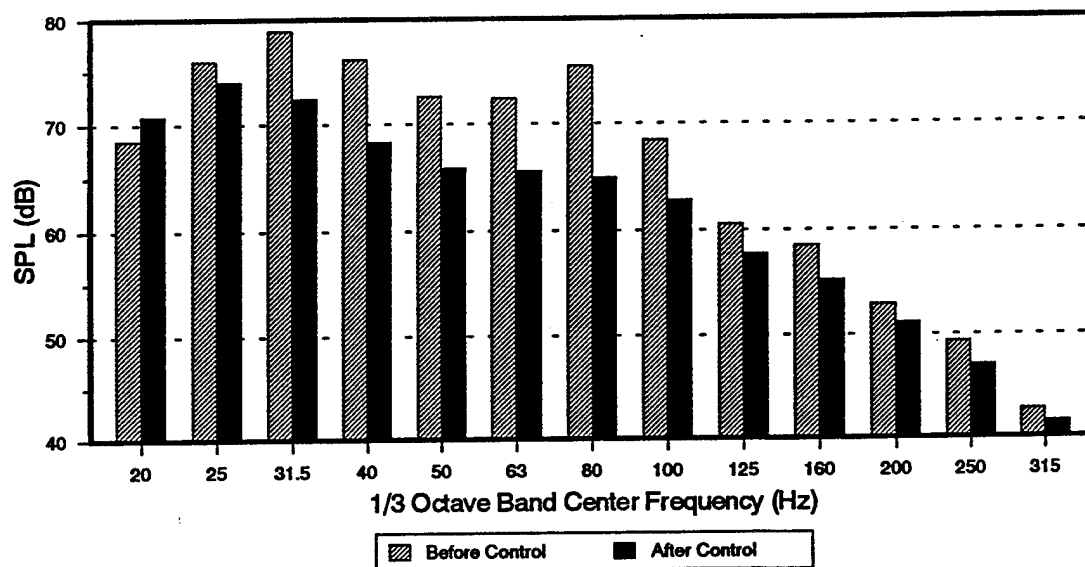


Figure 30. Error Microphone One-Third Octave Band Analysis, SI-SO Local ANR of Simulated Hush House.

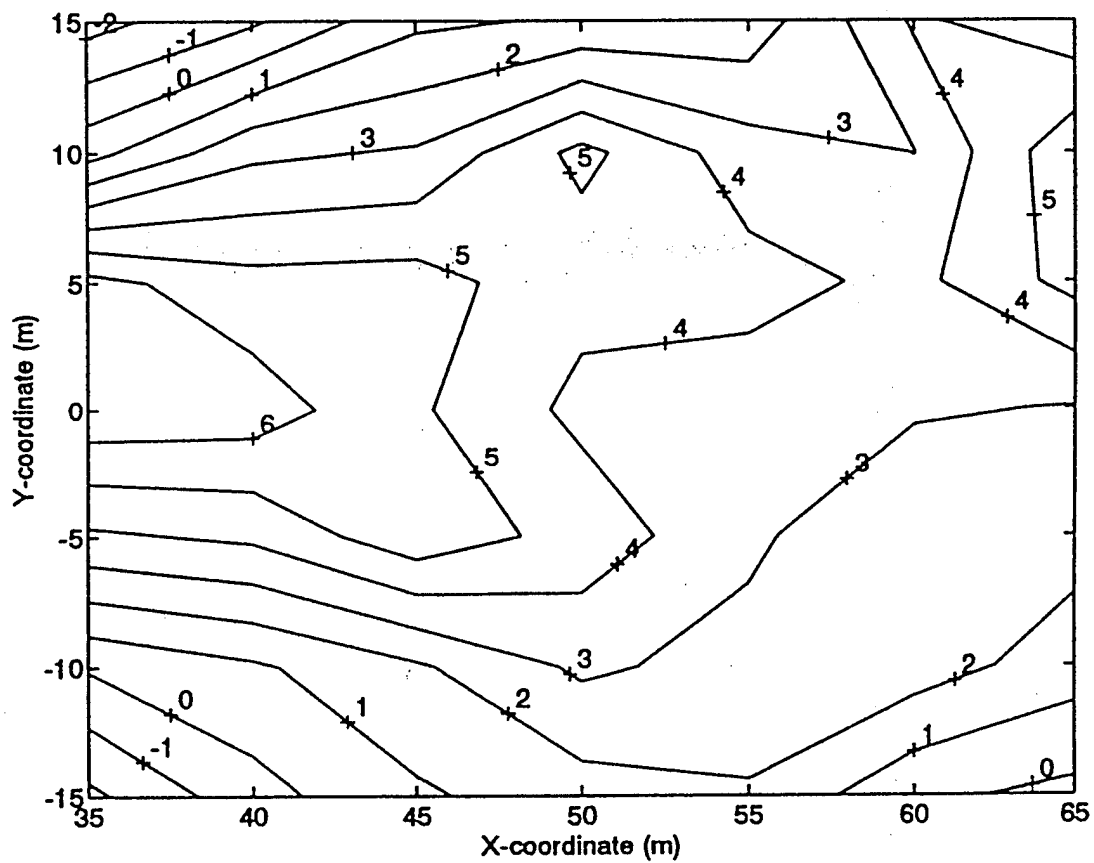


Figure 31. Total SPL Reduction Contours, SI-SO Local ANR of Simulated Hush House; Control Source at (17,0)m and Error Microphone at (40,0)m.

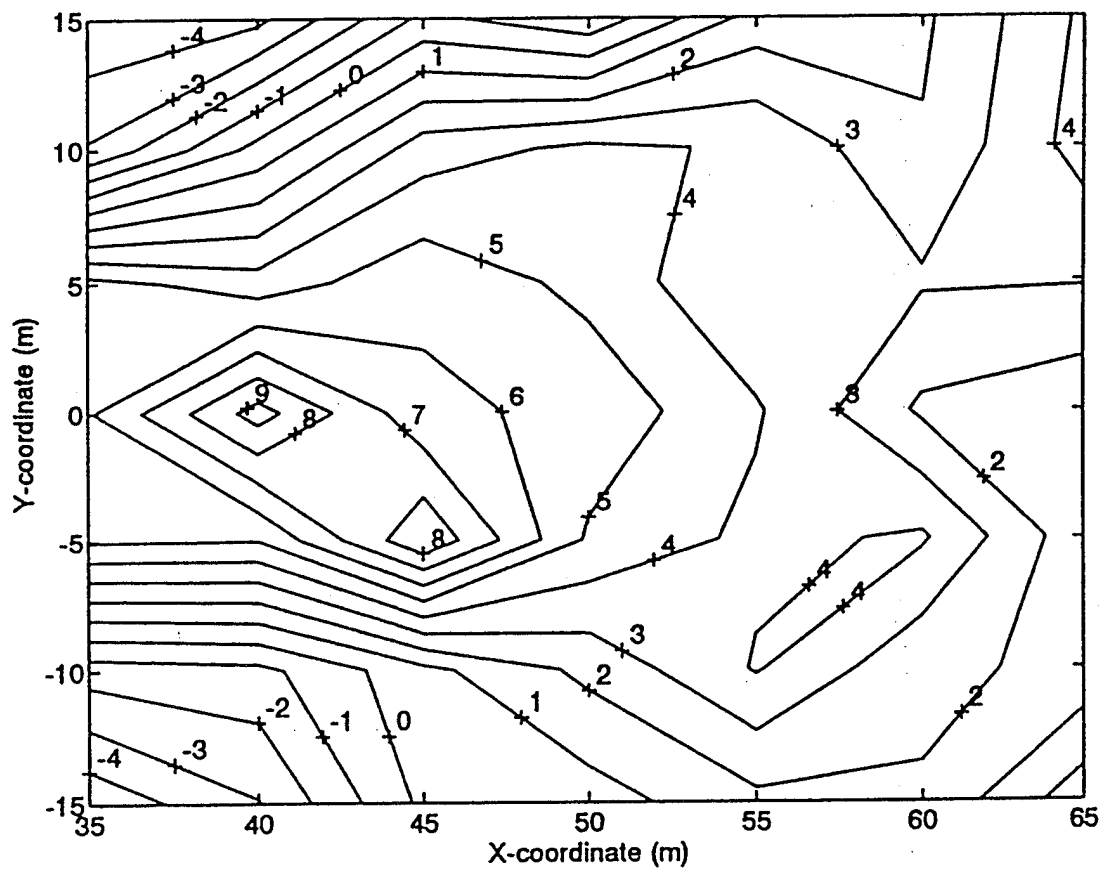


Figure 32. SPL Reduction Contours in 63 Hz One-Third Octave Band, SI-SO Local ANR of Simulated Hush House; Control Source at (17,0)m and Error Microphone at (40,0)m.

Three-Input, Three-Output Configuration

Multi-input, multi-output experiments were conducted using the simulated hush house. Microphones were again used as the reference and error sensors, and control sources were three conventional loudspeakers. 3I-3O control systems were implemented, with varying error sensor locations. The control loudspeakers were located along a line perpendicular to the exhaust tube, 30m from the engine, with a 5m spacing. The center control speaker was located along the exhaust tube axis. The reference microphone for the 3I-3O tests presented here was located at the top of the hill, approximately 10m from the jet engine exhaust.

The configuration for the first 3I-3O control system is shown in Figure 33. Following the (x,y) coordinate system used in the analytical study, described in *Analytical Results*, the three error sensors were located at coordinates of (40,0), (45,-5), and (45,5) m, where the origin is the engine exhaust. This configuration locates the error microphones in a small triangle.

The control, error, and reference signals were bandpass filtered between 25 and 250 Hz, again defining the controllable bandwidth of interest. The adaptive control FIR filter contained 100 coefficients and the sample rate was 800 Hz. The system identification was performed on the DSP board with an FIR filter containing 200 coefficients. The controller was allowed to converge for approximately 60 seconds.

The coherences between the reference microphone and the error microphones were similar in level to that shown in the plot of Figure 21, and the coherence through the control speakers in this experiment is similar to that shown in Figure 22.

The one-third octave band spectra for the center error microphone are shown in Figure 34. Reductions ranging from 8 to 10 dB were obtained in the one-third octave bands between 25 and 100 Hz. The total SPL reduction integrated over the 25 to 250 Hz bandwidth at the center error microphone was 5.9 dB.

Figure 35 shows a contour plot of the total SPL reduction obtained over the field point matrix, and Figures 36 and 37 show the reduction contours in the one-third octave bands with center frequencies of 40 Hz and 100 Hz, respectively. It is evident from the contour plots that a larger area of reduction is obtained with the 3I-3O

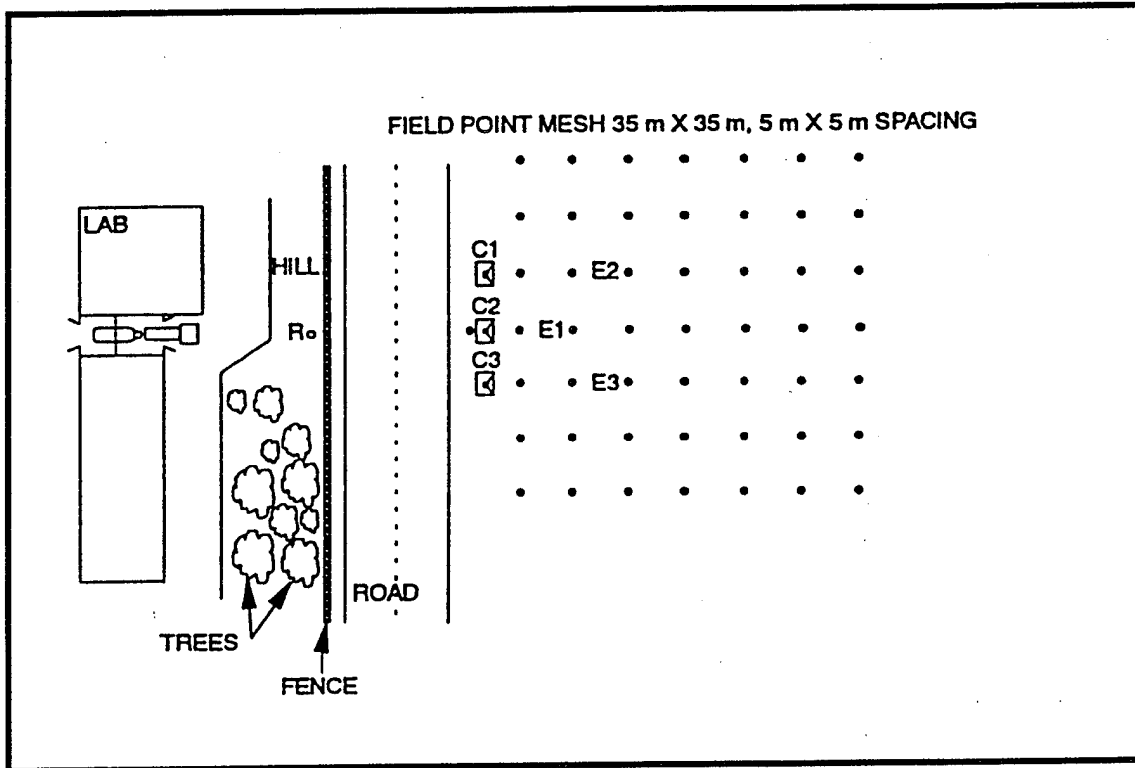


Figure 33. First Configuration for 3I-30 Local ANR of the Simulated Hush House.

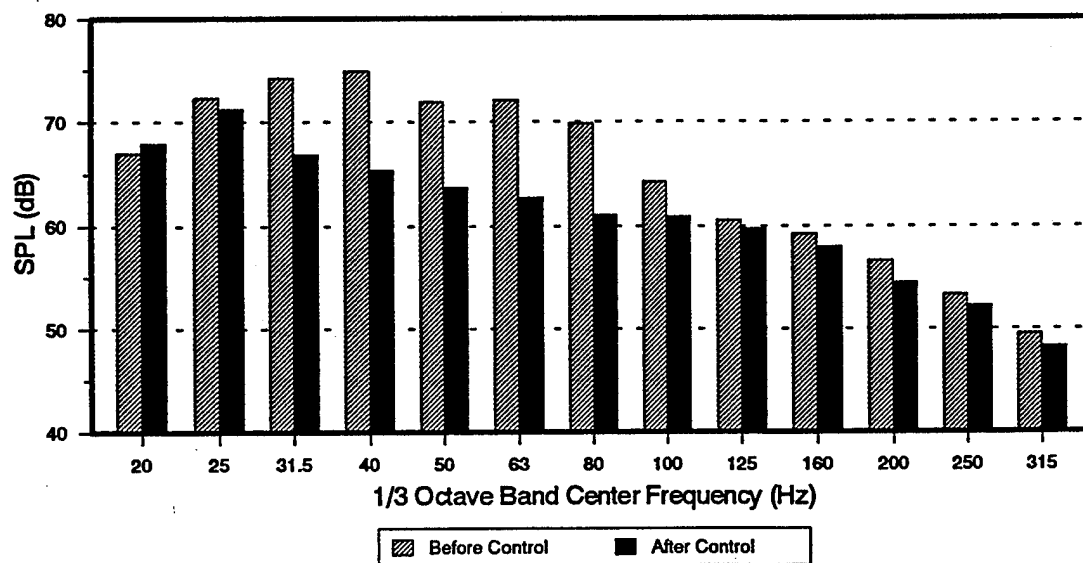


Figure 34. Error Microphone One-Third Octave Band Analysis, 3I-3O Local ANR of Simulated Hush House.

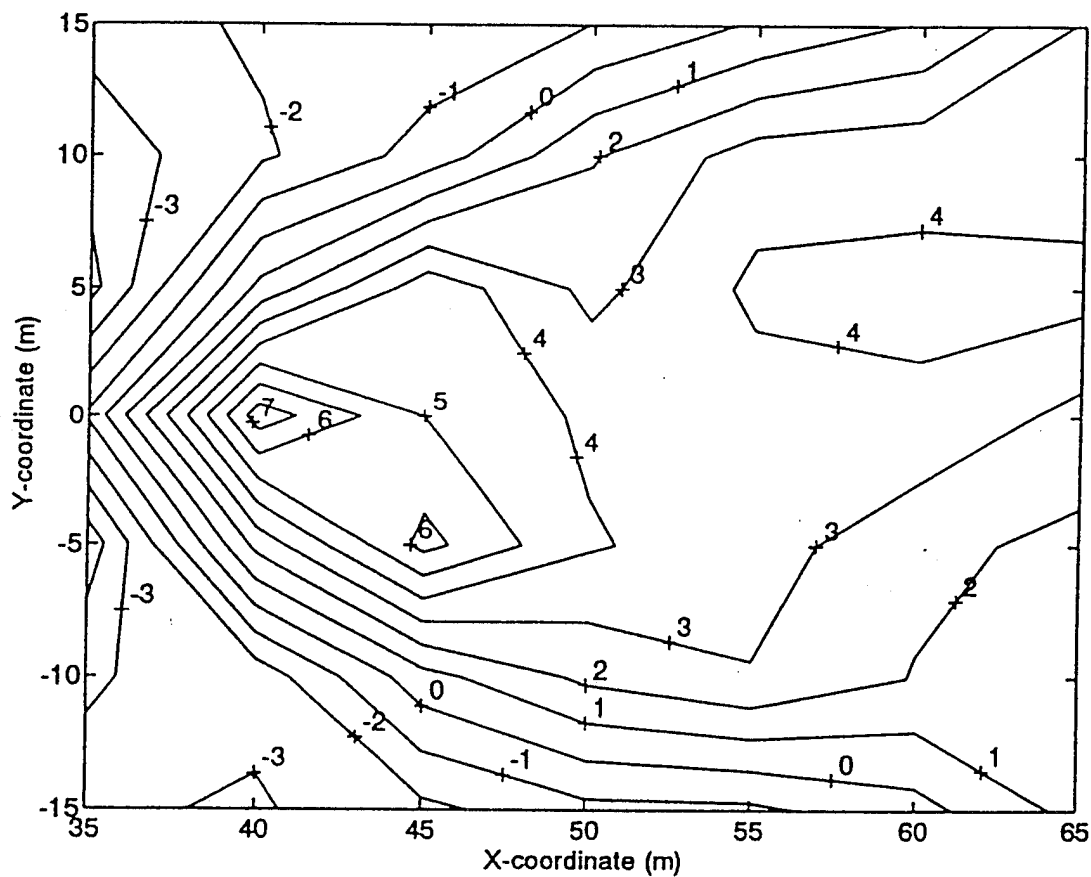


Figure 35. Total SPL Reduction Contours, 3I-30 Local ANR of Simulated Hush House; Control Sources at (30,0), (30,5), and (30,-5)m and Error Microphones at (40,0), (45,5), and (45,-5)m.

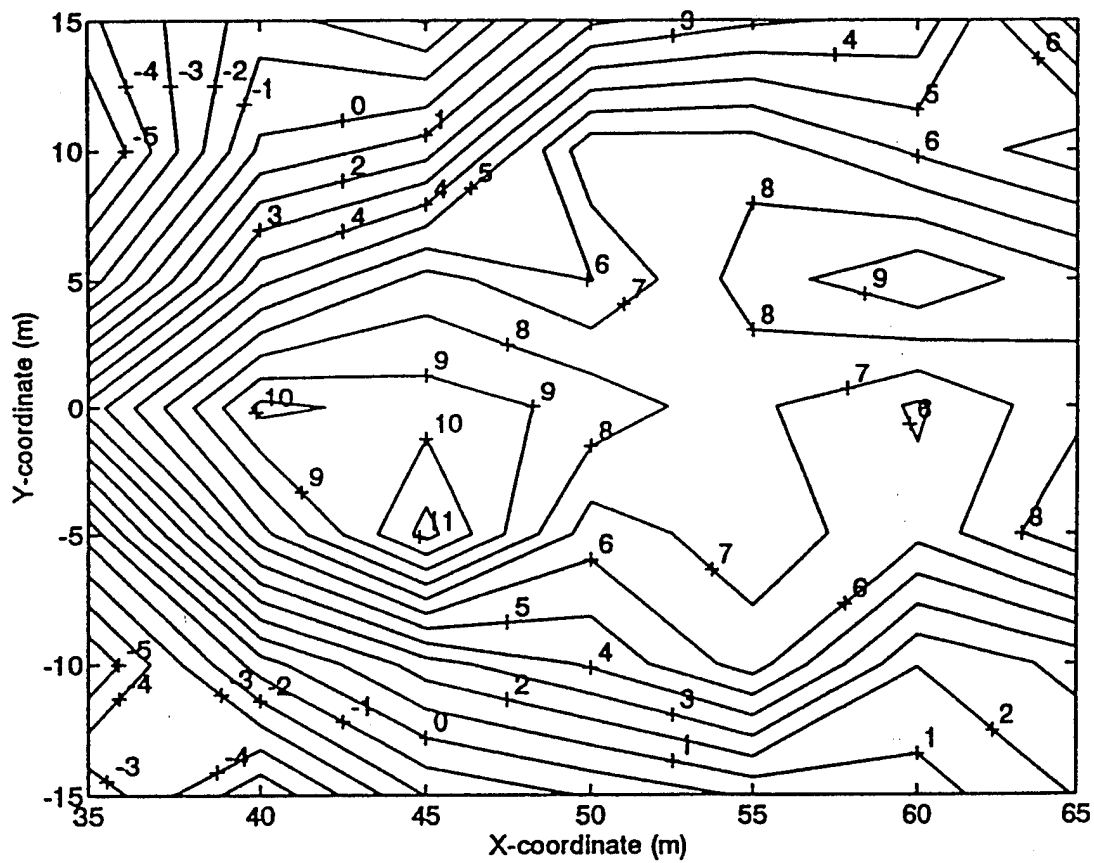


Figure 36. SPL Reduction Contours in 40 Hz One-Third Octave Band, 3I-30 Local ANR of Simulated Hush House; Control Sources at (30,0), (30,5), and (30,-5)m and Error Microphones at (40,0), (45,5), and (45,-5)m.

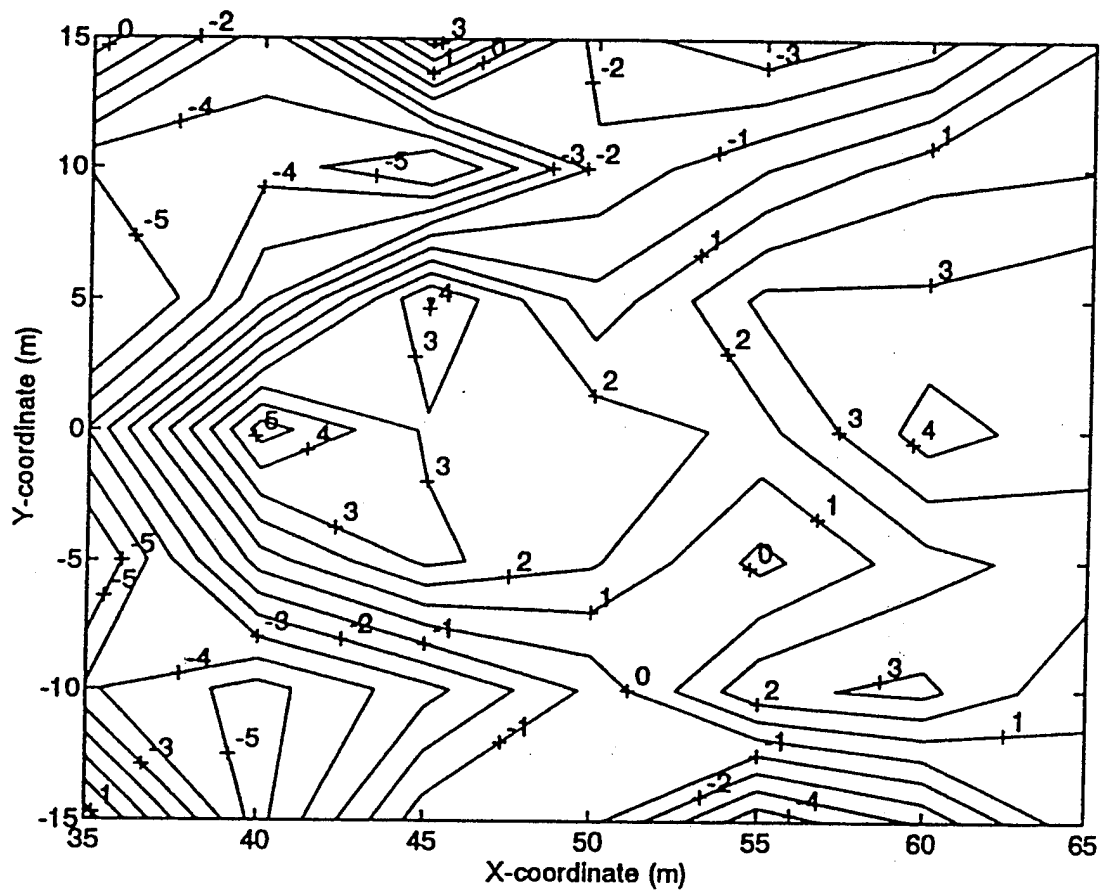


Figure 37. SPL Reduction Contours in 100 Hz One-Third Octave Band, 3I-30 Local ANR of Simulated Hush House; Control Sources at (30,0), (30,5), and (30,-5)m and Error Microphones at (40,0), (45,5), and (45,-5)m.

system, compared to the similar SI-SO case, as expected. (Compare Figure 25 with Figure 35 and Figure 26 with Figure 36.) The cone of reduction is wider for 3I-3O than for the SI-SO system, as predicted with the analytical model. Note that the amount of reduction at each of the error sensors is slightly less for 3I-3O than that achieved at the error sensor with the similar SI-SO system.

Another 3I-3O control system configuration is shown in Figure 38. The control sources were in the same positions as for the previous 3I-3O test. The three error sensors were located at coordinates of (40,0), (50,-7.5), and (50,7.5) m, following the (x,y) coordinate system previously defined, where the origin is the engine exhaust. This configuration has the error microphones situated in a larger triangle than the last experiment, in an attempt to enlarge further the area of attenuation.

Control system parameters were similar to those in the previous 3I-3O test. The coherences between the reference microphone and the error microphones were similar to that shown in the plot of Figure 21, and again the coherence through the control speakers is closely represented by Figure 22.

The one-third octave band spectra for the center error microphone are shown in Figure 39. Reductions ranging from 8 to 13 dB were obtained in the one-third octave bands between 25 and 100 Hz. The total SPL integrated over the 25 to 250 Hz bandwidth at the center error microphone was reduced by 6.3 dB.

Figure 40 shows a contour plot of the total SPL reduction obtained over the field point matrix, and Figures 41 and 42 show the reduction contours in the one-third octave bands with center frequencies of 40 Hz and 80 Hz, respectively. It is evident from the contour plots that spreading out the error sensors resulted in a slightly larger area of reduction than for the smaller triangular configuration, particularly at the lower frequencies.

Comparison of Results with Analytical Model

Reasonably good agreement was noted between the noise reduction contours predicted with the analytical model and those measured experimentally. Comparison of Figure 6 with Figure 26 and of Figure 7 with Figure 27 shows that the area

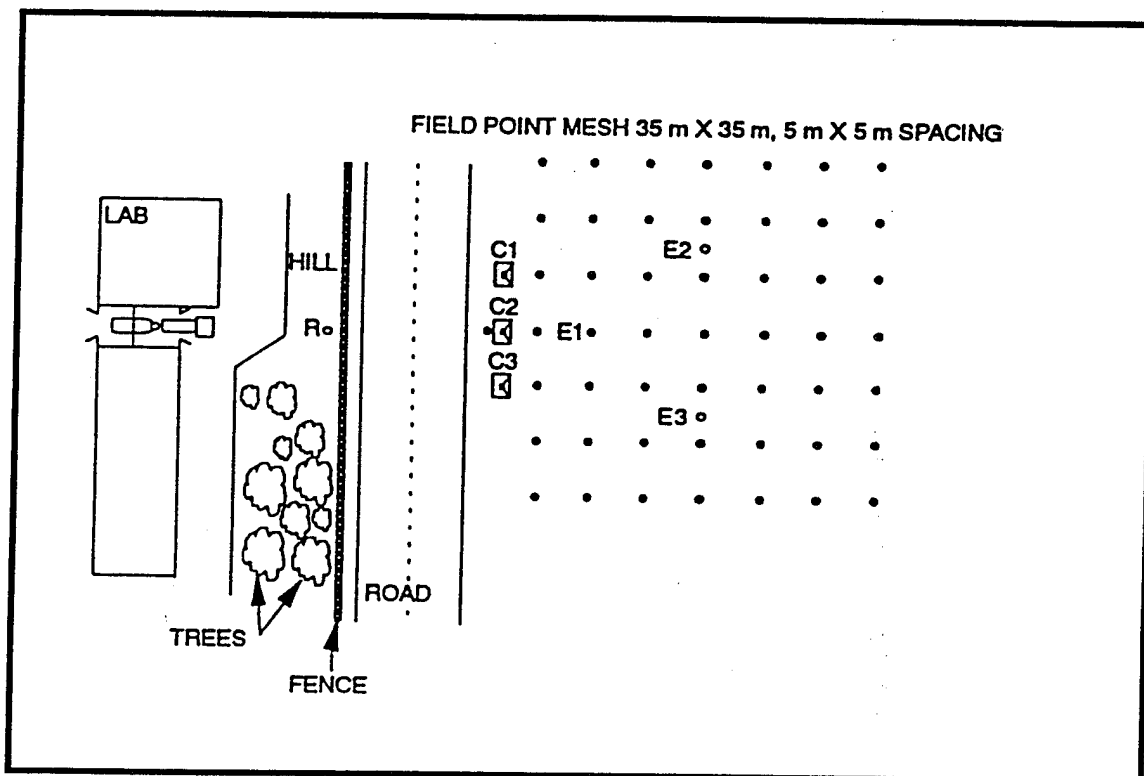


Figure 38. Second Configuration for 3I-30 Local ANR of Simulated Hush House.

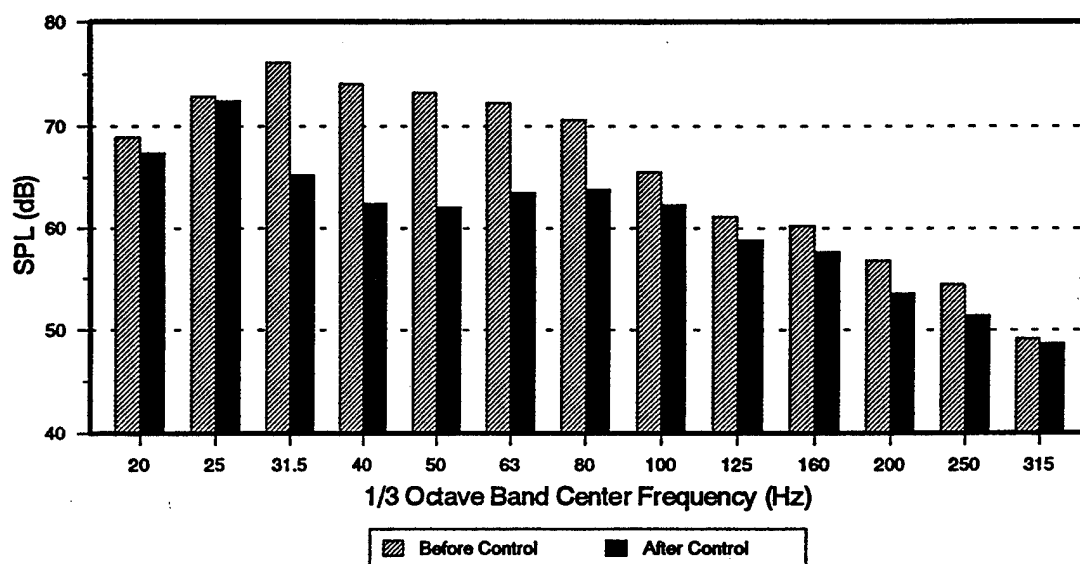


Figure 39. Error Microphone One-Third Octave Band Analysis, 3I-3O Local ANR of Simulated Hush House.

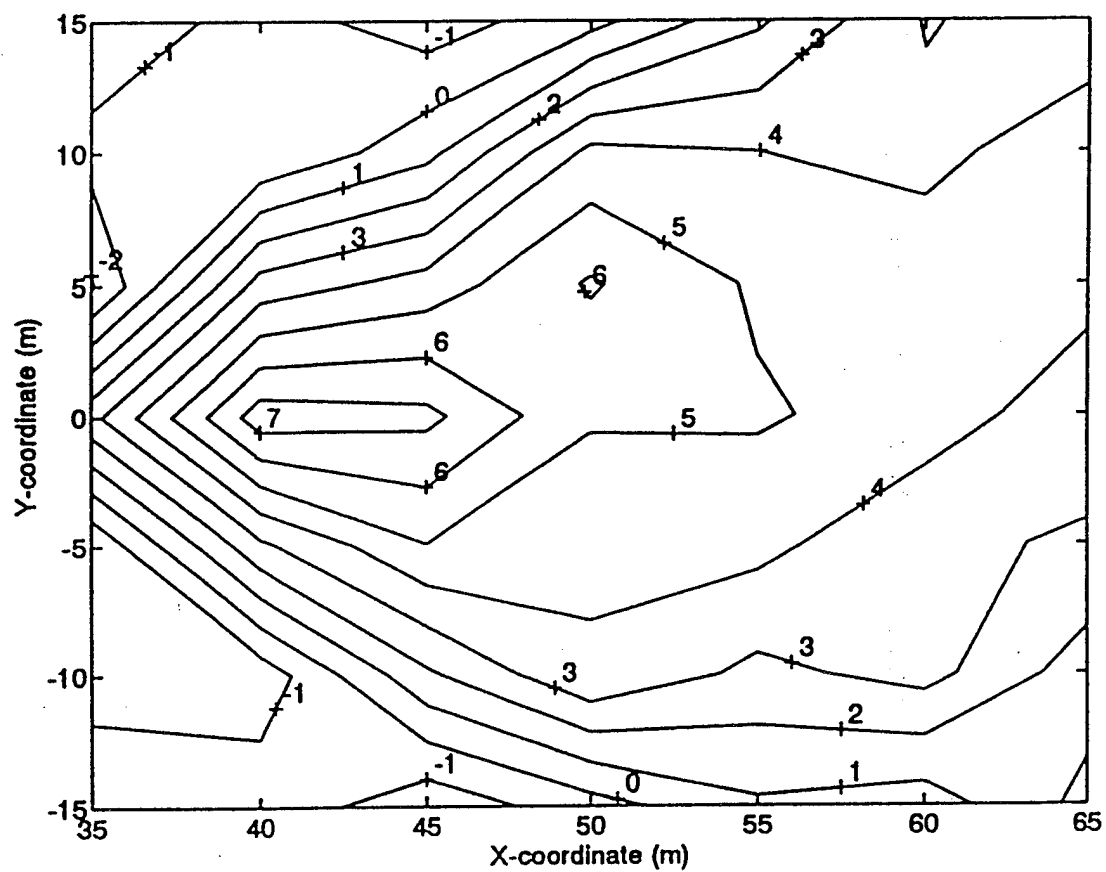


Figure 40. Total SPL Reduction Contours, 31-30 Local ANR of Simulated Hush House; Control Sources at (30,0), (30,5), and (30,-5)m and Error Microphones at (40,0), (50,7.5), and (50,-7.5)m.

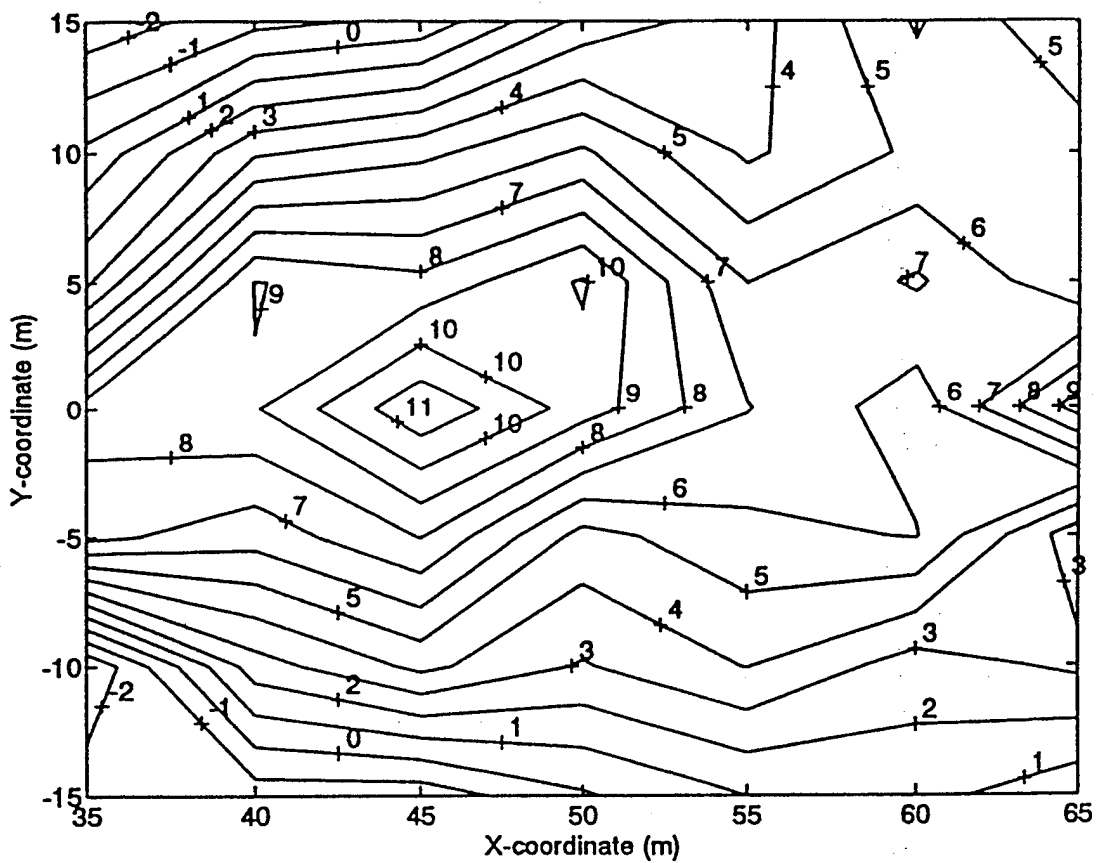


Figure 41. SPL Reduction Contours in 40 Hz One-Third Octave Band, 3I-3O Local ANR of Simulated Hush House; Control Sources at (30,0), (30,5), and (30,-5)m and Error Microphones at (40,0), (50,7.5), and (50,-7.5)m.

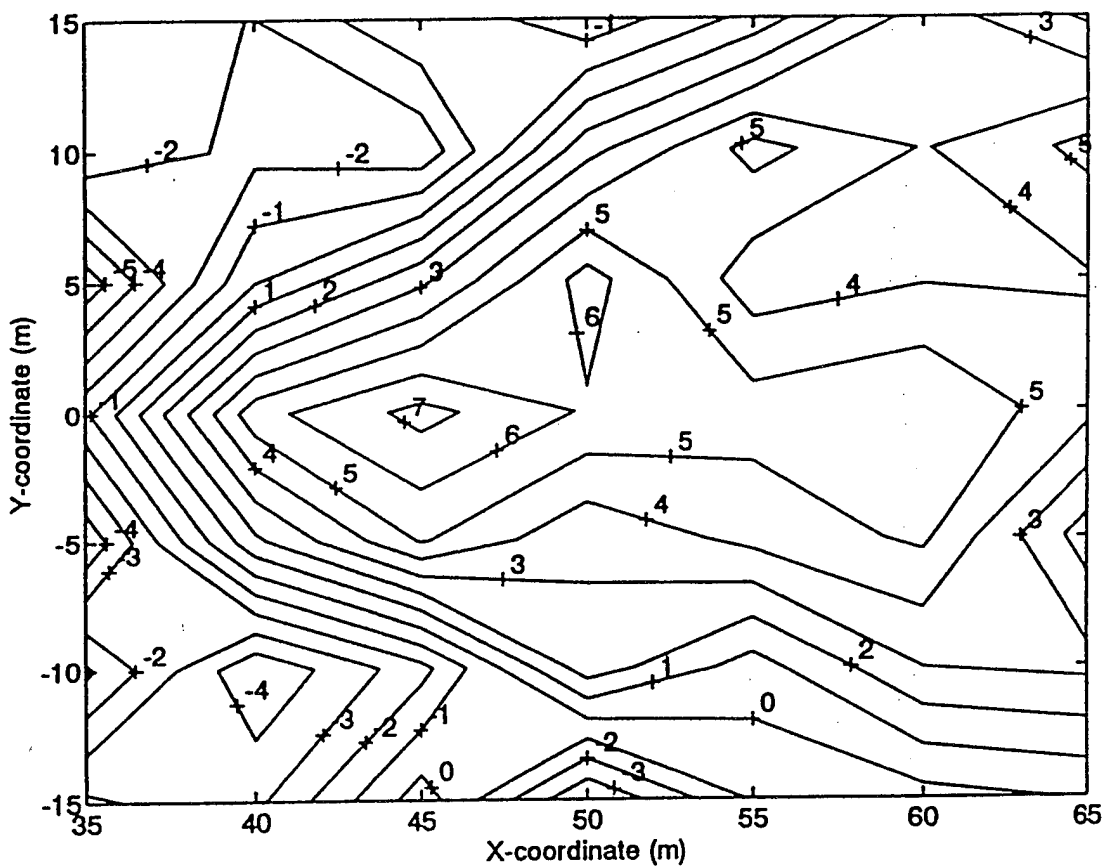


Figure 42. SPL Reduction Contours in 80 Hz One-Third Octave Band, 31-30 Local ANR of Simulated Hush House; Control Sources at (30,0), (30,5), and (30,-5)m and Error Microphones at (40,0), (50,7.5), and (50,-7.5)m.

over which attenuation is obtained for a SI-SO case agrees well between the simulation and the experiment. The amount of attenuation predicted is higher in the analytical model, but the model does not account for imperfect coherence between the reference and error and imperfect coherence of the control speaker input to output relationship. Also, the analytical model predicts the reduction at a single frequency, whereas the experimental results are integrated over one-third octave bands. The model also predicts reasonably well the attenuation pattern obtained with the 3I-3O systems. The contours predicted by the analytical model in Figures 9 and 10 can be compared to the experimental results in Figures 36 and 41, respectively, since they correspond to the same configuration. Again the area over which attenuation occurs shows relatively good agreement between the model and the measured results.

Thus the analytical model described earlier has been verified to give reasonably accurate predictions of the reduction contours which are obtained experimentally. The model has been shown to be a useful tool for design and evaluation of ANR configurations. This is valuable, since control configurations can be modeled to estimate their effectiveness and evaluated for their potential before they are experimentally implemented. The model can be used to predict attenuation patterns and the area over which attenuation will occur, and can be used as a guideline for determining optimal ANR configurations.

Unsuppressed Jet With WAS 3000 as Control Source

The MOAS system, including the WAS 3000 noise source, was implemented as a control source for local ANR; the disturbance source for this test was the Saeta 200 jet aircraft described in *Unsuppressed Jet*.

The configuration of the jet, the MOAS, and the reference and error microphones is shown in the diagram in Figure 43. The control source and error microphone were located along a line that was at an angle of approximately 45 degrees to the axis of the jet. The reference microphone was located at an angle of 60 degrees to the axis of the jet, since there was judged to be too much air flow from the jets at a nearby position at 45 degrees. The reference microphone was placed as far from the MOAS

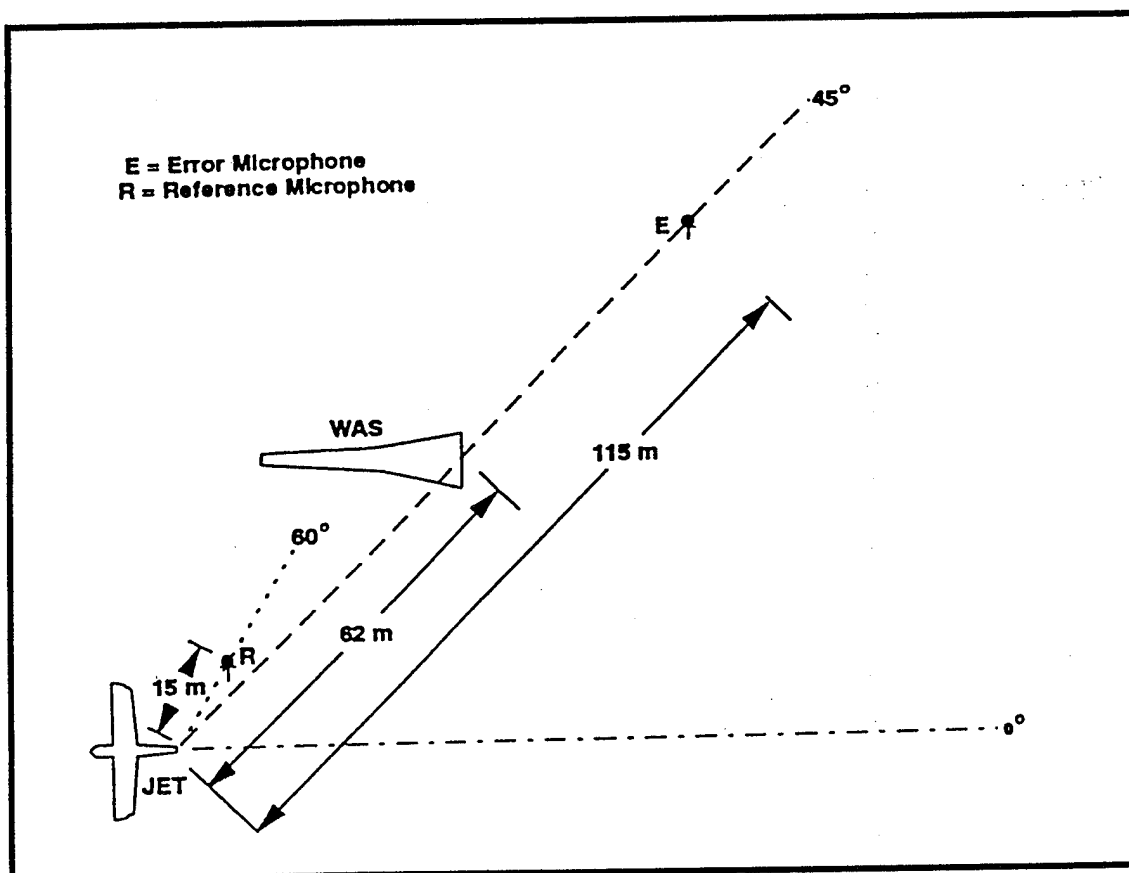


Figure 43. Configuration for SI-SO Local ANR of Unsuppressed Jet Aircraft, Using WAS 3000.

as was practical since the diesel engine and compressor which are part of the MOAS system created significant levels of tonal noise which corrupted the reference signal and reduced the reference to error coherence. Figure 44 contains a photo of the configuration from behind the error microphone.

The WAS 3000 was set to operate at 2.5 psig and approximately 2 amps, since this operating point resulted in sound pressure levels at the error microphone comparable to those from the jet engines. This is at the low end of the WAS 3000 operating range, but higher pressures and currents would have resulted in noise levels from the WAS 3000 greatly in excess of the jet noise levels, making noise reduction impossible.

A SI-SO system was implemented, and the control, error, and reference signals were bandpass filtered between 10 and 200 Hz, which defined the controllable bandwidth of interest. The adaptive control FIR filter contained 100 coefficients and the sample rate was 800 Hz. The system identification was performed on the DSP board with an FIR filter containing 200 coefficients. The controller was allowed to converge for approximately 120 seconds.

The coherence between the reference microphone and the error microphone with the jet engines and the MOAS diesel engine operating is shown in Figure 45. The two drops in coherence at about 58 Hz and 116 Hz are due to the tones generated by the MOAS engine. The coherence between the control signal into the WAS 3000 and the noise output at the error microphone was determined by playing white noise through the WAS 3000, operating at 2.5 psi and 2 amps, with the jet engines off. This coherence function, shown here for noise over a range of only 10 to 100 Hz, is shown in Figure 46. Again the signal corruption due to engine tones is seen. The overall level of coherence, approximately 0.8, is much poorer than those seen for the conventional loudspeakers, for example in Figure 22. This is due in part to the low level at which the WAS 3000 was operating, at the low end of its operating range. The level of coherence measured in a separate test, over the range from 100 to 200 Hz, is similar to the level of coherence from 10 to 100 Hz, shown in Figure 46.

The error microphone narrowband spectra before and after control are shown in Figure 47. Again note the peaks in the error signal at about 58 and 116 Hz, which are due to the diesel engine and compressor. Note that much of the significant

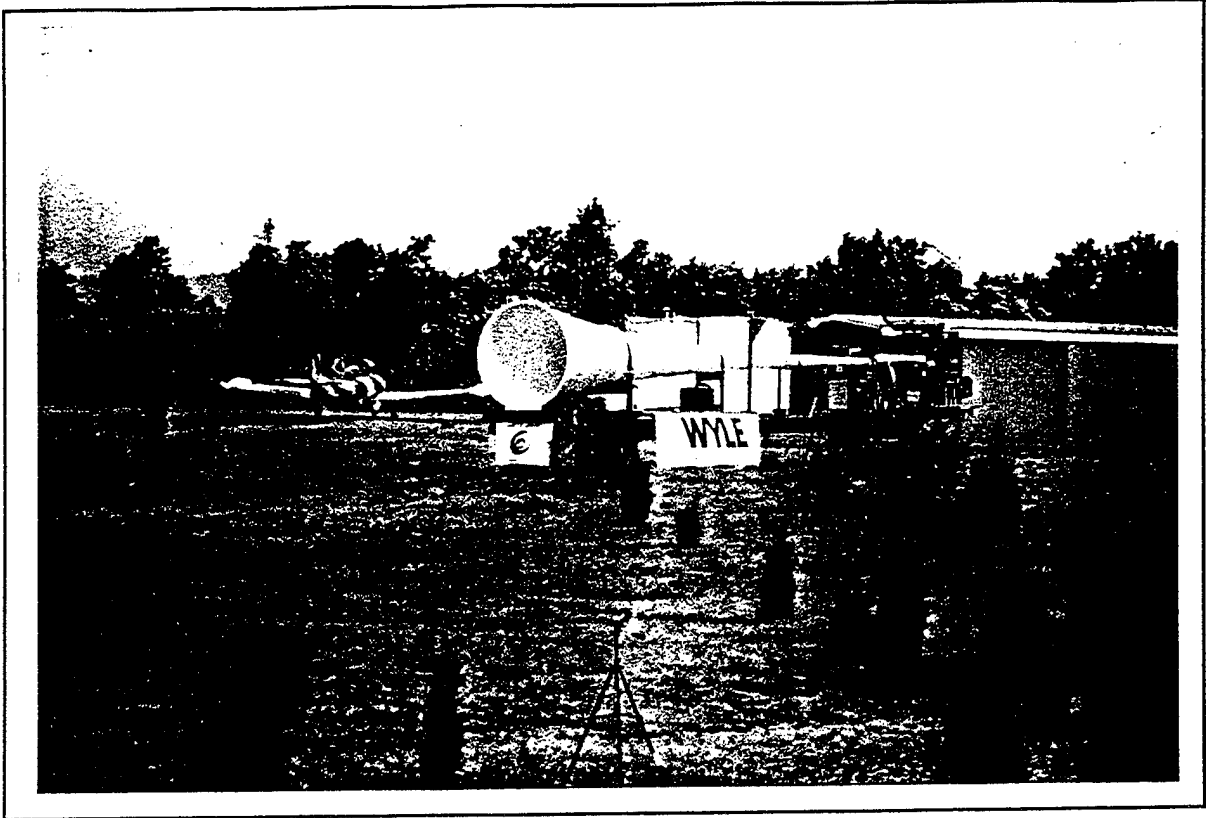


Figure 44. Photograph of Unsuppressed Jet Aircraft and WAS 3000 for Local ANR.

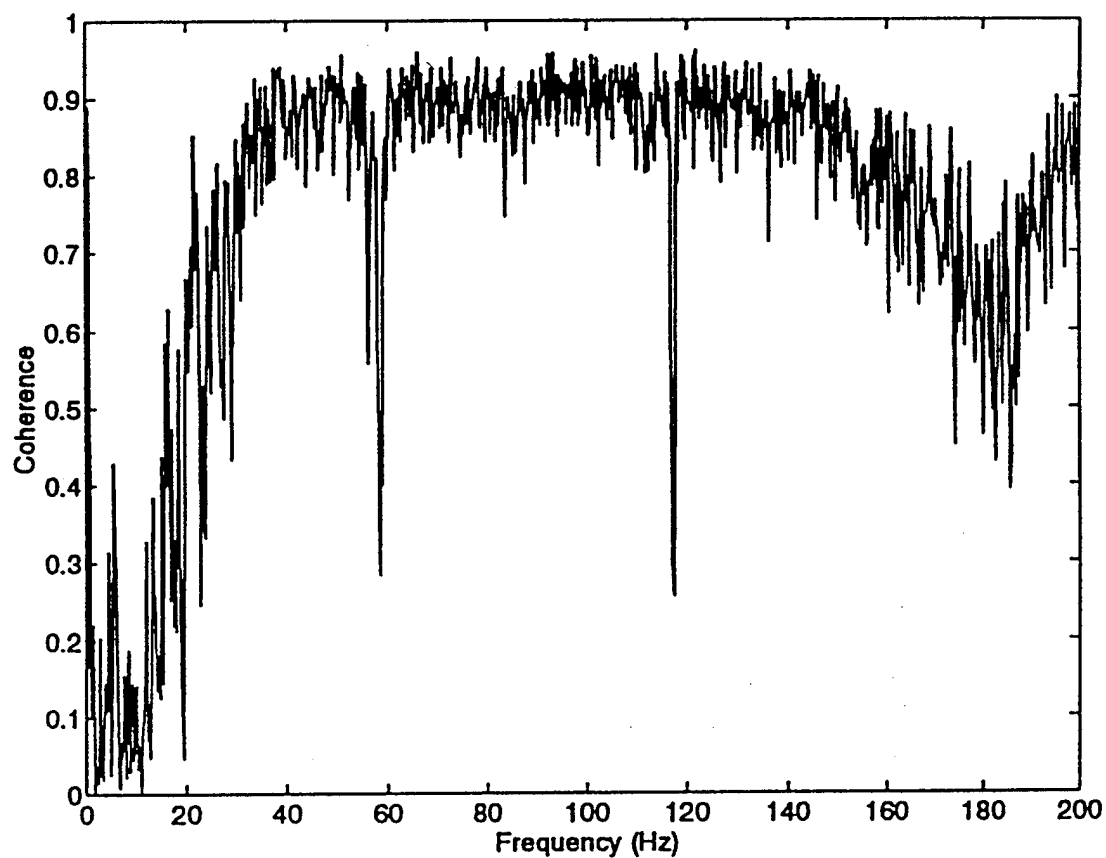


Figure 45. Coherence Between Reference Microphone and Error Microphone, SI-SO Local ANR of Unsuppressed Jet Aircraft.

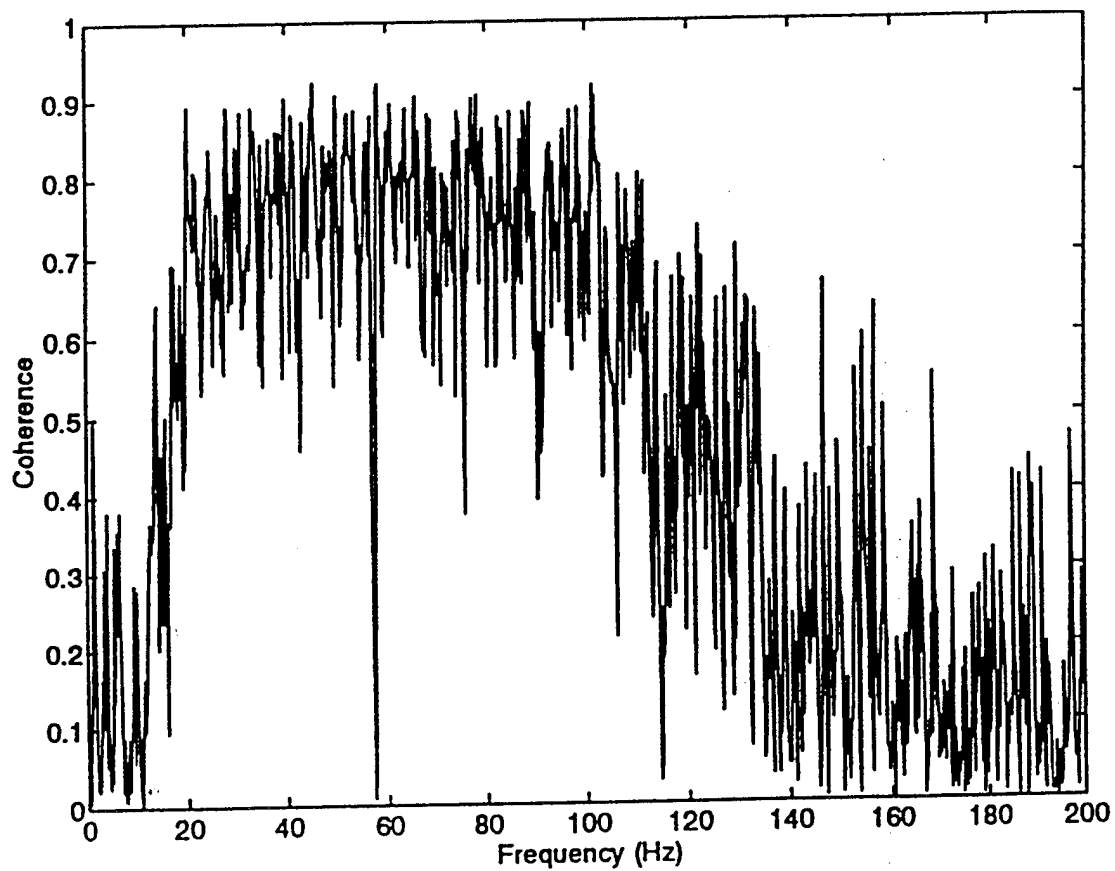


Figure 46. Coherence Between Input to WAS 3000 and Error Microphone, SI-SO Local ANR of Unsuppressed Jet Aircraft, 10 to 100 Hz.

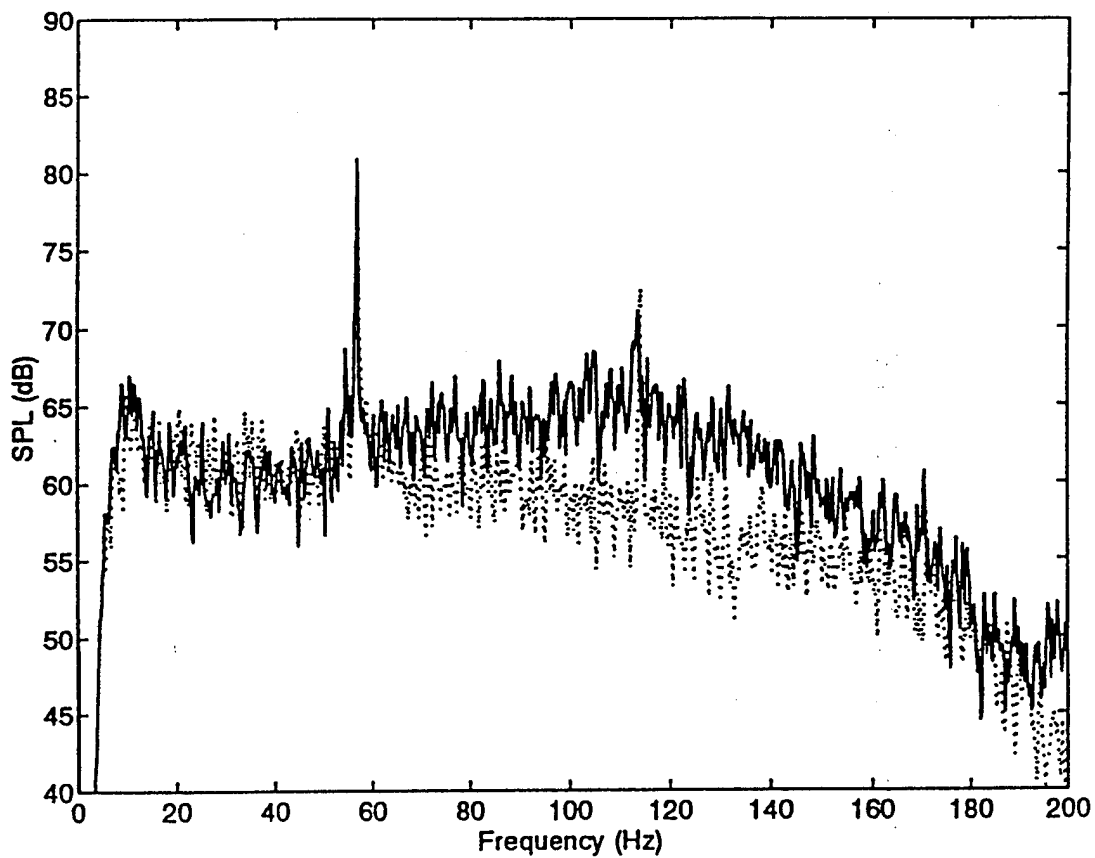


Figure 47. Error Microphone Spectra, SI-SO Local ANR of Unsuppressed Jet Aircraft Using WAS 3000.
—— before control; after control.

acoustic energy in the error spectrum before control is between 60 and 160 Hz, and this is the part of the spectra which exhibits the largest reduction. The one-third octave band analysis of the error microphone signal is shown in Figure 48. Again most of the reduction is evident in the one-third octave bands which have the highest levels before control. Reductions ranging from 5 to 7 dB are achieved in the one-third octave bands with center frequencies between 63 and 160 Hz. The one-third octave band with a center frequency of 63 Hz does not show as much reduction since the tone from the diesel engine, which dominates this band, was not significantly controlled. The controller could not reduce the tones generated by the diesel engine because of the low reference to error coherence at these frequencies, and perhaps for reasons related to acausality in the control system resulting from a disturbance noise source (the MOAS engine) located between the reference and error sensors.

The spectra in Figure 48 show little or no reduction in the bands at 40 Hz and below. This is true for a number of reasons. The controller devotes most of its control effort to the highest spectral levels, which in this case were at frequencies above 50 or 60 Hz. Once the levels above 60 Hz were reduced, the controller could devote its effort to the peaks at 58 Hz and at around 10 Hz, which dominate the remaining spectrum. However, the peak at 58 Hz could not be controlled for the reasons described in the previous paragraph, and the 10 Hz energy could not be controlled due to the poor coherences below 20 Hz in this experiment. If the spectrum had been dominated by higher levels of low-frequency noise below 50 Hz, greater levels of low-frequency reduction would have been seen.

Noise levels were measured in a small array around the error microphone to study the extent of noise reduction obtained. Noise reductions in the 100 Hz one-third octave band are shown in Figure 49. It can be seen that reductions of up to 6 dB were obtained up to 20m behind the error microphone, although the shape of the area of reduction is not well defined based on the small number of data points measured here.

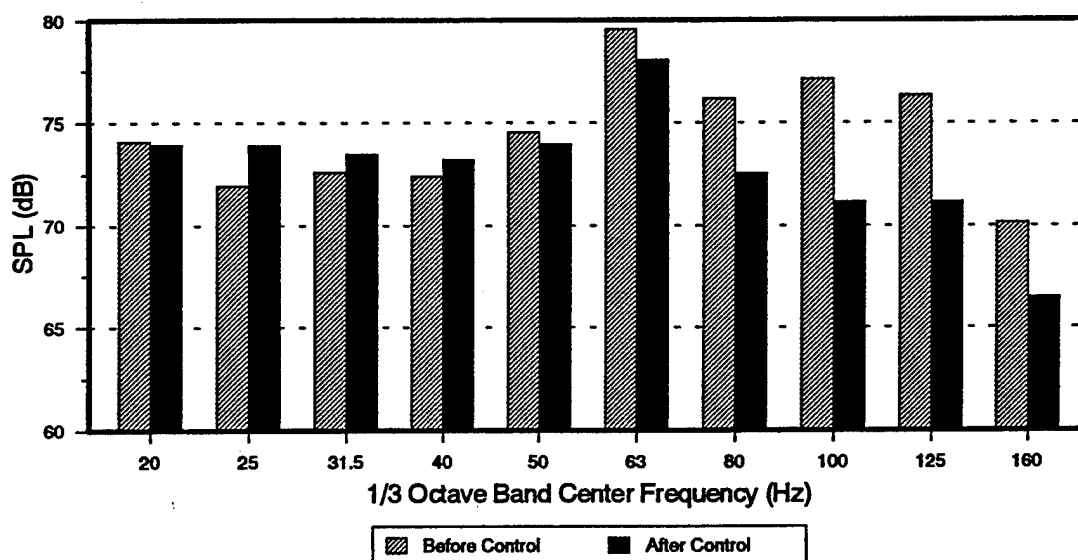


Figure 48. Error Microphone One-Third Octave Band Analysis, SI-SO Local ANR of Unsuppressed Jet Aircraft, Using WAS 3000.

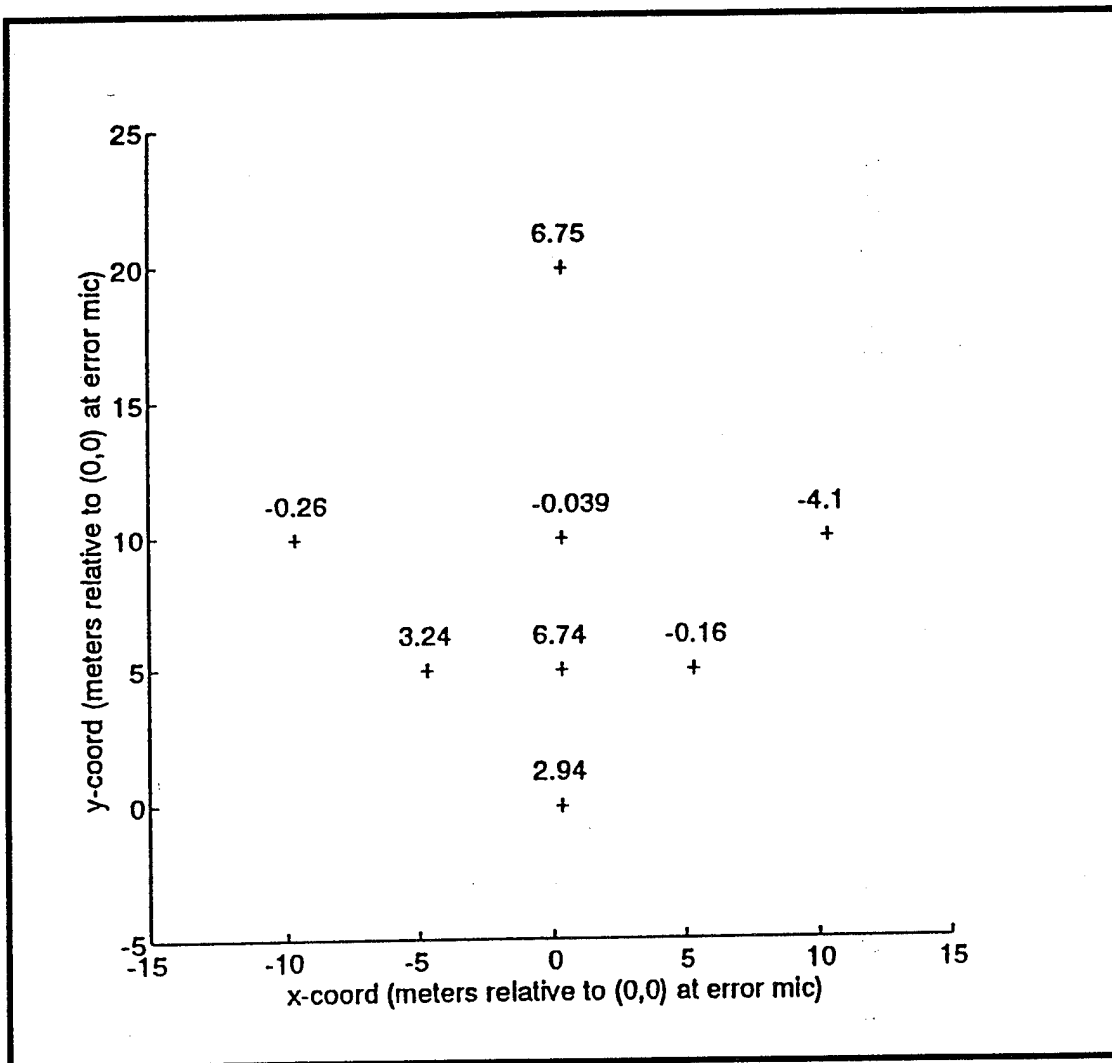


Figure 49. SPL Reductions in 100 Hz One-Third Octave Band, SI-SO Local ANR of Unsuppressed Jet Aircraft, Using WAS 3000; Control Source at (0,-53)m and Error Microphone at (0,0)m.

Global Active Noise Reduction

This section describes experiments of global ANR at the simulated hush house. Tests were conducted both using conventional loudspeakers and a WAS 3000 as control sources. For application to a full-scale hush house, conventional cabinet loudspeakers would not be sufficiently powerful for global ANR, as discussed in *Selection of Control Sources*; however, they were used in a global test at this smaller scale facility in order to gain understanding of the technical issues involved in global control of broadband noise.

Simulated Hush House With Conventional Loudspeakers

Active noise reduction of the simulated hush house was attempted using two Klipsch loudspeakers driven in parallel as a single control source in an SI-SO system. The loudspeakers were placed as close to the disturbance noise source as was practical. Figure 50 contains a diagram showing the configuration of the reference and error microphones and the control loudspeakers. The loudspeakers were placed on top of a scaffold approximately 3m high, which put them higher than the top of the exhaust deflector and almost at the same level as the error microphone and the microphones in the far-field array. The loudspeakers were approximately 3m from the exhaust deflector plate (and therefore approximately 8m from the jet engine exhaust nozzle). The reference microphone was about 0.5m above the ground, and about 0.5m from the deflector plate. The error microphone and field microphones were in the same locations as for the SI-SO local ANR tests described in *Single-Input, Single-Output Configuration*.

The control, reference, and error signals were all bandpass filtered between 25 and 200 Hz, thus determining the bandwidth of interest. The adaptive FIR control filter contained 100 coefficients, and the system identification was performed on the DSP board using a FIR filter containing 200 coefficients. The sample rate of the controller was 800 Hz, and the controller was allowed to converge for about 60 seconds.

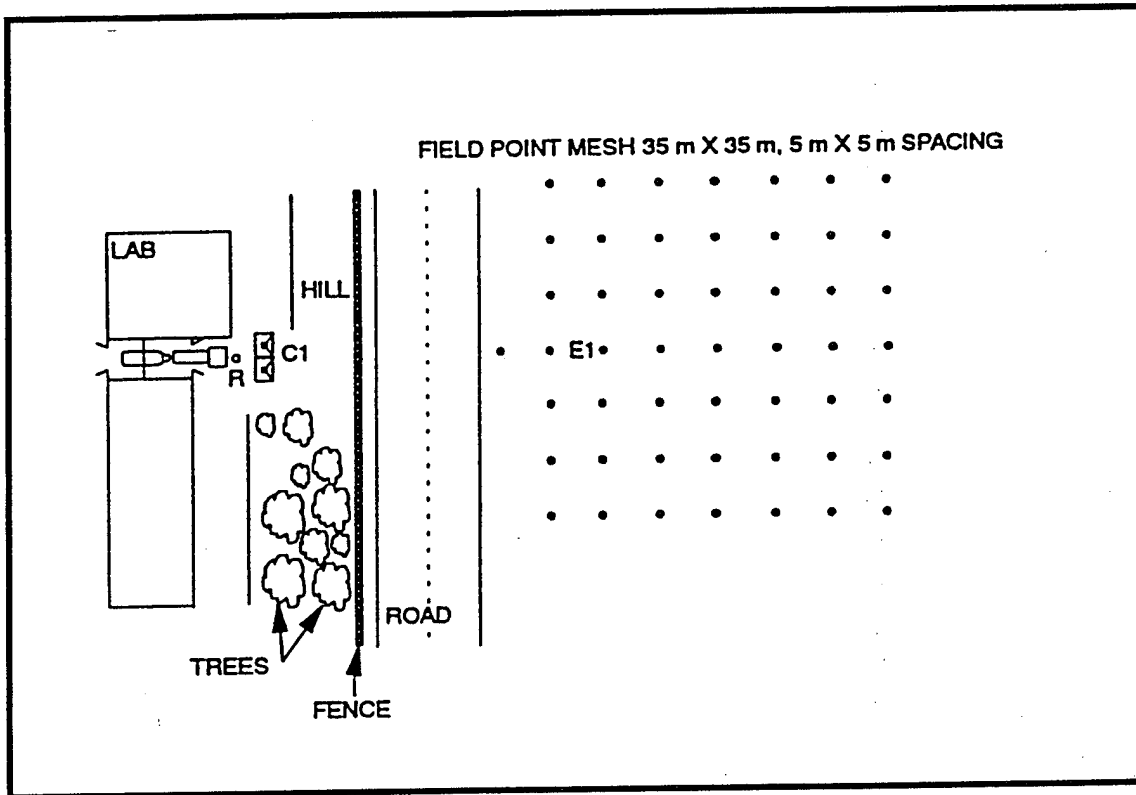


Figure 50. Configuration for SI-SO Global ANR of Simulated Hush House, Using Loudspeakers.

The coherence between the reference microphone and the error microphone, measured with the jet engine running in the hush house, is shown in Figure 51. This coherence is seen to be considerably lower than that in any of the local ANR experiments, since it was necessary to place the reference microphone so close to the disturbance source near the exhaust deflector. The coherence of white noise through the control loudspeakers to the error sensor is shown in Figure 52, and shows relatively good input to output coherence for the loudspeakers even though they were located farther away from the error microphone than for the local ANR tests.

The one-third octave band spectra for the error microphone before and after control are shown in Figure 53. The total reduction at the error microphone, integrated across the bandwidth, was 1.7 dB. The maximum reduction is about 3 dB in the one-third octave band with a center frequency of 50 Hz.

A contour plot showing the total SPL reduction over the field point matrix is shown in Figure 54, and the reduction contour plots in the one-third octave bands with center frequencies of 31.5 Hz and 50 Hz are shown in Figures 55 and 56, respectively. An extremely large area of attenuation, covering the entire 30m x 30m area, is evident with the global SI-SO control, but the amount of attenuation is much smaller than the reductions achieved in local ANR. The control performance is degraded due primarily to the poor reference to error coherence and feedback of the control loudspeaker output into the reference microphone signal. It is possible that somewhat greater reduction would have been shown with more powerful control loudspeakers.

Simulated Hush House With WAS 3000 Control Source

Global ANR of the simulated hush house was also attempted using the MOAS system, containing a WAS 3000, as the control source. For this experiment, the MOAS system was parked adjacent to the Turbo Lab building with the mouth of the horn approximately 2m from the exhaust deflector. The horn axis was approximately perpendicular to the augments tube axis; this orientation was chosen because it was the only practical way to fit the MOAS into the test facility. In this configuration, the effective center of the control source was very near the

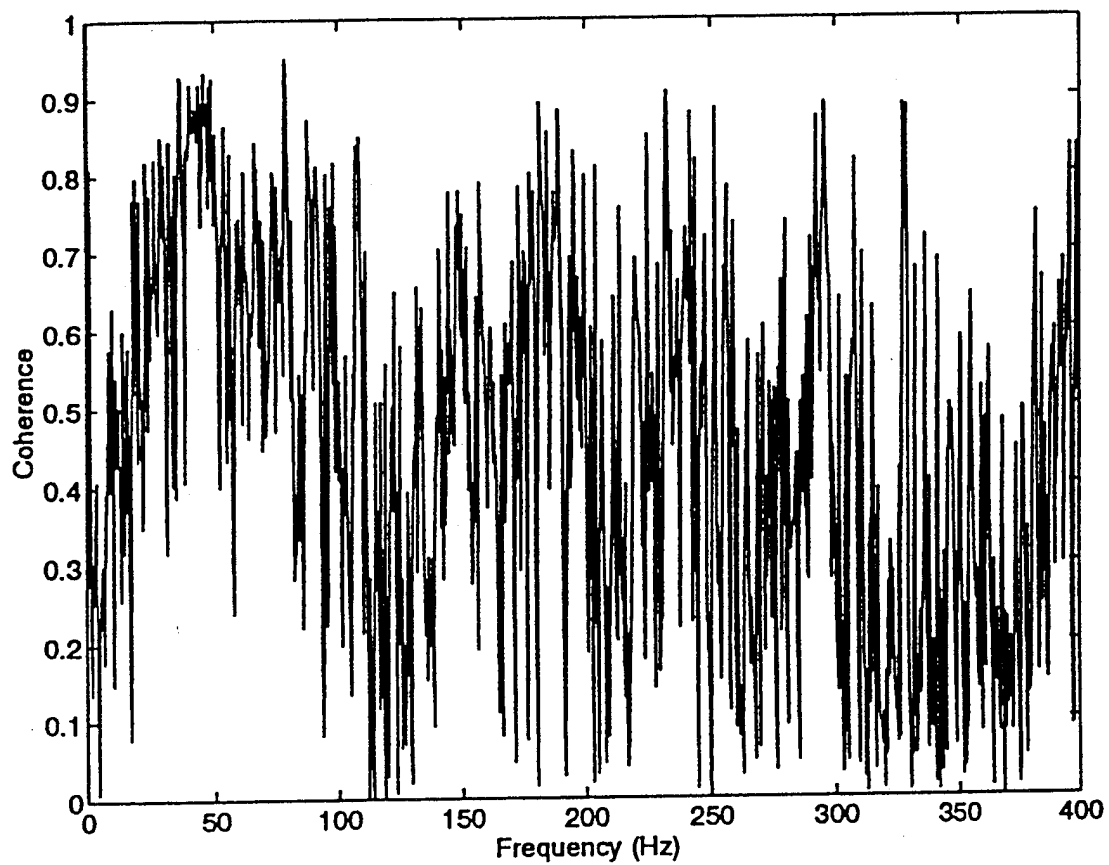


Figure 51. Coherence Between Reference Microphone and Error Microphone, SI-SO Global ANR of Simulated Hush House, Using Loudspeakers.

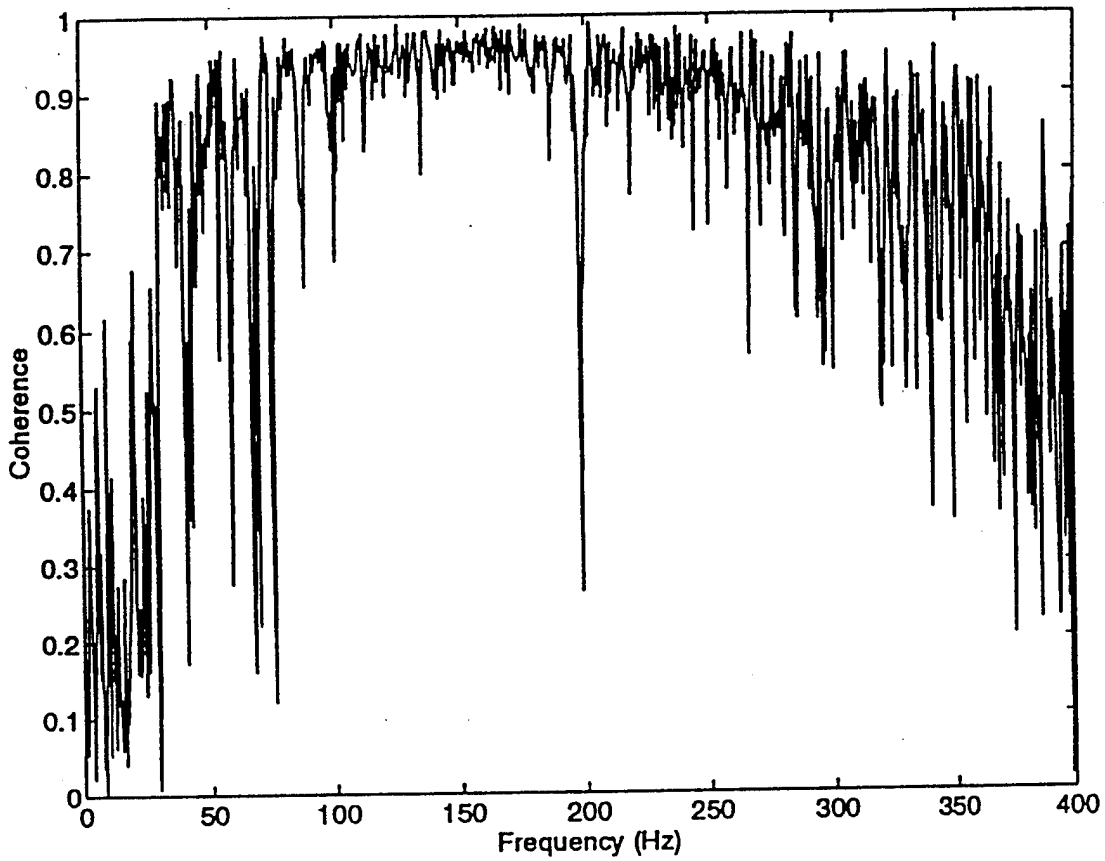


Figure 52. Coherence Between Input to Loudspeakers and Error Microphone, SI-SO Global ANR of Simulated Hush House.

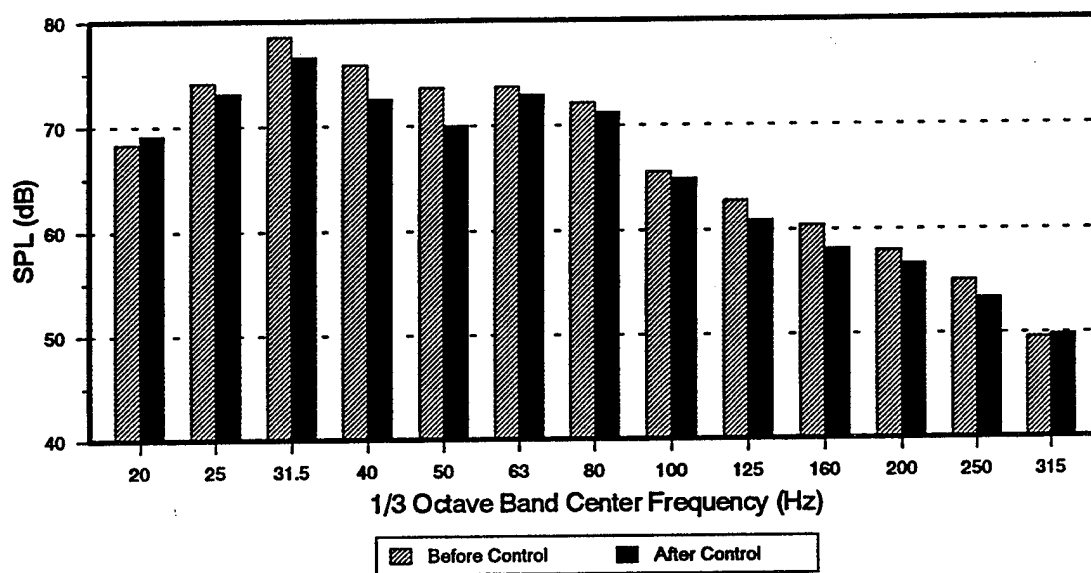


Figure 53. Error Microphone One-Third Octave Band Analysis, SI-SO Global ANR of Simulated Hush House, Using Loudspeakers.

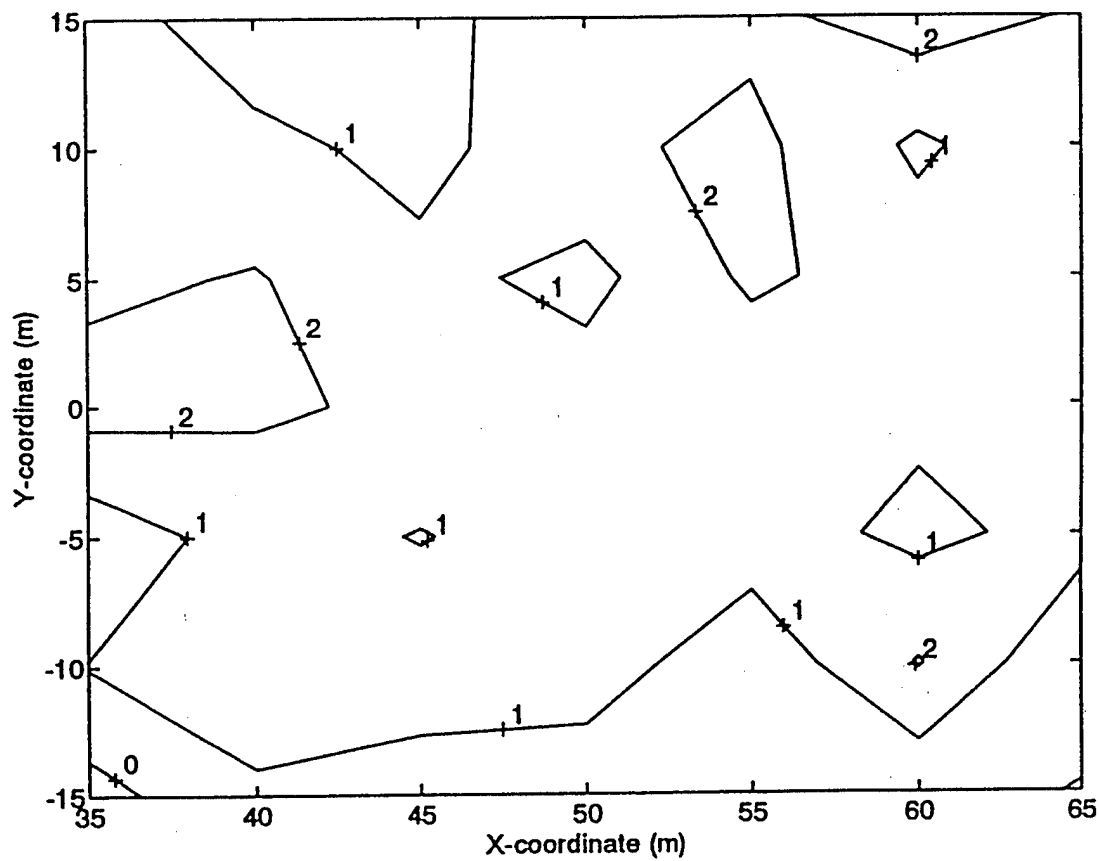


Figure 54. Total SPL Reduction Contours, SI-SO Global ANR of Simulated Hush House, Using Loudspeakers; Control Source at (8,0)m and Error Microphone at (40,0)m.

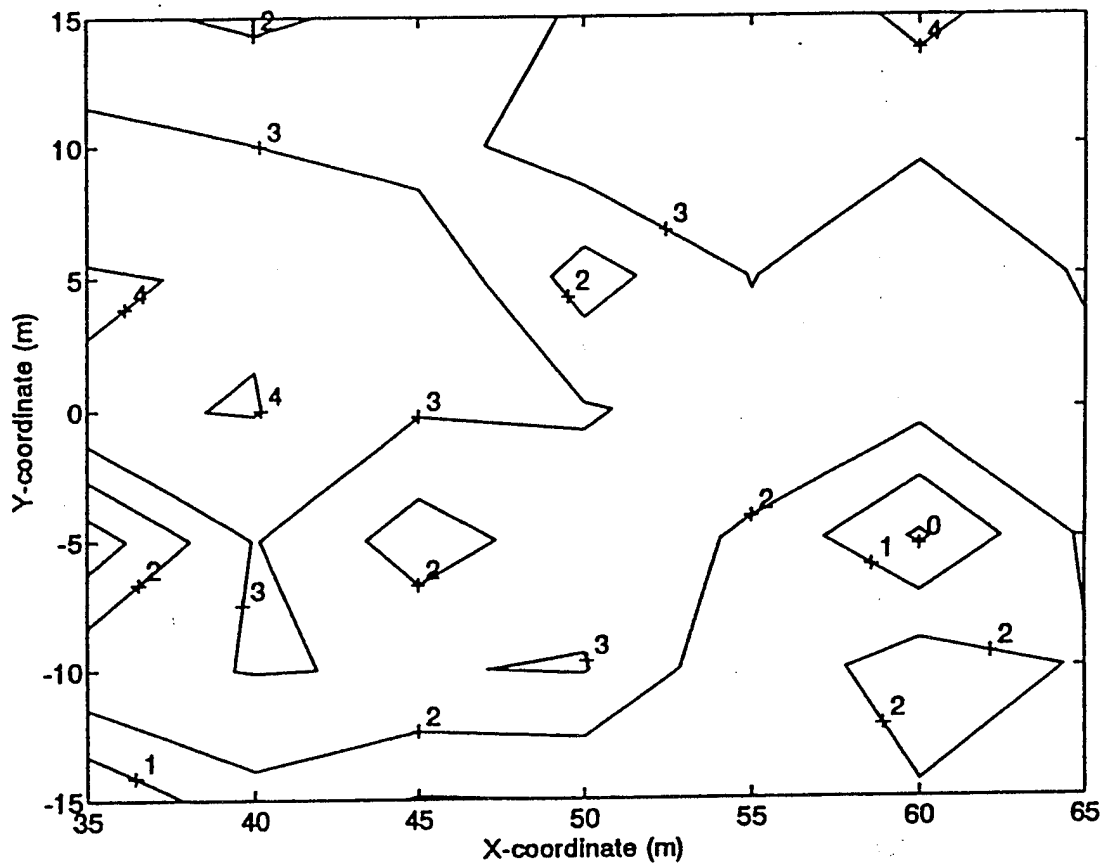


Figure 55. SPL Reduction Contours in 31.5 Hz One-Third Octave Band, SI-SO Global ANR of Simulated Hush House, Using Loudspeakers; Control Source at (8,0)m and Error Microphone at (40,0)m.

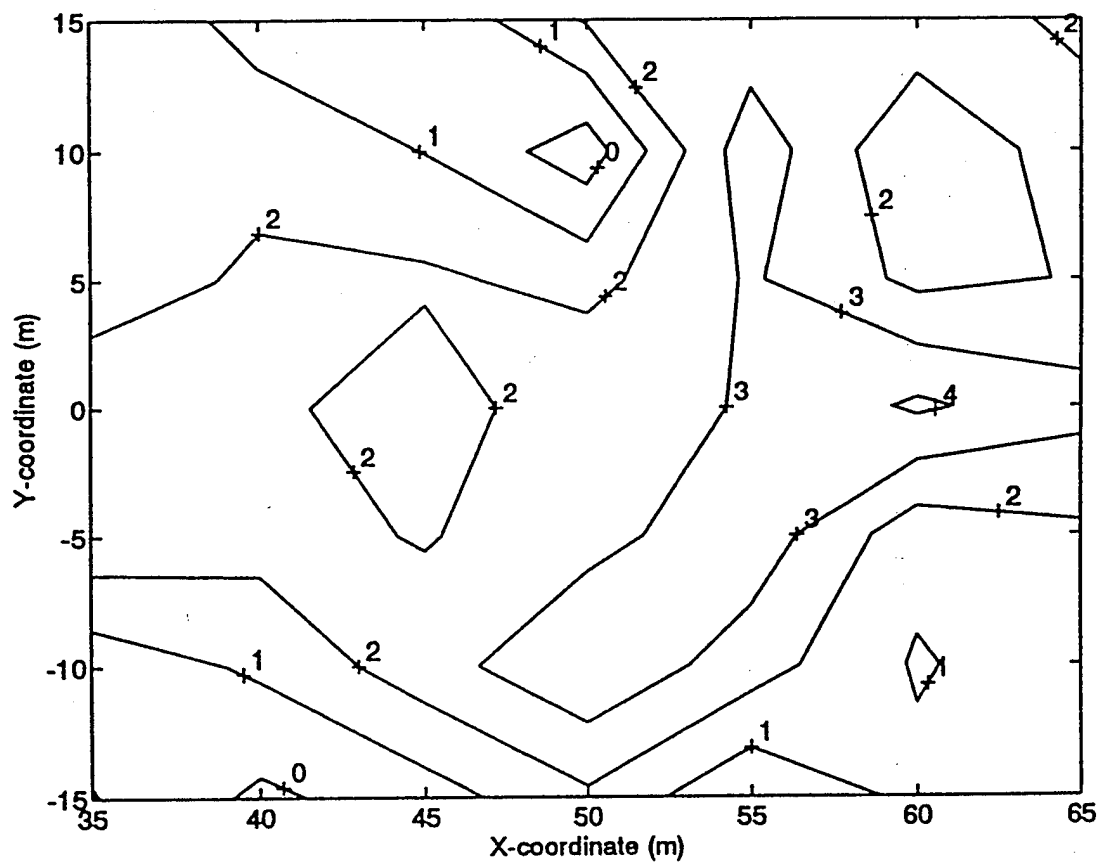


Figure 56. SPL Reduction Contours in 50 Hz One-Third Octave Band, SI-SO Global ANR of Simulated Hush House, Using Loudspeakers; Control Source at (8,0)m and Error Microphone at (40,0)m.

disturbance source, and the MOAS diesel engine and compressor were as far from the disturbance source as was practical. A picture showing the MOAS and the simulated hush house is shown in Figure 57.

Choice of a reference location involved many tradeoffs, involving coherence, feedback, and causality, as discussed in *The Importance of Reference and Error Signals*. The reference location was varied from the immediate vicinity of the exhaust deflector to the top of the hill. Although no reference location which met all the requirements was found, some results are presented here with the reference microphone at the top of the hill, similar to the location used in the majority of the local ANR tests. This position was chosen in order to maximize coherence. Figure 58 contains a diagram showing the configuration of the reference and error sensors and the MOAS horn which correspond to the data presented here.

The coherence between the reference microphone and the error microphone, with the jet engine running in the simulated hush house, is shown in Figure 59. The reference to error coherence is quite good, greater than 0.9, with the reference microphone at the top of the hill. However, this reference position is problematic on account of the causality issue; the reference microphone is not able to sense the disturbance early enough for the WAS 3000 control output to reach the error microphone in sufficient time.

The WAS 3000 was operated at virtually the bottom of its operating range, approximately 1.5 psi and 1.5 amps, in order for the control source noise level to be similar to that of the simulated hush house. At this operating point, the coherence through the MOAS over the 10 to 100 Hz frequency range is shown in Figure 60. Coherence values are relatively poor, in the range of 0.7 to 0.9 across most of the frequency range of interest.

Despite the obvious causality problem, control was attempted. The control, reference, and error signals were all bandpass filtered between 10 and 100 Hz, thus determining the bandwidth of interest. The adaptive FIR control filter used 100 coefficients, and the system identification was performed on the DSP board with a FIR filter containing 200 coefficients. The sample rate of the controller was 800 Hz. The controller went unstable in this experiment after approximately 90 seconds of

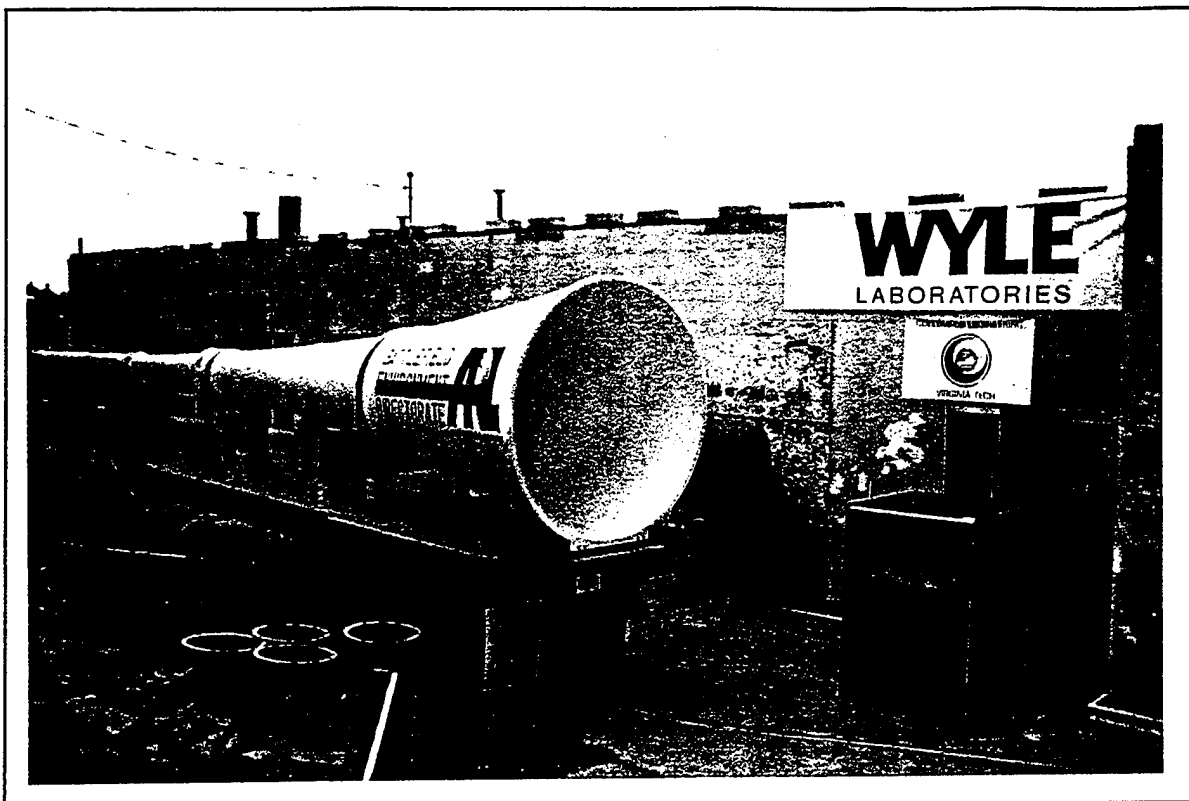


Figure 57. Photograph of Simulated Hush House and WAS 3000 Horn for Global ANR.

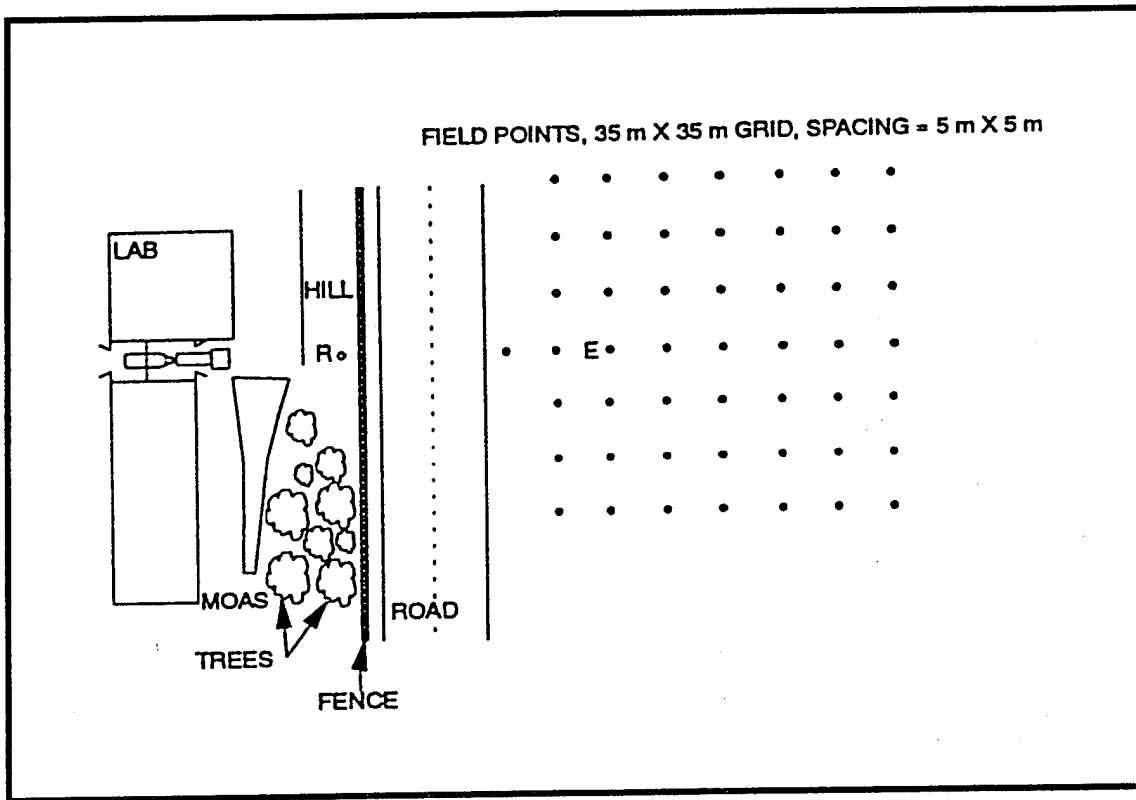


Figure 58. Configuration for SI-SO Global ANR of Simulated Hush House, Using WAS 3000.

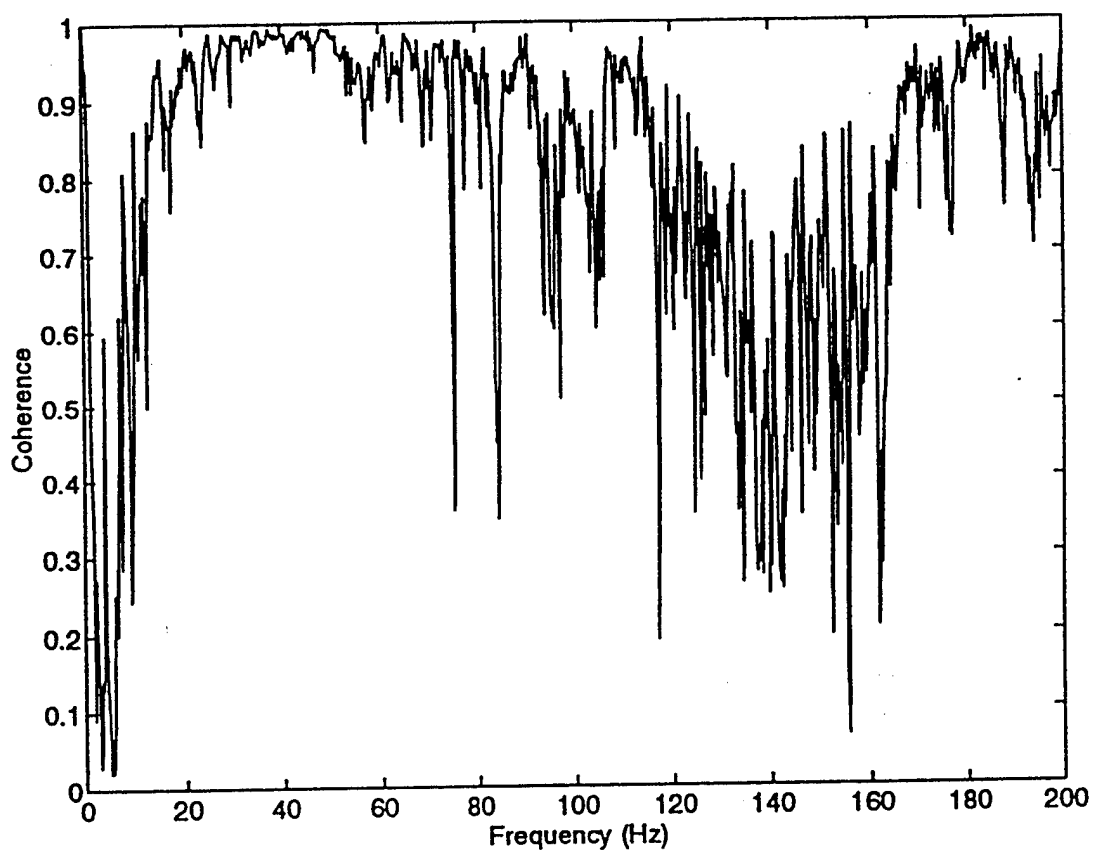


Figure 59. Coherence Between Reference Microphone and Error Microphone, SI-SO Global ANR of Simulated Hush House, Using WAS 3000.

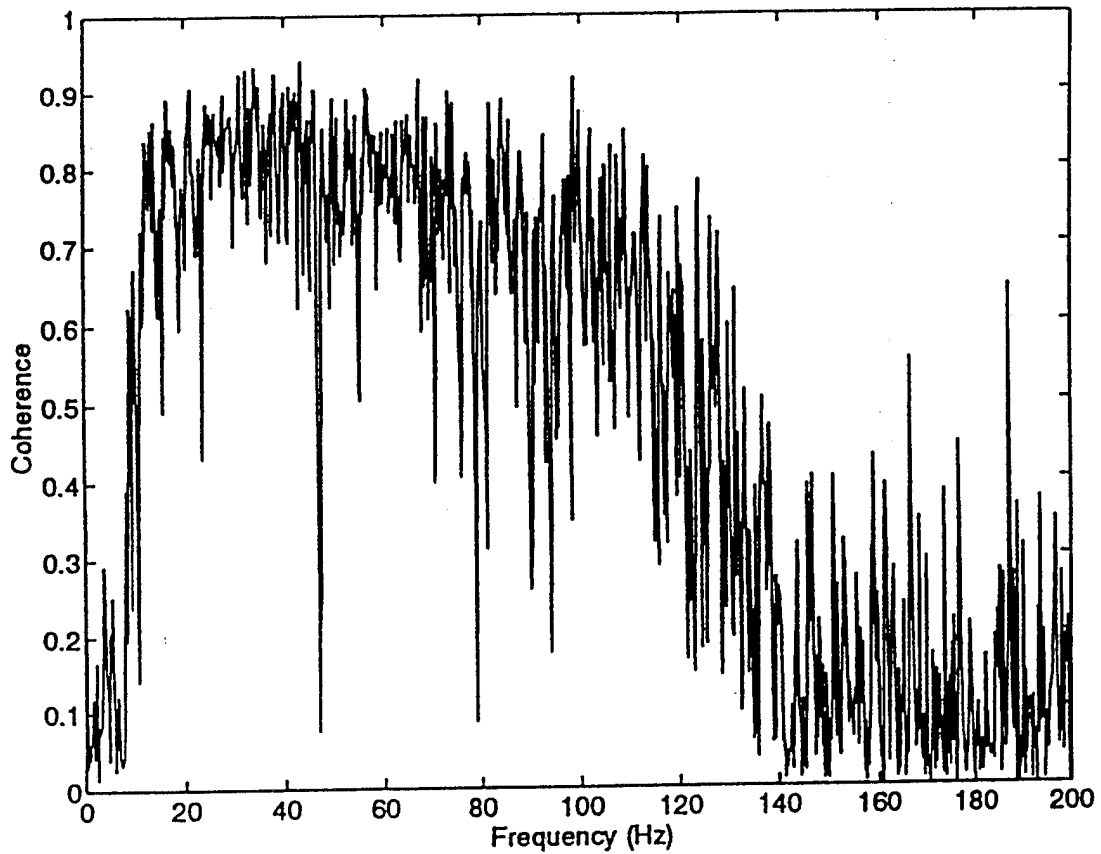


Figure 60. Coherence Between Input to WAS 3000 and Error Microphone, SI-SO Global ANR of Simulated Hush House, 10 to 100 Hz.

convergence. The one-third octave band spectra for the error microphone before control and just before the controller went unstable are shown in Figure 61. The reduction observed at the error microphone is only a few dB in some of the one-third octave bands; this probably represents random fluctuations rather than active control.

The global control experiment was repeated several times with a variety of reference microphone locations and with an accelerometer as a reference sensor, in attempts to reduce the causality and feedback problems. However, in most cases, the controller went unstable before any reduction was achieved, probably due to a combination of inadequate reference signal, acausality, control feedback, and the poor coherence of the WAS 3000 when operated at the low level needed for this application.

Attempts were made to address the control feedback problem by implementing a controller which utilized the feedback removal algorithm (discussed in Appendix A). However, use of this control code did not yield any significant improvements in noise reduction.

Potential of WAS 3000 as a Control Source

Although the global active noise reduction experiment using the WAS 3000 was not successful, the WAS 3000 was used as a control source, with some success, in application to local ANR, as described in *Unsuppressed Jet With WAS 3000 as Control Source*. However, no reductions were achieved in the local ANR experiment at frequencies below 50 Hz, where the real value of the WAS 3000 as a control source had been anticipated. Because the sound power level needed from the WAS 3000, in order to achieve ANR of the simulated hush house or the Saeta jet, was at the very low end of its operating range, this control source was rather poorly suited to the disturbance sources used in this program. However, at higher operating pressures and coil currents, suitable for application to louder disturbance sources such as actual hush houses, the WAS 3000 may be suitable.

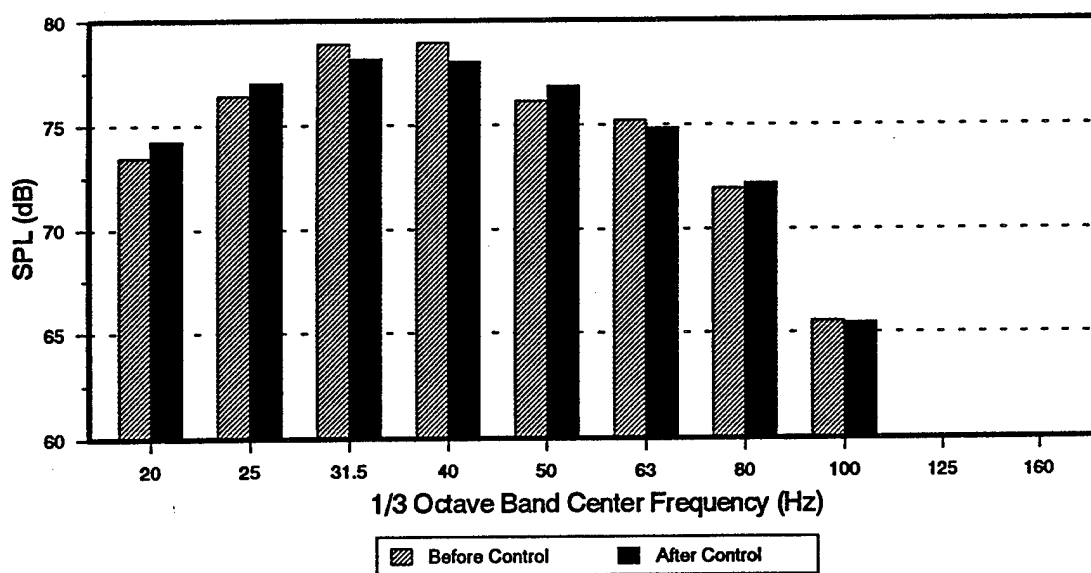


Figure 61. Error Microphone One-Third Octave Band Analysis, SI-SO Global ANR of Simulated Hush House, Using WAS 3000.

Coherence

It was suspected that the operation of the WAS 3000 at the low end of its operating range, and the resulting poor coherence values between the input and output of the WAS 3000, had contributed to the low levels of noise reduction achieved in local ANR. Poor coherence of the control source input and output can result in a non-linear control-to-error transfer function and thus a poor system identification (as described in Appendix A), as well as ineffective feedback removal, due to the inability to accurately model a non-linear or transitory control-to-reference transfer function. Therefore the coherence of the WAS 3000 and its potential as a control source were studied as a function of operating point, with emphasis on operation at high output levels.

Input to output coherence of the WAS 3000 was measured at a variety of pressure and current settings. With the WAS 3000 near the simulated hush house and an error microphone in the far field, as in the configuration shown in Figure 58, the coherence between white noise over a bandwidth of 10 to 200 Hz input to the WAS 3000 and the error microphone signal was measured. Figure 62 shows the coherence at 1.5 psi and 2 amps, similar to the level used in the previous ANR tests. Figure 63 shows the coherence of the WAS 3000 for the same configuration, but at an operating level of 2.5 psi and 4 amps. The coherence is markedly improved, to values of around 0.9, when the WAS 3000 is operated at the higher level, and there is less deviation of the coherence about the mean, especially on the frequency range between about 10 and 120 Hz. Additional tests over the higher range of operating points also indicated coherence values of 0.85 to 0.95 when the WAS 3000 is producing relatively high noise levels.

Feedback Removal

In order to demonstrate the ability of the controller to model the control-to-reference transfer function, and thus to remove the feedback of the control output into the reference signal, a feedback removal test was performed where the only task of the controller was to remove the control feedback into the reference microphone. (The feedback removal algorithm is described in Appendix A.) The reference microphone was located near the top of the hill similar to the location shown in Figure 58.

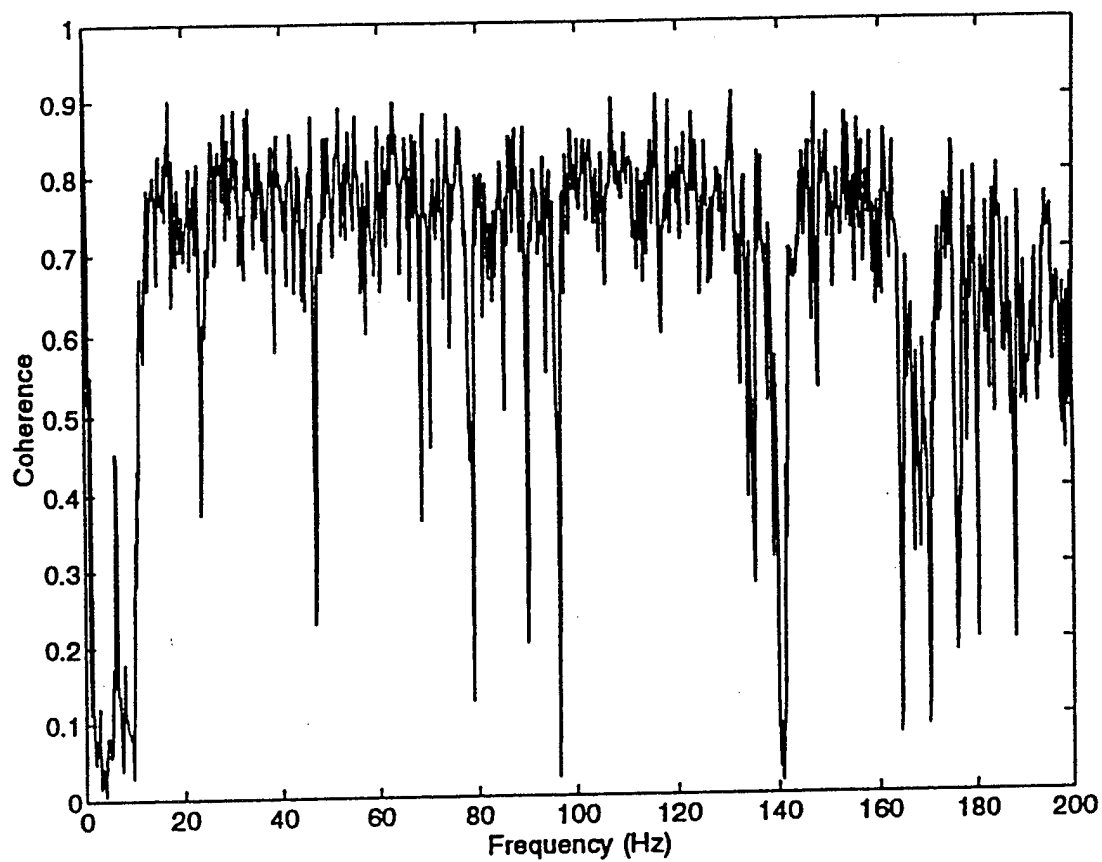


Figure 62. Coherence Between Input to WAS 3000 and Error Microphone, WAS 3000 at 1.5 psi and 2 amps.

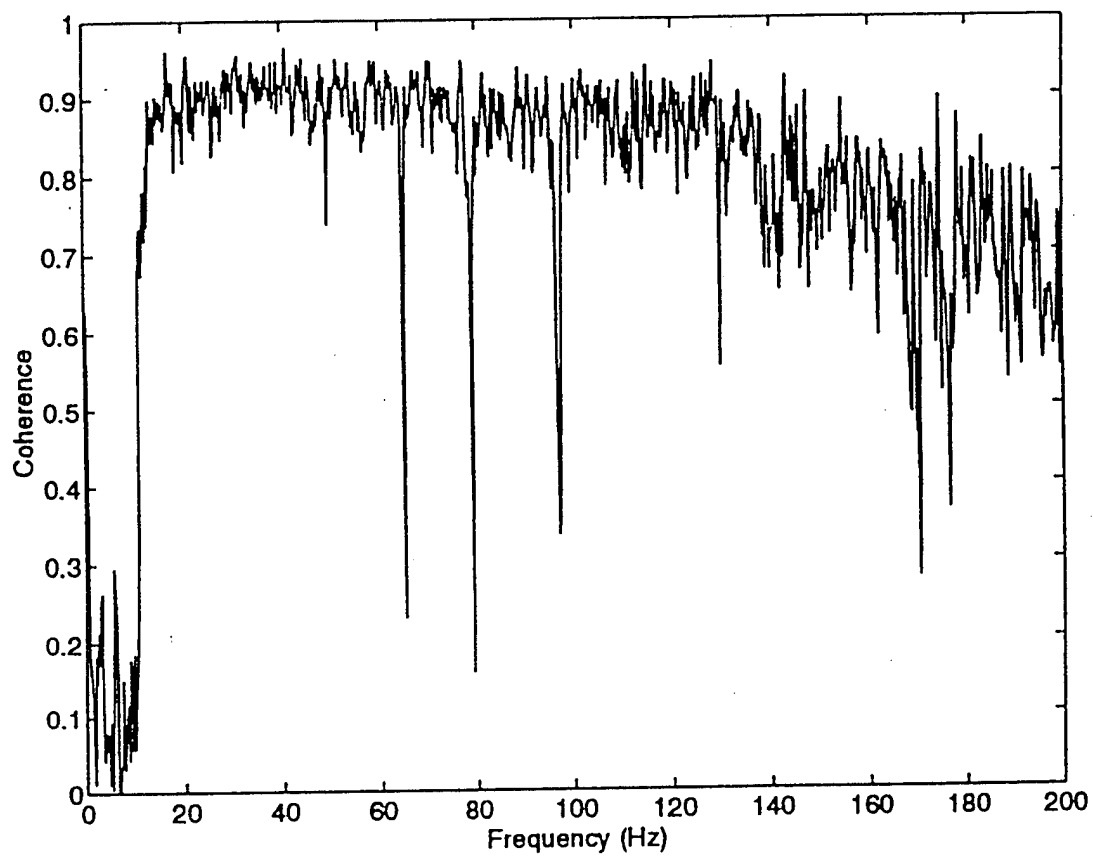


Figure 63. Coherence Between Input to WAS 3000 and Error Microphone, WAS 3000 at 2.5 psi and 4 amps.

A number of tests were conducted over a range of pressure and current settings. For the data shown here, the WAS 3000 was set to operate at 3.5 psi and 2 amps. The bandwidth was 10 to 100 Hz, and an adaptive controller was utilized to model the control-to-reference transfer function in order to evaluate how much feedback could be removed from the reference signal. The coherence between input to the WAS 3000 and reference microphone signal is shown in Figure 64.

A white noise signal over a bandwidth of 10 to 100 Hz was input to the WAS 3000 and the same electrical signal was used as the reference for the adaptive controller. Therefore the controller was attempting to predict the control source output with perfect knowledge of the signal input, and then to subtract the predicted signal from the measured signal. The resulting one-third octave band levels from the reference microphone signal, filtered by the controller, before and after feedback removal, are shown in Figure 65. From 6 to 12 dB of feedback removal was achieved in the one-third octave bands with center frequencies in the bandwidth of interest.

This test demonstrates the ability of the controller to design a filter which models the control-to-reference transfer function and then to remove a significant amount of the control output effects from the reference signal, when the WAS 3000 is operated at high levels. Thus it shows that the WAS 3000 output can be predicted and feedback removal can be performed if the WAS 3000 is operated at high output levels.

Control of a Broadband Disturbance at High Sound Level

A test was performed to evaluate the potential of the WAS 3000 as a control source for ANR when used to cancel high sound levels. The concept was to create a disturbance loud enough so that it was necessary to operate the WAS 3000 at a high level in order to cancel the disturbance. The configuration for this test is shown in Figure 66. The disturbance in this case was two Klipsch loudspeakers driven together at full power with white noise over a bandwidth of 25 to 100 Hz. The control source was the WAS operated at 3.5 psi and 6 amps. The reference signal was taken directly from the output of the same signal generator which was used as the disturbance signal and sent to the Klipsch loudspeakers. The signal to the disturbance speakers was given an additional delay, sufficiently long to produce a causal system.

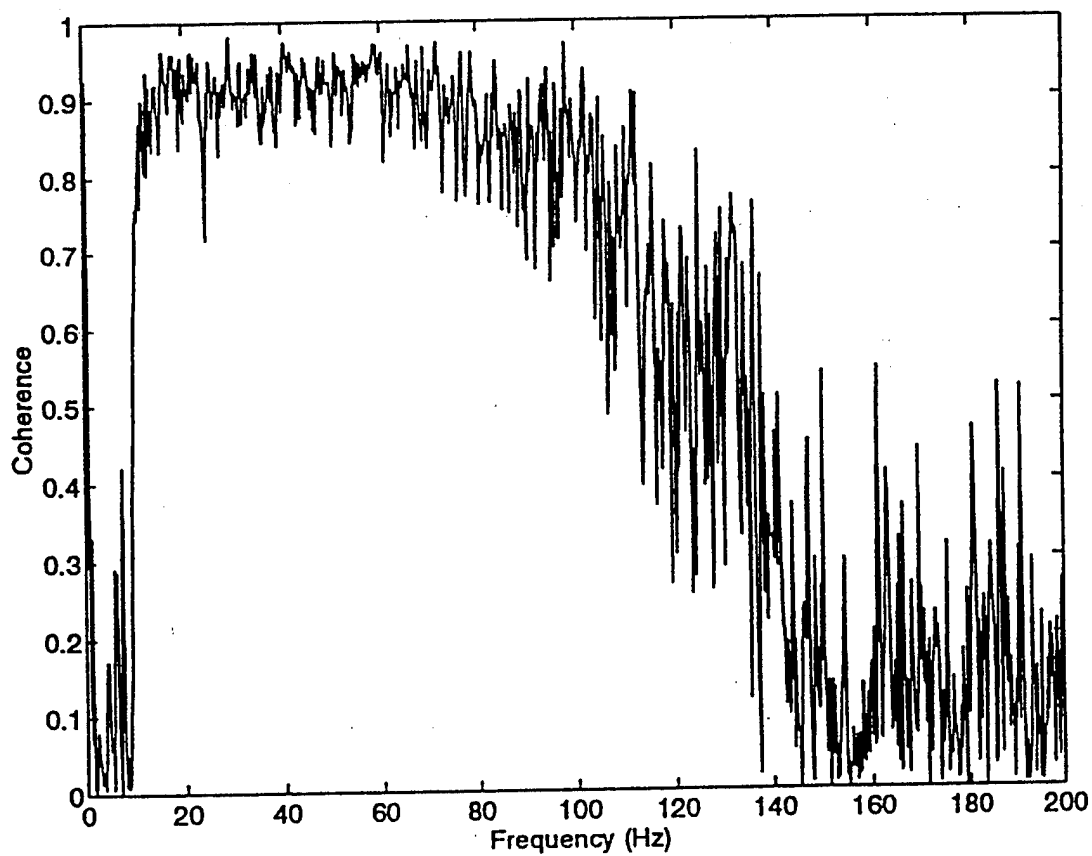


Figure 64. Coherence Between Input to WAS 3000 and Reference Microphone, WAS 3000 at 3.5 psi and 2 amps, Bandwidth = 10 to 100 Hz.

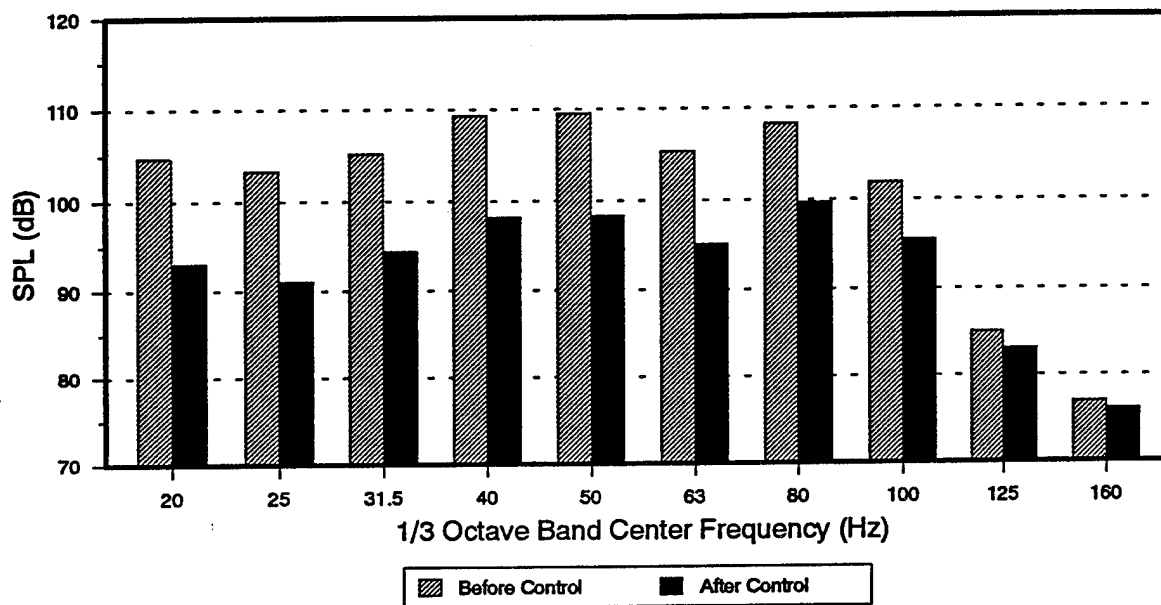


Figure 65. Reference Microphone One-Third Octave Band Analysis of Feedback Removal, WAS 3000 at 3.5 psi and 2 amps, Bandwidth = 10 to 100 Hz.

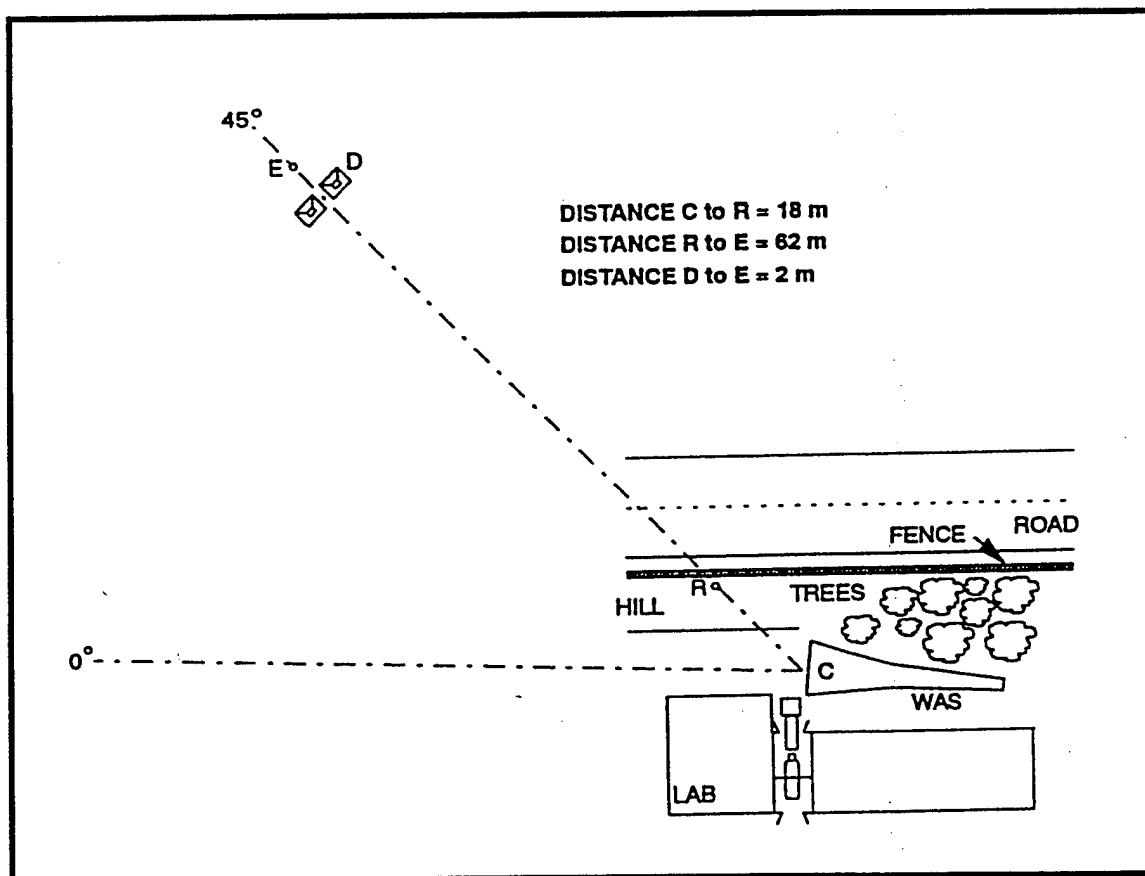


Figure 66. Configuration for ANR of Loudspeaker Noise at High Level, Using WAS 3000; Reference Microphone Not in Use.

The coherence of the input and output of the WAS 3000 and the input and output of the loudspeakers used as the disturbance are shown in Figures 67 and 68, respectively. Thus Figure 67 shows the control source coherence and Figure 68 represents the reference-to-error coherence. The resulting error signal before and after control is shown by one-third octave band levels in Figure 69. Reductions of 8 to 14 dB were achieved in the one-third octave bands where the error level was highest before control.

These tests demonstrate that the WAS 3000 can be used for ANR if operated at sufficiently high levels to result in good input to output coherence. Therefore, if a WAS 3000 were implemented as a control source for ANR of an extremely loud disturbance, such as an actual military hush house facility, it is possible that global ANR could be achieved.

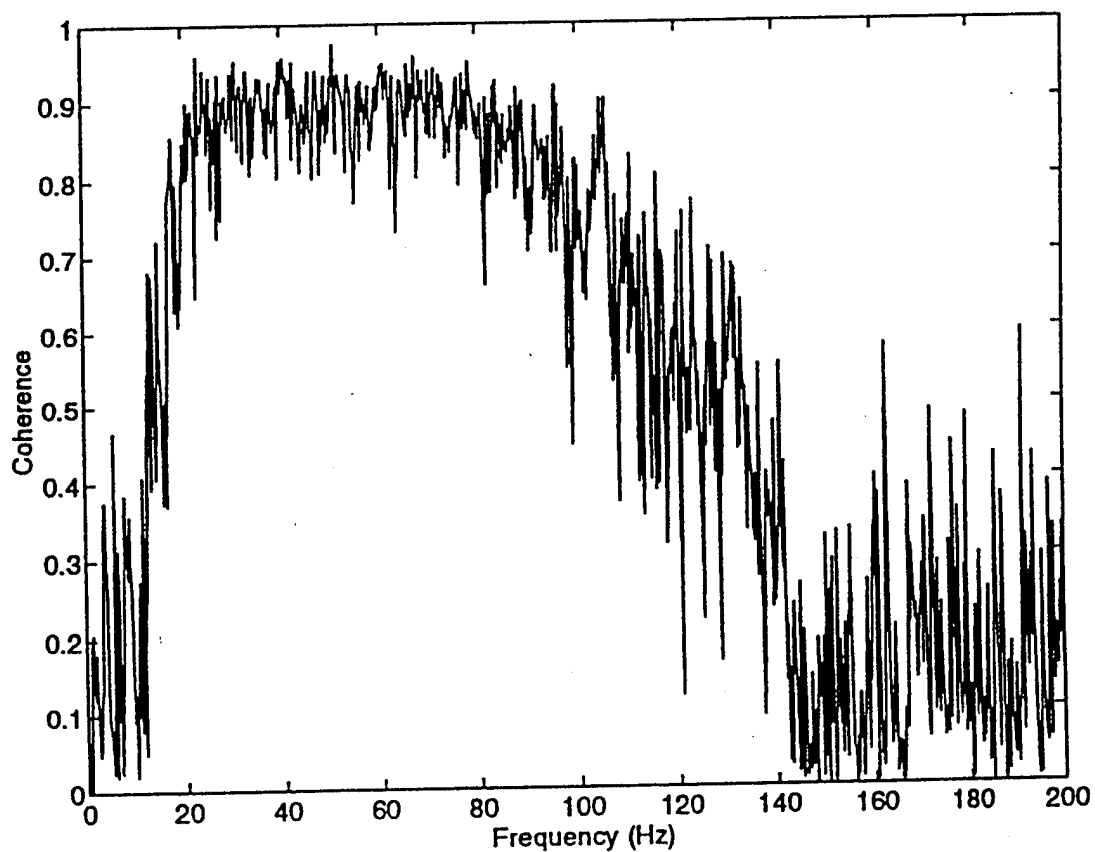


Figure 67. Coherence Between Input to WAS 3000 and Error Microphone, ANR of Loudspeaker Noise at High Level, WAS 3000 at 3.5 psi and 6 amps, Bandwidth = 10 to 100 Hz.

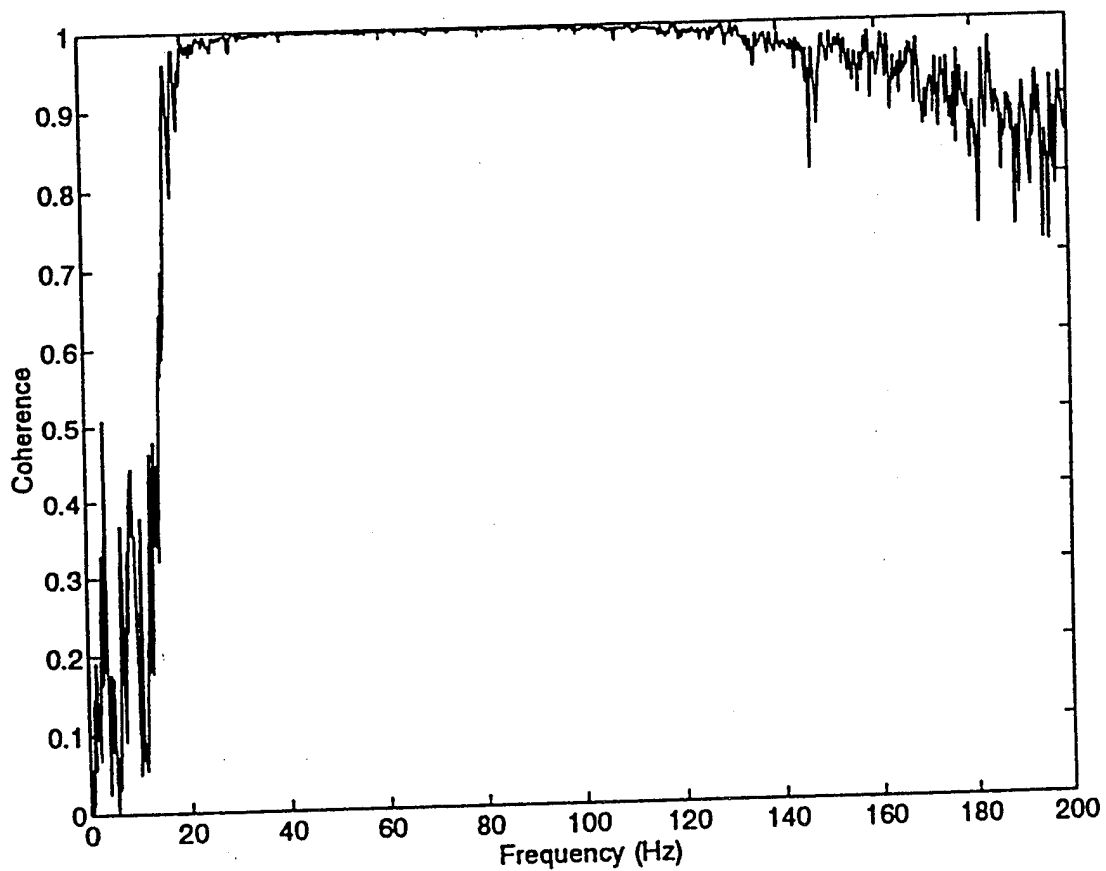


Figure 68. Coherence Between Input to Disturbance Loudspeakers (Reference Signal) and Error Microphone, ANR of Loudspeaker Noise at High Level.

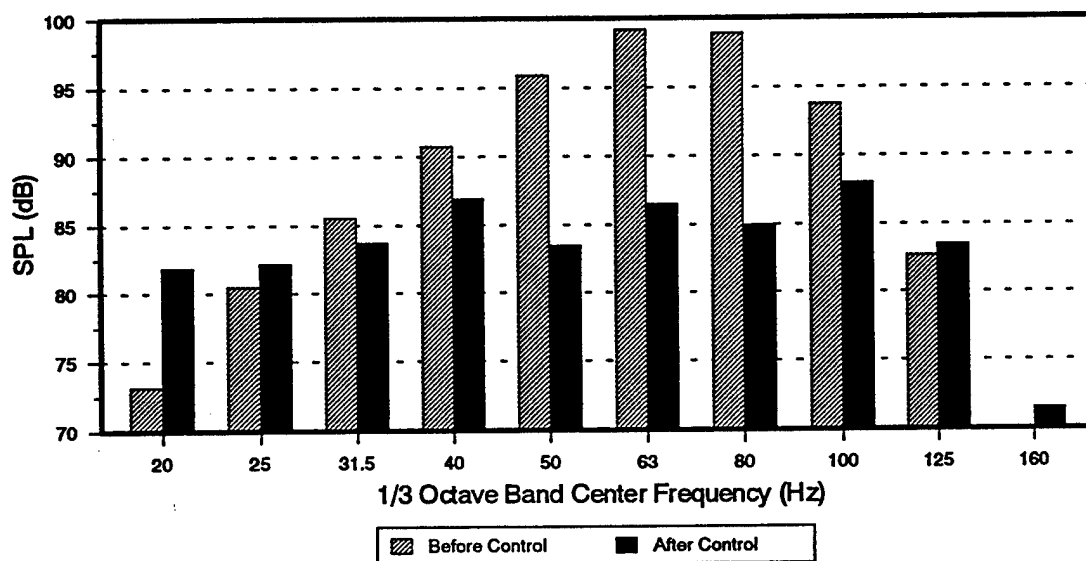


Figure 69. Error Microphone One-Third Octave Band Analysis, ANR of Loudspeaker Noise at High Level, Using WAS 3000, Bandwidth = 25 to 100 Hz.

CONCLUSIONS

The results of this study demonstrate that active noise reduction techniques can be used to significantly attenuate broadband, low-frequency jet engine runup noise from test cells and unsuppressed engines. When low-frequency noise reduction is attempted over a specific localized area at some distance from the engine exhaust, one-third octave band noise reductions of up to 15 dB can be obtained. One-third octave band noise reductions of 5 dB or greater can be achieved over areas in excess of 20m x 25m. Areas of effective noise reduction can be successfully predicted with an analytical model.

The study shows that the reduction of jet engine runup noise over a specific localized area is easier to achieve than global noise reduction when a feedforward control algorithm is applied. One major reason for this is the relative ease of obtaining an adequate reference signal for the active controller when a reference microphone is placed at some distance away from, rather than in the immediate vicinity of, the jet exhaust.

In addition, the study provides evidence that a high-intensity electropneumatic noise source, in this case the WAS 3000, may produce adequate sound power and may have sufficient linearity to be effectively used as a control source for the active reduction of low-frequency noise from Air Force hush houses.

The results of this study are promising, and additional investigation of both local and global active noise reduction is recommended. One focus of research should be enlarging the area over which noise reduction is achieved at large distances from jet noise sources. In addition, experiments using a full-scale hush house and military aircraft should be conducted to demonstrate that the ANR technique can be successfully applied on a military air field.

REFERENCES

1. Lee, R.A., "Far-Field Acoustic Data for the Texas ASE, Inc., Hush House," AFAMRL-TR-81-148, April 1982.
2. Leug, P., "Process of Silencing Sound Oscillations," U.S. Patent No. 2043416, 1936.
3. Eriksson, L.J., *et al.*, "Active Noise Control on Systems With Time-Varying Sources and Parameters", *Sound and Vib.*, July 1989.
4. Nelson, P.A., and Elliott, S.J., *Active Control of Sound*, Academic Press Ltd, London, 1992.
5. Stevens, J., and Ahuja, K., "The State-of-the-Art in Active Noise Control", AIAA Paper #90-3924, 13th AIAA Aeroacoustics Conference, October 1990.
6. Guicking, D., "Recent Advances in Active Noise Control," Second International Congress on Recent Developments in Air- and Structure-borne Sound and Vibration, Auburn Univ., 1992
7. Hasebe, M., *et al.*, "Study on Active Noise Control in Three-Dimensional Space Using Digital Signal Processor", *Inter-Noise 89*, 455-458.
8. Peterson, D.K., Weeks, W. A., Nowlin, W.C. , "Active Control of Complex Noise Problems Using a Broadband, Multichannel Controller," Proceedings of Noise-Con 94, Ft Lauderdale, FL, pp. 315-320.
9. Angevine, O.L., "Active Cancellation of the Hum of Large Electric Transformers," Proceedings of Inter-Noise 92, Toronto, Canada, pp. 313-316.
10. Hill, P.D., and Wheeler, R.J., "Application of Active Control to Combustion Turbine Exhaust Noise - Summary Report", STC Report 90-ITM5-ACTEX-R1, Westinghouse STC, Pittsburgh, PA, April 1992.
11. Nelson, P.A., and Elliott, S.J., "The Minimum Power Output of a Pair of Free-Field Monopole Sources", *J. Sound Vib.*, 105 (1), 173-178, 1986.
12. Vipperman, J.S., Burdisso, R.A., and Fuller, C.R., "Causality Analysis of Feedforward-Controlled Systems With Broadband Inputs", *J. Acoust. Soc. Am.*, 94 (1), 234-242, July 1993.
13. Meyer, W.A., "Theoretical Analysis of the Performance of an Air-Modulated Speaker," *J. Acoust. Soc. Am.*, 45 (4), 957-965, 1969.
14. Chapman, C.J., and Glendinning, A.G., "A Theoretical Analysis of a Compressed Air Loudspeaker," *J. Sound Vib.*, 138 (3), 493-499, 1990.

REFERENCES (Continued)

15. Glendinning, A.G., Elliott, S.J., and Nelson, P.A., "A High-Intensity Acoustic Source for Active Attenuation of Exhaust Noise," ISVR Technical Report No. 156, University of Southampton, UK, 1988.
16. Glendinning, A.G., Nelson P.A., and Elliott, S.J., "Experiments on a Compressed Air Loudspeaker," *J. Sound Vib.*, 138, 479-491, 1990.
17. Sabatier, J.M., "Pneumatic Loudspeaker Acoustic Generation System," National Center for Physical Acoustics, University of Mississippi, NCPA Report No. JMS91-01, Contract DACA 88-90-D-0047, December 1991.
18. Sabatier, J.M., "Acoustical Characterization of the Mother of All Speakers," National Center for Physical Acoustics, University of Mississippi, NCPA Report No. JMS0593-1, Contract DAAD 07-91-C-0139, May 1993.
19. Kennedy, B.W. *et al.*, "Mobile Acoustic System (MOAS) Field Characterization," Draft Report, U.S. Army Research Laboratory, White Sands, NM, 1993.
20. Eriksson, L.J., and Allie, M.C., "A Digital Sound Control System for Use in Turbulent Flows," Proceedings of Noise-Con 87, State College, PA.
21. Wang, J.S., and Crocker, M.J., "Tubular Windscreen Design for Microphones for In-Duct Fan Sound Power Measurements," *J. Acoust. Soc. Am.*, 55 (3), 568-575, March 1974.
22. Neise, W., "Theoretical and Experimental Investigations of Microphone Probes for Sound Measurements in Turbulent Flow," *J. Sound Vib.*, 39 (3), 371-400, April 1975.

APPENDIX A

Control Algorithm

Principles of Operation

The adaptive controller used in these experiments is a variable coefficient finite impulse response (FIR) filter adapted by a feedforward filtered-x least mean square (LMS) algorithm.^{A1,A2} The ability of such control systems to "adapt" or change in response to changes in their environment makes them useful in a wide range of applications which require a robust control system.

A block diagram of the control system for the single-input, single-output (SI-SO) case is shown in Figure A-1. The control signal time sequence u_k is obtained by filtering a reference signal, which is coherent with the disturbance signal x_k , through an adaptive finite impulse response (FIR) filter, $W(z)$. The output of an adaptive FIR filter is a linear combination of the input sequence and a number of adaptive filter coefficients. It is assumed here that the reference signal is an accurate representation of the disturbance signal and that there is no feedback from the control source into the reference signal. That is,

$$u_k = \sum_{j=0}^L W_{j,k} x_{k-j} \quad (A-1)$$

where $W_{j,k}$ is the j 'th filter coefficient at the k 'th time step, L is the FIR filter order and the subscript k indicates a signal sample at time t_k . Since the transfer function of a FIR filter contains only zeroes and no poles, where the zeroes are the roots of the numerator and poles are the roots of the denominator, the FIR is inherently stable. The filter output can also be expressed in convolution form as $u = W(z) * x_k$, where $*$ denotes convolution.

The boxes T_{de} , the disturbance path transfer function, and T_{ce} , the control path transfer function, in Figure A-1 describe the relationships between the disturbance and error signals and the control and error signals, respectively. These transfer functions represent the changes in the signals due to physical propagation of the acoustic waves, the frequency response of the control source, and the frequency response of the error transducer. The signal d_k represents the acoustic signal from

the disturbance source as it reaches the error sensor, as a function of the time step, k . The signal y_k represents the acoustic output of the control source resulting from the control input u_k . The error signal e_k is the sum of the signals from the disturbance and control sources.

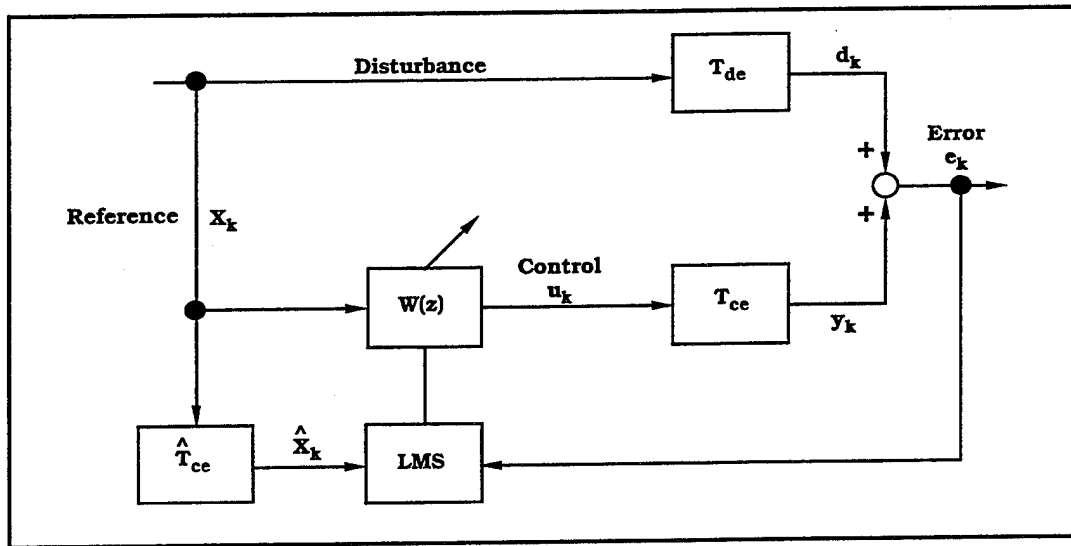


Figure A-1. Block Diagram of SI-SO Adaptive Feedforward Control System.

The error signal, e_k , is supplied to the controller by a microphone in the acoustic field. The set of filter coefficients W_j are updated at each time step by the controller in order to minimize a cost function, which is representative of the quantity to be minimized, in this case acoustic pressure. The cost function is formed as the mean square value of the error signal as follows:

$$C(W_j) = E[e_k^2] \quad (A-2)$$

where $E[\cdot]$ is the expected value operator. It can be shown that the equation above defines a quadratic surface, expressed as a function of the FIR filter weights, although the derivation is not presented here. The minimum of this surface may be found using a gradient descent method.

The gradient of the mean-square error function can be found by differentiating with respect to the weighting coefficients, W . Setting the partial derivative equal to zero, a solution can be obtained for the optimal weighting coefficients necessary to minimize the mean-square error. However, this solution requires performing a matrix inversion, which is computationally intensive; therefore the controller does

not use this method to find the optimal coefficients. Instead, a method of steepest descent is employed, using the quadratic surface defined by the cost function. The Least Mean Square (LMS) descent algorithm uses an estimate of the gradient based on instantaneous values of the error and reference signals, and has been shown to converge to the optimal solution.^{A3}

The result of the application of the Least Mean Square (LMS) algorithm to minimize the cost function yields a set of recursive equations to update the filter coefficients at each time step. The derivation can be found in detail in the references^{A4,A5} and is not presented here for brevity. The filter update equation for the single-input, single-output (SI-SO) case is

$$W_{j,k+1} = W_{j,k} - 2\mu e_k \tilde{x}_{k-j}; \quad j = 0, 1, \dots, L \quad (A-3)$$

where the signal \tilde{x}_{k-j} is known as the filtered-x signal, or filtered reference, and μ is a convergence parameter which controls the rate of convergence toward the optimal solution and the stability of the minimization process. Gradual convergence by a series of relatively small steps can ameliorate the effects of gradient and measurement noise, in many practical cases. The LMS algorithm requires a knowledge of both the error signal and the filtered-x signal.

In practice, the effect of the LMS algorithm on the spectrum of the error signal is a reduction of levels at the frequencies which contribute the most energy to the overall spectrum, since they make the greatest contribution to the cost function. Therefore spectral peaks tend to be attenuated first.

Since it takes a finite amount of time for the acoustic signal to propagate from the control source to the error microphone, it is necessary for the controller to account for this associated transfer function. The finite propagation time results in a phase and magnitude alteration which, if not accounted for, may create system instabilities or poor system performance.

The filtered-x version of the LMS algorithm accounts for this by modifying the reference signal input, x_k , by an estimate of the appropriate control path transfer function, indicated as \hat{T}_{ce} in Figure A-1, before supplying the signal to the FIR filter. This transfer function must be known in order to obtain the filtered-x signal; therefore an estimate of the control path transfer function T_{ce} is necessary before

control can be initiated. In practice, the control path transfer function is commonly identified experimentally for the actual system, and then modelled, as described in the following subsection of this appendix.

While these equations describe a system with a single input and single output, they can readily be expanded to describe a system with multiple inputs and multiple outputs.

For a multiple-input, multiple-output (MI-MO) controller, the reference signal is fed forward to an array of adaptive FIR filters whose outputs drive N_c control actuators. The filter coefficients are updated to minimize a cost function that is now defined as the sum of the mean square value of the error signals. That is,

$$C = \sum_{s=0}^{N_s} E [(e_s)_k^2] \quad (A-4)$$

where $(e_s)_k$ is the s 'th error sensor signal, and N_s is the number of error sensors.

The update equation for the filter coefficients can be shown to be as follows:^{A2}

$$W_{rj}(k+1) = W_{rj}(k) - 2\mu \sum_{s=1}^{N_s} (e_s)_k (\tilde{x}_{rs})_{k-j} \quad j=0,1,\dots,L \quad r=1,\dots,N_c \quad (A-5)$$

where $(\tilde{x}_{rs})_k$ is the disturbance signal filtered by the transfer function between the r 'th control actuator and the s 'th error sensor. Thus it is clear from Equation (A-5) that there are $N_s \times N_c$ transfer functions that need to be measured and modelled with digital filters.

System Identification of the Control Path Transfer Function(s)

An estimate of the control path transfer function, i.e., a "system identification," is necessary to obtain the filtered reference signal. The estimate is obtained by experimentally measuring the transfer function and then modelling it with either a FIR or an infinite impulse response (IIR) filter. An IIR filter is a recursive filter, in that the filter output is a function of both the input sequence and the output sequence. The IIR filter model is expressed as:

$$\hat{T}_{ce}(z) = \frac{B(z)}{1 + A(z)} = \frac{b_0 + b_1 z^{-1} + \dots + b_m z^{-m}}{1 + a_1 z^{-1} + a_p z^{-p}} \quad (A-6)$$

which has m zeroes and p poles, where the zeroes are the polynomial roots of the numerator and poles are the roots of the denominator. Since both zeroes and poles are included, a IIR filter is capable of accurately modelling a transfer function with sharp resonances and anti-resonances; for example, those characteristic of the vibration of lightly damped structures. An IIR filter may be much more efficient and more accurate than an FIR filter, with only zeroes and no poles, at modelling certain transfer functions. However, a disadvantage of IIR filters is that they are subject to instability if any of the poles are unstable.

Two methods of obtaining a digital model of the control path transfer function were used in this study: an "off-line" method and an "on-line" method. In the "off-line" method, the control source is first driven with white noise, the transfer function between the control input and the error sensor output is measured, and an IIR or FIR filter is designed, using a separate computer program, to model this transfer function in both magnitude and phase. The digital filter is designed by a curve-fit technique which solves a system of equations for the coefficients of the filter.^{A6} In the "on-line" method, the model of a FIR filter is performed directly on the same digital signal processing (DSP) board which is used to implement control. A white noise signal is sent through the controller to the control source and the coefficients of the digital filter are adapted in real time, in a method similar to the control algorithm which solves for the coefficients of the adaptive FIR compensating filter.^{A4} The number of filter coefficients must be chosen, and can be adjusted based on the complexity of the filter required; the larger the number of coefficients, the more computations that are required by the controller.

Since an IIR filter has both poles and zeroes, potential for instability exists if an IIR filter is used for the system identification if any of the poles of the filter are located outside of the unit circle in the complex z -plane. In the event that the IIR filter design yields unstable poles, the poles are "reciprocated" across the unit circle into the stable region, inside the unit circle. The process of reciprocation involves replacing each unstable pole with its inverse in order to reflect it across the unit circle into the stable region.^{A1} This distorts the phase response of the model somewhat, but inversion of a small number of slightly unstable poles in a large filter still yields a model with a satisfactory match of both magnitude and phase response.

Feedback Removal

The feedforward algorithm assumes that there is no significant contribution from the output of the control source, or feedback, in the reference signal. If there exists significant feedback of the control signal into the reference, the coherence between the reference and the error will be degraded, and it is possible that this feedback loop will cause the control system to become unstable. This potential instability is one of the difficulties involved in achieving global control, especially when both the control source and the reference sensor are determined from acoustic signals.

It is possible to attempt to electronically remove the control feedback present in the reference signal, using the control algorithm.^{A7} This technique is known as feedback removal (FBR), and a control block diagram of the FBR method is shown in Figure A-2. The control-to-reference transfer function, T_{cr} , is measured directly, and then modeled by a digital filter. The control output signal is then filtered through the model of T_{cr} , called \hat{T}_{cr} , and subtracted from the measured reference signal. Ideally, the measured reference minus the version of the control signal which has been filtered through \hat{T}_{cr} yields a new reference signal with the feedback removed. In this technique, it is extremely important that the model of T_{cr} is accurate, since any significant modelling errors will result in control feedback content in the reference signal.

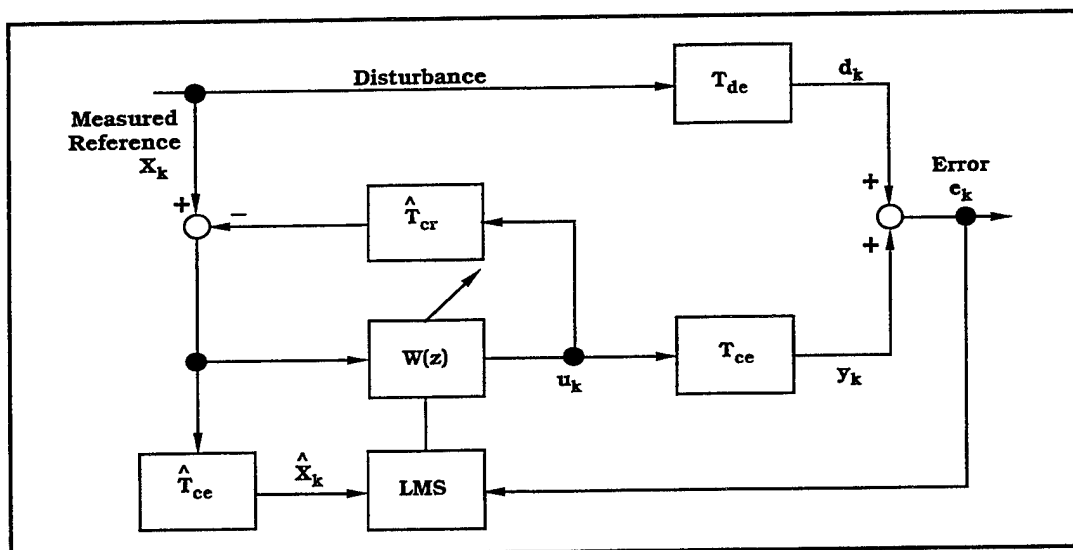


Figure A-2. Block Diagram of Control System With Feedback Removal.

REFERENCES FOR APPENDIX A

- A1. Widrow, B., and Stearns, S., *Adaptive Signal Processing*, Prentice Hall, NJ, 1985.
- A2. Elliott, S.J., et al., "A Multiple Error LMS Algorithm and Its Application to Active Control of Sound and Vibration", *IEEE Transactions on Acoustics, Speech, and Signal Processing*, Vol. ASSP-35, No. 10, 1423-1434, October 1987.
- A3. Stevens, J., and Ahuja, K., "The State-of-the-Art in Active Noise Control", AIAA Paper #90-3924, 13th AIAA Aeroacoustics Conference, October 1990.
- A4. Vipperman, J.S., Burdisso, R.A., and Fuller, C.R., "Active Control of Broadband Structural Vibration Using the LMS Adaptive Algorithm," *J. Sound Vib.*, 166 (2), 283-299, 1993.
- A5. Smith, J.P., "Active Control of Broadband Acoustic Radiation From Structures," M.S. Thesis, VPI&SU, Blacksburg, VA, 1993.
- A6. Smith, J.O., "Techniques for Digital Filter Design and System Identification with Application to the Violin," Ph.D. dissertation, Stanford Univ., CA, 1983.
- A7. Nelson, P.A., and Elliott, S.J., *Active Control of Sound*, Academic Press Ltd, London, 1992.

APPENDIX B

Description of the Analytical Model

The analytical model used in this study implements simple monopole sources as the disturbance and control sources radiating in the presence of a reflecting plane. The pressure at a radius r due to a monopole harmonic acoustic source radiating into free space is expressed as:

$$p(r) = \frac{A}{r} e^{-jkr} \quad (B-1)$$

where A is the source amplitude (which can be complex), and k is the wavenumber.

In the presence of a reflecting plane, each source will result in two pressure waves at the observation point, a direct wave and a reflected wave. The reflected wave, and thus the reflecting plane, can be accounted for by including an image source symmetrically located about the plane of reflection for each acoustic source above the plane. Therefore the sound pressure radiated by a single source to the observation point is given by the sum of the pressures due to the actual source and the image source.

Figure B-1 contains a diagram of the general arrangement showing the observation point labeled E and the disturbance and control sources, labeled D and C , respectively. The total pressure observed at the error location E will be a summation of the pressures at that point due to the disturbance source and the control source, and their respective image sources. The pressure at point E is

$$P_c = P_{de} + P_{d_{ie}} + P_{ce} + P_{c_{ie}} = \frac{A_d}{r_{de}} e^{-jkr_{de}} + \frac{A_{d_i}}{r_{d_{ie}}} e^{-jkr_{d_{ie}}} + \frac{A_c}{r_{ce}} e^{-jkr_{ce}} + \frac{A_{c_i}}{r_{c_{ie}}} e^{-jkr_{c_{ie}}} \quad (B-2)$$

where A_d and A_c are the complex amplitudes of the disturbance and source, respectively, the subscript i refers to the image source, P_{mn} denotes the pressure at point n due to the source at point m , and r_{mn} represents the distance from point m to point n .

For a single disturbance monopole source, N_e observation points, and N_c control sources, Equation (B-2) becomes a system of equations which can be expressed in matrix form as:

$$[P_e]_{N_e \times 1} = [P_{de}]_{N_e \times 1} + [P_{d_{ie}}]_{N_e \times 1} + \{[R_{ce}] + [R_{c_{ie}}]\}_{N_e \times N_c} [A_c]_{N_c \times 1} \quad (B-3)$$

where $[R_{ce}]$ and $[R_{c_{ie}}]$ are matrices of the last two terms of Equation (4.3), respectively, with the complex control amplitudes factored out.

If $N_c = N_e$, letting $[P_e] = 0$ and solving for the complex control input amplitude matrix $[A_c]$ yields:

$$[A_c] = -[MR_{ce}]^{-1} [MP_{de}] \quad (B-4)$$

where:

$$[MR_{ce}]_{N_e \times N_c} = [R_{ce}] + [R_{c_{ie}}] \quad \text{and} \quad [MP_{de}]_{N_e \times 1} = [P_{de}] + [P_{d_{ie}}] \quad (B-5)$$

If $N_c \geq N_e$, the "pseudo inverse" is implemented to solve for the $[A_c]$ that minimizes $[P_e]$ as follows:

$$[A_c] = -\{[MR_{ce}]^T [MR_{ce}]\}^{-1} [MR_{ce}]^T [MP_{de}] \quad (B-6)$$

The transpose in Equation (B-6) is a Hermetian transpose, which is the transpose of complex conjugates. Once the control amplitudes are known, the pressure at any point in space due to both the disturbance and control sources can be found in order to evaluate the area of reduction and the amount of attenuation.

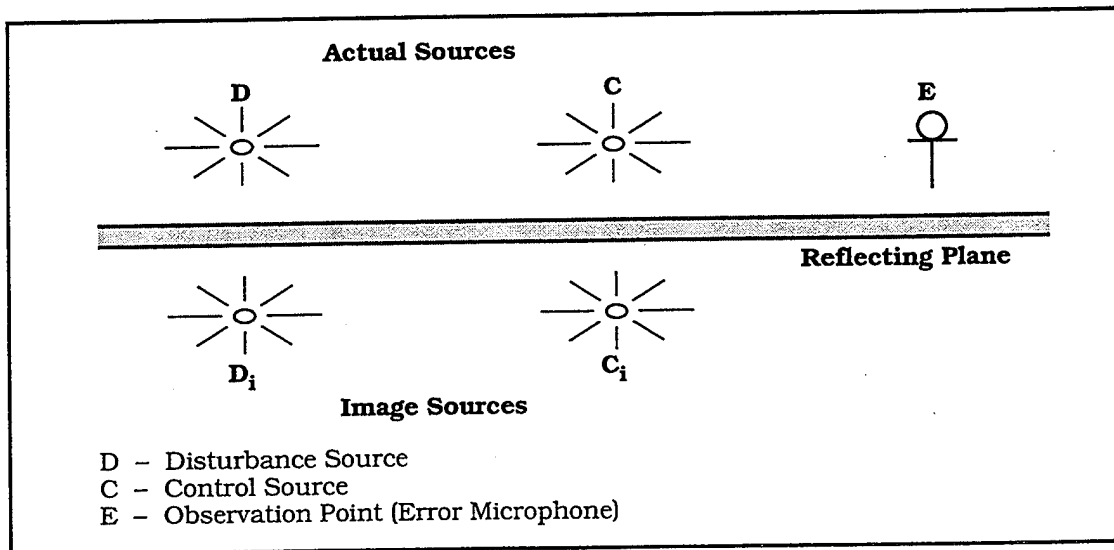


Figure B-1. Schematic of Disturbance, Control Source, and Observation Point.